Aus dem

Department für Frauengesundheit Tübingen

Universitäts-Frauenklinik

Establishing a three-dimensional organoid model of primary breast cancer for assessing effects of oncolytic virotherapy

Inaugural-Dissertation
zur Erlangung des Doktorgrades
der Medizin

der Medizinischen Fakultät
der Eberhard Karls Universität
zu Tübingen

vorgelegt von

Carter, Mary Elisabeth

2023

Dekan:	Professor Dr. B. Pichler
1. Berichterstatter:	Professor Dr. A. Hartkopf
2. Berichterstatter:	Professor Dr. F. Stubenrauch
3. Berichterstatter:	Professor Dr. I. Juhasz-Böss

Tag der Disputation: 13.02.2023

Content

List of figures

List of tables

List of abbreviations

Abbreviation	**Meaning**
advDMEM/F12 +/+/+	Gibco Advanced Dulbecco's Modified Eagle Medium/F-12 with the addition of 1% GlutaMAX, 1% 4-(2-hydroxyethyl)-1-piperazineethanesulfonic acid and 1% penicillin-streptomycin
ANOVA	One-way analysis of variance
ASC	Adult stem cells
BRCA	Breast cancer susceptibility genes
BSA	Bovine serum albumin
CD	Cytosine deaminase
CDK	Cyclin-dependent kinase
d	Days
DCIS	Ductal carcinoma *in situ*
DMEM	Dulbecco's modified Eagle's medium
EDTA	Ethylenediaminetetraacetic acid

EGF	Epidermal growth factor
ER	Oestrogen receptor
FDA	United States Food and Drug Administration
FGF	Fibroblast growth factor
GFP	Green fluorescent protein
GLV-0b347	Vaccinia virus expressing a red fluorescent protein
GLV-1h94	Vaccinia virus expressing a suicide gene
GM-CSF	Granulocyte macrophage colony-stimulating factor
HEPES	4-(2-hydroxyethyl)-1-piperazineethanesulfonic acid
HER2	Human epidermal growth factor receptor 2
hpi	Hours post infection
HSV-1	Herpes simplex virus type 1
H-1PV	Parvovirus H1
IFN	Interferon
L-WRN	L-WRN: L cell line engineered to secrete Wnt3a, R spondin 3, and Noggin (L-WRN) conditioned medium
MeV	Measles vaccine viruses
MeV-GFP	Measles virus expressing the GFP marker gene
MeV-SCD	Measles virus expressing a suicide gene
MHC	Major histocompatibility complex
MOCK	Untreated organoids
MOI	Multiplicity of infection
NDV	Newcastle Disease virus
p	Passages
PARP	Poly adenosine diphosphate ribose polymerase
PBS	Dulbecco's phosphate-buffered saline
PD-L1	Programmed death-ligand 1
PIK3CA	phosphatidylinositol-4,5-bisphosphate 3-kinase, catalytic subunit alpha
PR	Progesterone receptor
PSC	Pluripotent stem cells

RUC-GFP	*Renilla reniformis* luciferase – *Aequorea victoria* green fluorescent fusion protein
RFP	Red fluorescent protein
RV	Reovirus
SCD	Super cytosine deaminase
SCID	Severe combined immuno-deficient
SLAM	Signalling lymphocyte activation molecule
TK	Thymidine kinase
TNBC	Triple negative breast cancer
TNM	Tumour, Node, and Metastases
UPRT	Uracil phosphoribosyltransferase
VGF	Vaccinia (virus) growth factor
5-FC	5-fluorocytosine
5-FU	5-fluorouracil
5-FUMP	5-fluorouridine monophosphate

1 Introduction

1.1 Epidemiology and prognosis of breast cancer

Unfortunately, one in eight women will be diagnosed with breast cancer in their life [1]. In 2019 around 268 000 women were diagnosed with breast cancer in the United States. Indeed, breast cancer alone will make up approximately 30% of new cancer diagnoses this year in women. Additionally, this type of cancer is one of the three most common causes of death in women due to cancer. For example, breast cancer is the most common cause of cancer-associated deaths in women aged between 20-59 years [1].

In comparison to other tumour entities, breast cancer has a relatively good prognosis. The current five-year survival rate is around 90% in the first five years after diagnosis. The ten-year survival rate is around 83%. The high survival rate is due to a combination of effective therapies as well as an improved detection scheme [1, 2]. Nevertheless, even decades later patients can still suffer from a relapse in form of distant metastases.

1.2 Classification of breast cancer

1.2.1 *Tumour, Node, Metastases staging classification for breast cancer*

Breast cancer can be staged according to the Tumour, Node, and Metastases (TNM) staging system. The tables below are based on the TNM classification criteria of the 8th edition of the TNM staging system. The classification system evaluates three different categories: tumour, lymph nodes and distant metastases. The determined stage influences disease management, and the patient's treatment as well as prognosis [3].

Table 1 Classification of primary tumour (T) [3]

Primary tumour stage	Description
T0	No primary tumour
Tis **Tis (DCIS)** **Tis (Paget)**	Carcinoma *in situ* Ductal carcinoma *in situ* (DCIS) Paget disease of the nipple with no additional invasive carcinoma and/or DCIS
T1	Size of tumour lesion ≤ 20 mm
T2	Size of tumour lesion > 20 mm but ≤ 50 mm
T3	Size of tumour lesion > 50 mm
T4	No defined size but additional infiltration of the chest wall and/or skin

Table 2 Classification of regional lymph nodes (N) [3]

Regional lymph nodes	Description
	Clinical classification
cNX	No assessment of regional lymph nodes possible
cN0	No regional lymph node metastases
cN1	Metastases in movable ipsilateral regional lymph nodes in axillary level I and II
cN2	Metastases in fixed ipsilateral regional lymph nodes in axillary level I and II or internal mammary nodes
cN3	Metastases in ipsilateral lymph nodes in axillary level III, in mammary lymph nodes and in axillary level I/II, in ipsilateral supraclavicular lymph nodes
	Pathological classification
pNX	No assessment of regional lymph nodes possible
pN0	No regional lymph node metastases

pN1	Micrometastases (mi), metastases in one to three axillary lymph nodes, metastases ipsilateral internal mammary sentinel nodes
pN2	Metastases in four to nine axillary lymph nodes, positive internal mammary lymph nodes
pN3	Metastases in ≥ 10 axillary lymph nodes, ipsilateral internal mammary lymph nodes with at least one in axillary lymph nodes, > 3 axillary lymph nodes and internal mammary lymph nodes detected by sentinel lymph node biopsy, or supraclavicular lymph nodes

Table 3 Classification of distant metastases (M) [3]

Distant metastases	Description
M0	No evidence of distant metastases or metastases ≤ 0.2 mm
M1	Distant metastases > 0.2 mm

Table 4 Staging of breast cancer according to TNM classification [3]

Primary tumour stage (T)	Regional lymph nodes (N)	Distant metastases (M)	Stage group
Tis	N0	M0	0
T1	N0	M0	IA
T0	N1mi	M0	IB
T1	N1mi	M0	IB
T0	N1	M0	IIA
T1	N1	M0	IIA
T2	N0	M0	IIA
T2	N1	M0	IIB
T3	N0	M0	IIB
T0	N2	M0	IIIA
T1	N2	M0	IIIA

T2	N2	M0	IIIA
T3	N1	M0	IIIA
T3	N2	M0	IIIA
T4	N0	M0	IIIB
T4	N1	M0	IIIB
T4	N2	M0	IIIB
Any T	N3	M0	IIC
Any T	Any N	M1	IV

1.2.2 *Histological classification of breast cancer*

Breast cancer has a heterogeneous pathology that can be classified into different groups. These groups include infiltrating ductal carcinoma, infiltrating lobular carcinoma and mixed ductal/lobular carcinoma [4].

Between 70 - 80% of lesions in the breast are classified as infiltrating ductal carcinoma. The cells grow in clusters with different manifestations of gland formation [5]. Macroscopically lesions of this subtype are hard, gritty and of a grey to white colour. The neighbouring tissue is infiltrated in a diffuse manner thereby resulting in an irregular structure often resembling a star [5]. The hardness of these lesions is due to the reactive fibrosis through invasion into the mammary tissue [5]. Three different grades of infiltrating ductal carcinoma can be differentiated. Grade 1 lesions are well differentiated and infiltrate the neighbouring in solid nests. There is rarely nuclear pleomorphism and next to no mitotic activity. Grade 2 lesions are moderately differentiated. Additionally, some glandular differentiation can be found. The mitotic rate is low and only a few nuclear pleomorphisms can be found. Grade 3 lesions are hardly differentiated. The cells grow in solid clusters and show no glandular differentiation. The nuclei are atypical and a high mitotic rate can be seen [5].

Between 5 - 10% of lesions in the breast are classified as infiltrating lobular carcinoma. This subtype displays a characteristic growth pattern including the infiltration of mammary stroma and neighbouring fatty tissue. The lobular carcinoma cells are small cells which infiltrate singly or in small clusters [6]. A

small reactive fibrosis in the neighbouring tissue can sometimes be seen. In some cases the infiltrating lobular carcinoma is difficult to differentiate from an infiltrating ductal carcinoma [7]. E-cadherin staining can help in these cases [7]. Infiltrating lobular carcinoma demonstrates certain characteristics. These carcinomas have been seen to infiltrate bilaterally and often in a multicentre manner [8, 9]. Additionally, infiltrating lobular carcinomas are oestrogen receptor (ER) positive. Yet the expression rate of ER can vary [8, 10]. The prognosis of infiltrating lobular carcinomas and infiltrating ductal carcinomas has been subject of many studies with varying results [8, 11, 12]. The majority of research found that infiltrating lobular carcinomas metastasize more often to unusual sites such as the peritoneum in comparison to other breast cancer subtypes [13].

Seven percent of lesions in the breast are classified as mixed infiltrating ductal/lobular carcinoma. This group combines the histological characteristics of both subtypes [6].

1.2.3 *Hormone receptor classification of breast cancer*

Breast cancer survival and outcome can be correlated with two important hormone receptors, namely ER and progesterone receptors (PR) [14]. The expression of these receptors influences different parameters of a patient's survival [15, 16]. ER expression seems to be beneficial for the five-year survival yet this effect cannot be seen in long-term survival [17]. Typically ER-positive breast cancer is well differentiated with a low mitotic rate [14]. Genetic mutations often correlate with a poor outcome. These types of genetic mutations are less likely to be found in ER-positive breast cancer [14].

The expression rate of PR is independent of ER [18]. PR-positive breast cancer indicates a better overall survival than PR-negative breast cancer [18].

1.2.4 *Molecular classification of breast cancer*

Using molecular testing, breast cancer subtypes can be divided into further subtypes. Four subtypes are most commonly distinguished in the literature: luminal A and B subtype, human epidermal growth factor receptor 2 (Her2)-enriched and basal-like [6].

Luminal subtypes are associated with ER-positive breast cancer [6, 14]. The cells of this breast cancer type show a similar genetic morphology to the normal epithelium lining the lumen of the breasts such as the characteristic expression of cytokeratin 8 and 18 [6, 14]. The differentiation into luminal A and B subtypes has an influence on the individual prognosis with luminal B indicating an unfavourable prognosis [19, 20].

Luminal A breast cancer plays an important role in breast cancer as 40% of breast cancers can be classified as this type [14]. This molecular pattern of breast cancer correlates with an increased expression of genes in connection with ER expression pathways. A decreased expression of Her2 and other genes in association with proliferation can be seen [21, 22].

In comparison, luminal B breast cancer has an increased expression of Her2 and other genes in association with proliferation. Frequently, a lower expression of ER can be seen [19, 22]. Nevertheless, the differentiation between Luminal A and B in the clinical routine is challenging.

Another molecular subtype is Her2 enriched breast cancer. In these cases the expression of Her2 and other genes associated with cell proliferation are increased. A decreased expression of luminal and basal gene expression profiles can be seen. However, the Her2-enriched subtype is not equivalent to clinical Her2 positivity and, in particular, hormonal receptor-positive HER2-positive tumours are often luminal carcinomas [6, 14].

Basal-like breast cancer correlates to ER-, PR- and HER2-negative, so-called triple-negative breast cancer (TNBC) [14]. There is an association between the mutation status of the breast cancer susceptibility genes (BRCA) and TNBC. In particular germ-line mutations within the BRCA-1 gene increase the risk for TNBC [23, 24].

1.3 Treatment of breast cancer

There are different treatment options for non-metastatic and metastatic disease which will be described separately below.

The primary treatment goal in the non-metastatic situation is to destroy all tumour cells and therefore decrease the risk of (distant) recurrence. Local and systemic treatment is available. Local treatment includes surgery and/or removal of regional lymph nodes as well as radiotherapy. Systemic therapy may be given preoperatively (neoadjuvant) or postoperatively (adjuvant) [25]. The choice of systemic therapy is determined by clinical subtypes: Hormone receptor-positive breast cancer is treated with endocrine therapy and, in case of a high risk of relapse (e.g. if lymph nodes are involved or in young patients), with additional chemotherapy. Her2-positive breast cancer is treated with HER2-directed targeted (antibody) treatment and chemotherapy. TNBC is treated with chemotherapy and (in high risk cases) with immunotherapy [25].

Regrettably, metastatic breast cancer remains currently incurable. The therapeutic aim is to achieve a stable disease and maintain quality of life [25].

1.3.1 *Treatment of non-metastatic breast cancer*

Surgery

The aim of surgery in the treatment of breast cancer is to achieve the removal of the tumour and, where possible, to maintain the functions of the mammary glands. Typical approaches include a total mastectomy or a local excision (lumpectomy; breast conserving therapy) [25]. Research suggests radiation therapy is most beneficial for improved outcome in patients with cancer-positive lymph nodes [26]. The surgical margins are checked throughout the operation to ensure pathological negative margins [27]. Negative surgical margins are associated with lower recurrence rates in comparison to positive surgical margins [28, 29]. Recent studies have shown a comparable survival rate of patients being treated with breast conserving therapy (when combined with radiation therapy) or mastectomies; some studies even indicate an improved survival for the first treatment option [30-33]. Clinical trials showed that neoadjuvant chemotherapy before breast conserving surgery may have a

higher local recurrence rate than adjuvant therapy. However, the distant recurrence rate was the same in both the adjuvant and neoadjuvant chemotherapy setting in combination with breast conserving therapy [34].

Regional lymph nodes are approached in a diagnostic and therapeutic manner. The choice of surgery may depend on positive lymph nodes and neoadjuvant therapy. In patients that have clinically involved lymph nodes (i.e. palpable lymph nodes or pathologic lymph nodes on imaging modalities), dissection of the axillary lymph nodes is recommended, whereas patients without clinical lymph nodes, sentinel node biopsy may be sufficient. Of note is that axillary lymph node dissection leads to an increase of lymphedema in comparison to sentinel lymph removal [35, 36]. Therefore, the necessity of axillary lymph node dissection needs to be well thought out.

Radiation therapy

Radiation therapy may be aimed at the breast, the chest wall or regional lymph nodes [25]. Negative surgical margins, patients that had been treated using breast conserving surgery, patients with large multicentric tumours and patients with lymph node involvement should be followed by breast irradiation to reduce the risk of recurrence [37, 38]. Moreover, younger patients and patients with high-risk characteristics benefit most from radiation therapy [38].

Endocrine therapy

Endocrine therapy aims to prevent patients that express the ER- and PR-receptor from hormonal growth-stimulation [25]. Tamoxifen is given to pre- or postmenopausal patients. Tamoxifen selectively modifies ER and prevents oestrogen from binding to ER [25]. In contrast to tamoxifen, aromatase inhibitors are only effective in postmenopausal patients or in premenopausal patients that receive chemical castration using gonadotropin-releasing hormone agonists or have received oophorectomy (see below). The mechanism of action is based on inhibiting the conversion of androgens to oestrogens, thereby lowering the concentration of circulating oestrogen [25]. Research has shown that aromatase inhibitors are more effective than tamoxifen, particularly in for

postmenopausal women [39, 40]. For premenopausal patients at high risk of relapse ovarian suppression might be part of the treatment. This can be induced by using gonadotropin-releasing hormone agonists or oophorectomy and should be combined with tamoxifen or aromatase inhibitor treatment [25]. The duration of endocrine therapy should be at least five years and, according to individual risk analysis, up to 10 years [41, 42].

Chemotherapy

Chemotherapy is indicated for high-risk patients, like women with triple-negative or HER2-positive breast cancer. In hormonal receptor positive, HER2-negative patients the efficacy of chemotherapy is comparably low and, due to the high level of side effects, it should only be used in high-risk cases. This decision can be based on tumour, size, grading and proliferation (as measured by the Ki67 proliferation index). New data have indicated that RNA-based risk scores can help to decide whether chemotherapy should be used or not [43-45]. Chemotherapy for breast cancer usually consists of anthracyclines and taxanes [46]. However, as anthracyclines are associated with long-term side effects such as heart failure, recent data suggests that omitting anthracyclines, especially in HER2-positive patients, can also be considered [47].

HER2-targeted therapy

Targeted therapies for Her2-positive breast cancer have led to great improvements for these patients. Her2-gene overexpression has been shown to correlate with a poorer outcome [47]. Therefore, targeting Her2 overexpression is an important part of therapy for Her2-positive breast cancer. Her2-targeting drugs include antibodies like trastuzumab and pertuzumab as well as tyrosin-kinase inhibitors like lapatinib, neratinib and tucatinib [47]. Moreover, antibody-drug-conjugates such as trastuzumab-emtansine and trastuzumab-deruxtecan are also available. In the non-metastatic situation, trastuzumab, when combined with chemotherapy, leads to a reduction of recurrence rates and an improved overall survival [48, 49]. Current research has focused on reducing side effects through lowering the number of parallel chemotherapeutic agents for low-risk patients, whereas high-risk patients benefit from the addition of further HER2-

directed agents like pertuzumab and neratinib [25]. Moreover, HER2-directed treatment of patients that do not respond to neoadjuvant HER2-directed treatment benefit from a postneoadjuvant therapy with trastuzumab-emtansine [50].

1.3.2 *Treatment of metastatic breast cancer*

Metastatic breast cancer includes a variety of patients differing in localisation, size and number of metastases [51]. Treatment aims are to prolong survival, reduce symptoms and improve of quality of life [52, 53]. These factors need to be weighed against the potential side effects. Although systemic therapy plays a major role in treating patients with metastatic breast cancer, local therapy might be useful to treat symptomatic patients. Whether local therapy improves survival, however, is unclear. This might be the case in patients with a small number of metastases (oligometastatic disease) [54]. Hormone-receptor and Her2-positive breast cancer should be subject to endocrine therapy with additional cyclin-dependent kinase (CDK) 4/6 inhibitors [25]. Further treatment options such as everolimus or phosphatidylinositol-4,5-bisphosphate 3-kinase, catalytic subunit alpha (PIK3CA) inhibitors can be used to avoid chemotherapy. If chemotherapy is necessary, single-agent chemotherapy should be used to maintain a balance between treatment results and quality of life [55].

In HER2-positive and TNBC patients monochemotherapy still is the treatment of choice already in the first line of metastatic therapy [25]. Treatment for HER2-positive patients should be combined with HER2-directed therapy. In triple negative patients immunotherapy (atezolizumab or pembrolizumab) should be used if the tumour and/or the surrounding immune cells express the programmed death-ligand 1 (PD-L1) receptor [56]. Moreover antibody-drug conjugates are highly effective in patients with HER2-positive (trastuzumab-emtansine, trastuzumab-deruxtecan) or triple-negative (sagituzumab-govitecan) breast cancer [57]. Patients with a pathogenic germline mutation in the BRCA1 or BRCA2 genes moreover benefit from targeted inhibitors of the poly adenosine diphosphate ribose polymerase (PARP) enzymes [58, 59]. PARP

inhibitors result in a disruption of DNA repair and replication by binding to BRCA1/2 mutated proteins and causing selective killing of the cells [59].

1.4 Patient-derived organoids

In order to enable the best possible research for future treatment options representative experimental cancer models are important. Such cancer models are indispensable for functional analysis of various cancers such as breast cancer. Human tumour cell lines have been the preferred method for cancer research [60]. Additionally, rodent xenografts have been used in which the human tumour cells are injected into immune-comprised animals [61]. Drost *et al.* summarized the disadvantages of tumour cell line models [60]. During establishment the cells undergo immense genetic alterations to adapt to the new environment. This adaption can lead to a shift in the genetic diversity of the cells and they may not represent the original tumour from which the cells were derived from. Additionally, establishing control lines derived from healthy tissue is difficult and only possible through conditional reprogramming [60, 62]. Yet this method does not guarantee successful cloning [63, 64]. Another aspect to consider when using tumour cell lines is that the structure and cellular interactions are not the same as in the original tissue. Kamb *et al.* reported that cells from tumour cell lines are different in cell architecture and complexity compared with their original tumour cells; original tumour cells form a complex structure with surrounding inflammatory or vascular cells [61]. Xenograft models are an improvement on cell cultures as they incorporate some type of stroma yet this is of murine origin and not human [61]. The interaction between host and xenograft may be different from the interaction with the originally derived tumour cells [61]. Moreover, xenograft models are developed to fulfil research needs such as easy production. Original tumours often develop over many years and therefore are not well represented by the xenograft model [61]. The main disadvantage in this model is similar to the aforementioned cell lines, namely, the genetic profile of the xenograft does not capture and represent the diverse genetic and epigenetic makeup of the original tumour [61]. During the process of establishing the model, clonal selection can be observed [65, 66]. The exact mechanism of potential selection is unknown and still subject to

current research. Research has utilized severe combined immune-deficient (SCID) mice. These mice have no murine B- and T-cell immunity [67]. More representative results could be achieved as the murine immune system does not interfere with the research conducted. However, some mice develop functional murine clones within months which have the potential to interfere with research and invalidate results [67].

In the past few years, the term organoid has evolved. Today we commonly understand an organoid culture to be a three-dimensional structure derived from stem cells that are cell-type specific for an organ. Additionally, the cells are capable of self-organization thereby resulting in a structure known for the particular organ [60, 68]. Organoid cell cultures can be grown from two types of stem cells, i.e. pluripotent stem cells (PSC) and adult stem cells (ASC) specific for an organ or tissue [69, 70]. Cultivation of PSC has been available for longer than cultivation of ASC. In the beginning, ASC did not seem to have the same proliferation potential *in vitro*. Enhanced replication of the environment was needed to reach the maximum proliferation potential for ASC. When the environment was improved and more representative of the naturally occurring environment, it has been possible to cultivate ASC. The additional factors needed for ASC cultivation include epidermal growth factor, proto-oncogene Wnt3, Wnt-signal amplifier R-spondin and the BMP-inhibitor Noggin. The addition of these factors to the culture environment has enabled many research groups to grow organoid cell cultures derived from tissue samples thereby resulting in an efficient and self-organizing model [60, 70].

So far, organoid cultures have been described from many different organs and tissue samples derived from colon, oesophagus, pancreas, stomach, liver, endometrium, and breast cancer [60, 71]. Organoid models have been shown to mirror the tumour epithelium. The phenotype of growing organoids is similar to the original tumour epithelium. This can also be seen at a genetic level [60]. For example, Raimondi *et al.* [72] established an organoid model of pancreatic cancer and healthy pancreatic tissue and used it to determine the effects of oncolytic adenoviruses. The authors concluded that the response of the pancreatic organoid model to oncolytic adenoviruses might be indicative of in-

patient responses of primary pancreatic tumours and metastases [72]. In 2018, Sachs *et al.* managed to set up a biobank of breast cancer tissue samples. The culture conditions for human mammary epithelial organoids have already been established that create organoids which exhibit the histological and genetic features of the original tumours [71].

Sachs *et al*. compared the response of organoid cultures to tamoxifen and the corresponding tumours to tamoxifen. The data showed matching responses between organoids and patients [71]. Consequently, organoid models might have the potential to predict patients' responses to different therapeutic agents.

1.5 Oncolytic virotherapy

1.5.1 *Introduction to oncolytic virotherapy*

Two of the main reasons for the development of a tumour are the combined changes in genetic and epigenetic characteristics of a cell. These changes result in a higher probability of cells becoming immortal [73]. Parallel to these changes, the evolving tumour cell produces so-called "neo-antigens" which should cause the cell to be detected by the immune system. However, instead the cell manages to circumvent the detection of the immune system by manipulating it [73]. This effect is due to the decreased reaction to signals from the innate immune system, reduced expression of neo-antigens, and prevention of immune cells from infiltrating the tumour [73]. These changes in the tumour environment shield the cell from the immune system but, interestingly, make it more vulnerable to viral infection [74].

The aim of any new therapy should be the selective destruction of tumour cells. Oncolytic viruses represent a new approach to cancer treatment. In contrast to classic gene therapy, where replication incompetent viruses are used, oncolytic viruses are replication competent [75]. Oncolytic viruses aim to selectively infect tumour cells followed by the replication of the viruses and destruction of the tumour cells, a process called oncolysis (Figure 1-1). The subsequent release of these additional infectious viruses causes the infection and oncolysis of neighbouring tumour cells [75, 76].

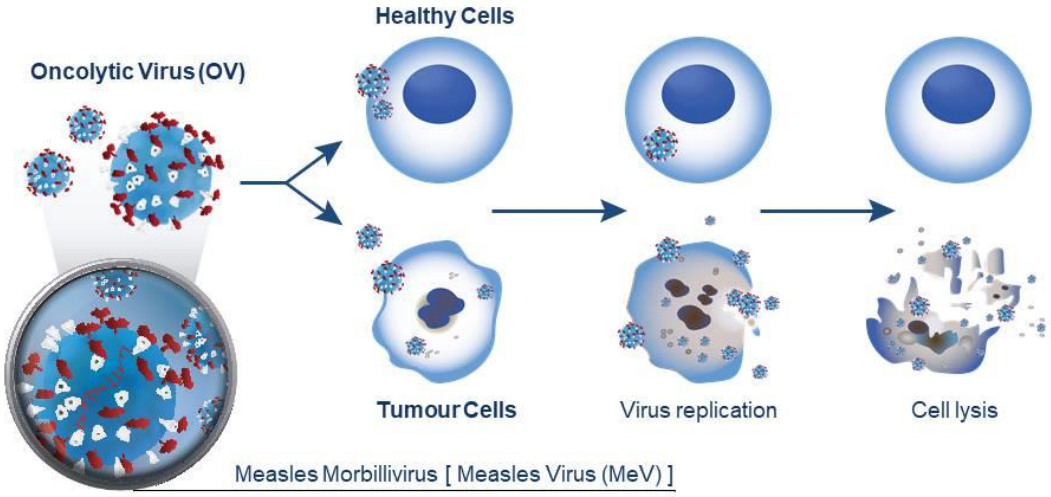

Figure 1-1 Oncolysis resulting from infection with oncolytic viruses

At the same time, a tumour-specific immune response is induced, thereby resulting in a further enhancement of the oncolytic effects [75]. Therefore, the combination of immune therapies such as immune checkpoint inhibitors, that release the brakes on the immune system, with oncolytic viruses might be a promising therapeutic strategy; corresponding clinical trials are currently being undertaken (NCT02919449; NCT01937117).

During the 20th century wild-type oncolytic viruses were used and their effects on tumour cells investigated. Research conducted on oncolytic viruses led to an important differentiation of oncolytic viruses into two groups. The first group includes oncolytic viruses with natural or intrinsic anti-neoplastic characteristics. The second group includes oncolytic viruses that have been genetically modified to enhance tumour-selectivity [77]. The enhancement of tumour selectivity is important in order to improve patient safety. Additionally, the aim is to reduce side effects locally and systemically as well as to maximize the oncolytic effect on the tumour.

The mechanisms of host cell selectivity of viruses have naturally evolved through evolution to improve the penetration into the host cells. In some case the cell selectivity also improved tumour selectivity. For example, viruses

interfere with many cell functions including cell division and cell death to enable viral survival [77]. Cells undergo changes during carcinogenesis. These alterations are often similar to the changes viruses induce in cells such as alteration of the interferon (IFN) pathways or changes to the cell cycle and cell death. Alterations in IFN signalling can improve the oncolytic effect on tumour cells through facilitated viral spread. This results in a higher susceptibility of tumour cells to oncolytic viruses [78]. In these cases natural selection leading to host cell selectivity has coincided with better tumour selectivity to enhance tumour-selectivity [77].

Viruses with natural oncolytic potential include vaccinia viruses, Newcastle Disease viruses (NDV), measles vaccine viruses (MeV), parvovirus H1 (H-1PV) and reoviruses (RV) [77]. The experience gained in science through the use of living viruses for vaccinations has shown that viruses are safe for use in patients [79]. For instance, a measles vaccine has been readily available for many years. The measles virus has shown to replicate preferably in tumour cells. This effect was larger when a vaccine measles strain was used in comparison to a wild-type measles virus [77]. In the example of the measles virus the vaccine strain enters the host cell mainly through CD46 receptor-dependent uptake. During carcinogenesis tumour cells often overexpress the CD46 receptor thereby making the tumour more susceptible to infection [80]. Another example for vaccine viruses with oncolytic properties is the vaccinia virus. The vaccine for vaccinia virus was used for the eradication of smallpox [81]. The application of this virus is safe for patients and mild or flu-like symptoms have been reported after the application of this vaccinia virus [77]. Therefore vaccinia viruses have potential as a future oncolytic virus.

Work with genetically engineered oncolytic viruses started in the 1990s [82]. The hope was to increase tumour selectivity and the oncolytic potential in comparison to the previously known naturally occurring oncolytic viruses. In some cases viruses without naturally occurring oncolytic effect were genetically engineered to create novel oncolytic viruses. Herpes simplex virus type 1 (HSV-1) was the first oncolytic virus to be genetically modified by creating a thymidine kinase-negative mutant of HSV-1 [83]. Many studies followed this development

[82]. After identifying viruses with oncolytic potential, the next step was to genetically engineer these viruses for selective replication in tumour cells. More recently, an activated immune response against the tumour cells caused by the oncolytic viruses is understood to be important for their action [84-86].

There are three main different ways to achieve improved tumour selectivity. Firstly, viruses are modified to ensure selective uptake into tumour cells. Secondly, gene manipulation is utilized to allow tumour cell-specific replication. Thirdly, the insertion of promoters into the viral genome enables tumour-dependent replication. Additionally, gene deletions can also result in reduction of toxicity caused by the viruses thereby facilitating the clinical application [78]. The vaccinia virus is an example for the combination of natural occurring tumour selectivity and genetic engineering. Tumour selectivity is enhanced through the deletion of the thymidine kinase (TK) gene and vaccinia (virus) growth factor (VGF) gene. TK deletion facilitates viral replication independent of the cell cycle. VGF deletion allows neighbouring cells to be infected [87]. The pathways for enhanced replication of vaccinia viruses are often amplified through carcinogenesis. Therefore, the dependency on these pathways allows tumour specific replication of the virus [87].

Therapeutic transgenes are another way to enhance the effectiveness of an oncolytic virus. The insertion of a suicide gene cytosine deaminase (CD) in a vaccinia virus has been subject to research [88]. The enzymatic activity includes the conversion of 5-fluorocytosine (5-FC) to 5-fluorouracil (5-FU) and 5-fluoro-uridine monophosphate (5-FUMP) [89]. 5-FC alone has little toxic effect and is used to treat fungal infections. 5-FU is a cytotoxic agent that is used for the treatment of breast cancer. 5-FUMP is the activated form of 5-FU [90, 91]. Derivatives are antimetabolites that are built into the DNA and RNA resulting in interference with important cellular functions such as DNA repair, DNA/RNA synthesis and protein synthesis [92, 93]. The addition of the suicide gene CD in a vaccinia virus has been found to enhance the therapeutic effect of an oncolytic virotherapy [88].

Additionally, oncolytic viruses can be armed with transgenes to evoke an immune response against infected tumour cells. Talimogene laherparepvec (T-VEC/OncoVEX^{GM-CSF}) is an HSV-1 that has been genetically engineered to improve the systemic antitumour response by integrating the gene for the granulocyte macrophage colony-stimulating factor (GM-CSF) [94]. The production of GM-CSF during infection with OncoVEX^{GM-CSF} provokes an antigen-specific T-cell response and a decrease of T-regulatory cells [95-99].

Transgenes can also be utilized to incorporate fluorescent proteins into the viral genome. The aim is to monitor the viral infection and spread. A fluorescent protein often used in oncolytic virus research is the *Renilla reniformis* luciferase – *Aequorea victoria* green fluorescent fusion protein (RUC-GFP). The addition of the RUC-GFP cassette into the viral genome can be used to image the viral spread [100].

The oncolytic viruses which are currently being developed should preferably not infect healthy cells but rather infect the tumour cells due to their activated or deregulated pathways [74]. The aim is to achieve a maximum activation in the tumour cell and little or no toxicity to normal cells. The feasibility of this approach has been demonstrated in preclinical models and patients [101-103]. Additionally, some oncolytic viruses have the potential to disrupt the vascular system around the tumour cells [104-107].

Promising tumour responses following the application of oncolytic viruses were confirmed in early clinical trials. For example, the oncolytic virus ONYX-015, a genetically modified adenovirus, was shown to replicate in tumour cells, and cause infiltration of immune cells into the tumour [108, 109]. Importantly, a large randomized clinical trial phase 3 trial using OncoVEX^{GM-CSF} in patients with advanced melanoma was undertaken. A therapeutic benefit was shown in this clinical trial thereby leading to the registration of OncoVEX^{GM-CSF} in the United States and the European Union [94]. This was the first time that these regulatory authorities had approved an oncolytic virus for a malignant disease. Currently, fourteen different oncolytic viruses have been investigated in eighteen published clinical trials that included breast cancer patients. These

trials demonstrate that oncolytic viruses are well tolerated and safe for use in patients and display clinical activity [110]. However, with the exception of the reovirus pelareorep, these trials only studied a small number of patients with different advanced tumours including some with breast cancer. In addition to the published trials, there are many different oncolytic viruses which are also currently being tested in clinical trials but are not yet published [110, 111].

1.5.2 *Oncolytic measles virus*

1.5.2.1 MeV-GFP

Figure 1-2 Depiction of relevant parts of the MeV-GFP genome [112]

The gene encoding for the green fluorescent protein (GFP) has been inserted in front of the N gene. N = nucleocapsid gene; P = phosphoprotein gene; M = matrix protein gene; F = fusion protein gene; H = haemagglutinin gene; L = large protein gene

Measles viruses belong to the family of paramyxoviruses. Measles viruses are characterized by single-stranded negative-sense linear RNA [113]. The RNA is surrounded by ribonucleoproteins as well as a layer of different proteins. The layer contains the haemagglutinin protein and the fusion protein [114]. Measles viruses are capable of causing syncytia formation and DNA fragmentation [115].

Measles viruses need haemagglutinin protein to attach to receptors on the host cell. These receptors for attachment include CD46, signalling lymphocyte activation molecule (SLAM, CD150) and Nectin 4 [80, 116]. CD46 is essential for intercellular fusion of the measles virus and all human cells apart from erythrocytes express this protein. The infection with a measles virus results in an expression of envelope glycoproteins, haemagglutinin and fusion proteins. The fusion with neighbouring cells is triggered through interaction with CD46 of neighbouring cells, thereby resulting in syncytia [80]. The syncytia formation results in a recruitment of neighbouring cells for viral infection. This recruitment leads to a spread of viral infection. The influence on neighbouring uninfected cells is called bystander effect [115].

In order to utilize the measles virus for oncolytic virotherapy the goal is to achieve efficient viral spread from the originally infected cells to neighbouring cells. The efficient spread through syncytia formation and enhanced specificity through CD46 expression are premises for an oncolytic virotherapy.

Research has shown that CD46 is overexpressed in the transformation from healthy cells to malignant cells. This transformation may be relevant for cancerous cells to evade the complement system and therefore evade elimination. CD46 is an important protein for inhibiting the activation of the complement system directed towards autologous cells. The CD46 receptor density plays an important role for the formation of syncytia and the viral entry increases with the receptor density [117]. Therefore, an increased receptor density as potentially expressed on cancerous cell could result in a higher perceptibility for measles virus infection. This makes it an interesting virus for potential oncolytic virotherapy.

The infection with an oncolytic measles virus additionally results in an increase of IFN-β. This response is enhanced through cell-cell fusion. The rise in basal IFN-β has the potential to trigger an immune response directed against the tumour [116].

Oncolytic measles viruses are based on the strain of measles viruses which have been used for vaccine purposes for many years. The years of vaccination have shown the excellent patient safety. Oncolytic measles viruses have been pre-clinically investigated and are undergoing clinical trials for use in cancer patients for a variety of cancer entities as for example ovarian cancer or breast cancer [118, 119].

The genome of MeV-GFP is based in the viral genome of the vaccine measles virus. However, one alteration has been made (Figure 1-2). A gene for the expression of a green fluorescent protein (GFP) has been added, namely the rucGFP gene. GFP originates from the jellyfish *Aequorea victoria* and does not naturally occur in vaccinia viruses [120]. GFP has become a well-established and very important marker for gene expression. The expression of rucGFP

gene allows the monitoring of the viral infection and spread *ex vivo* and potentially *in vivo.*

1.5.2.2 MeV-SCD

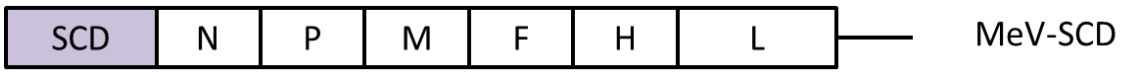

Figure 1-3 Depiction of the relevant parts of the MeV-SCD genome [112, 121]

The gene encoding for the suicide gene (SCD) has been inserted in front of the N gene. N = nucleocapsid gene; P = phosphoprotein gene; M = matrix protein gene; F = fusion protein gene; H = haemagglutinin gene; L = large protein gene

MeV-SCD is an oncolytic measles virus with an additional suicide gene called super cytosine deaminase (SCD) (Figure 1-3). MeV-SCD has a similar measles backbone to MeV-GFP. The GFP gene has been replaced with SCD. [122]. The yeast-derived suicide genes that encode for a fusion gene encoding both cytosine deaminase and uracil phosphoribosyltransferase (called FCU1 [89] or SCD [123]) which expresses a chimeric protein that converts the non-toxic prodrug 5-FC into highly cytotoxic compound 5-FU and subsequently 5-FUMP, thereby bypassing an important mechanism of chemoresistance for 5-FU [112]. 5-FU is a cytotoxic agent that is used for the treatment of breast cancer, and 5-FUMP is the activated form of 5-FU [90, 91]. Cytosine deaminase catalyzes the conversion to 5-FU and uracil phosphoribosyltransferase (UPRT) catalyzes the subsequent conversion of 5-FU to 5-FUMP. Therefore, UPRT has the potential to sensitize chemoresistant cancer cells to 5-FU [112]

Derivatives are anti-metabolites that are built into the DNA and RNA resulting in interference with important cellular functions such as DNA repair, DNA/RNA synthesis and protein synthesis [92, 93]. An anti-tumour effect of SCD on cancer cells has already been demonstrated in an adenovirus model [122]. An oncolytic measles virus expressing SCD has also been clinically used and demonstrated efficacy [124]. Viral replication and spread will allow the suicide gene to spread at the same time and enhance the therapeutic effect.

MeV-SCD has been used in previous research and demonstrated tumour specific replication in experiments in human hepatoma and ovarian cancer cells [112, 123]. The MeV-SCD virus used in the following experiments was used in research on ovarian cancer cells. The data suggest that the measles virus infects, replicates and lyses tumour cells. The addition of the aforementioned prodrug 5-FC enhances the oncolytic effect. The expression of the suicide gene was positive in the infected tumour cells [112].

MeV-SCD was used in the following experiments.

1.5.3 *Oncolytic vaccinia virus*

1.5.3.1 Vaccinia virus

Vaccinia viruses belong to the poxvirus family. The genome is characterized by a linear double-stranded DNA [125]. There is not one wild-type vaccinia virus but many. These vaccinia viruses are then named differently according to the viral genome/backbone. The Western Reserve and Lister vaccinia viruses will be described later. In the following more in-depth detail is provided to the genetically engineered GLV-0b347 originating from the wild-type Western Reserve vaccinia virus. 1h94 is a genetically engineered vaccinia virus derived from the wild-type Lister vaccinia virus [126].

Specialized entry and replication in tumour cells is found in some wild-type vaccinia viruses and in attenuated vaccinia viruses [127]. Attenuated vaccinia viruses have additional gene deletions or insertions to reduce the virulence of the wild-type virus [126].

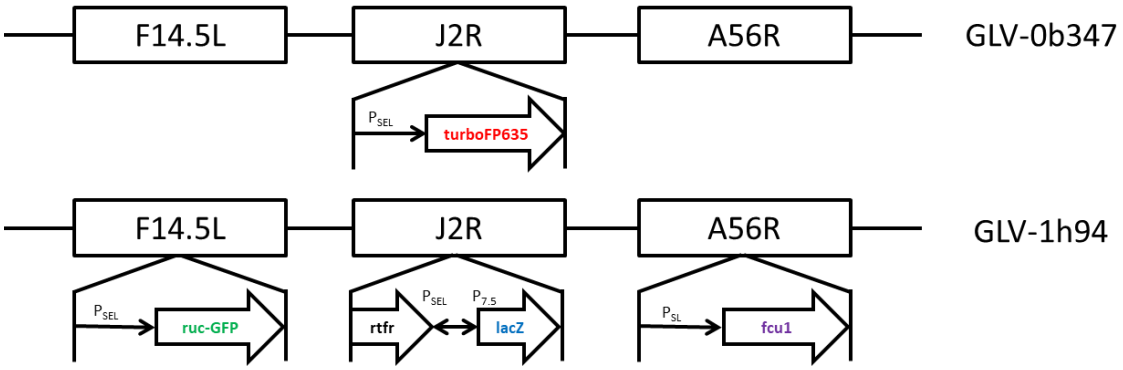

Figure 1-4 Viral genomes [121]

The viral genome of GLV wild-type viruses either with a *Lister* or *Western Reserve* backbone generally differ from one another. However, the genes that have been deleted are the same in both viruses. Therefore, they are summarized as one viral genome to give an overview.

F14.5L = open reading frame encoding 49 amino acids; J2R = non-essential gene encoding thymidine kinase; A56R = non-essential gene encoding haemagglutinin; turboFP365 = far red mutant of the red fluorescent protein from sea anemone *Entacmaea quadricolor*; ruc-GFP = R*enilla reniformis* luciferase – *Aequorea victoria* green fluorescent fusion protein; rtfr = reverse gene of human transferrin receptor; lacZ = β-galactosidase; gusA = β-glucoronidase; P(SEL) = VACV (vaccinia virus) synthetic early/late promoter; P(SL) = VACV synthetic late promoter; P(7.5) = VACV early/late promoter; P(11) = VACV late P11 promoter

The genome of the vaccinia virus can be changed to achieve different goals. In the following virus changes to the viral genome have been made to facilitate the monitoring of viral infection and to enhance the therapeutic effect.

1.5.3.2 GLV-0b347

The vaccinia virus GLV-0b347 is derived from a Western Reserve vaccinia virus and therefore contains a Western Reserve genome (backbone) (Figure 1-4). The only modification that has been made to the virus is the disruption of the J2R gene locus. This results in an attenuation of the vaccinia virus [126]. The J2R gene locus is non-essential and encodes for thymidine kinase [127]. The J2R gene locus in the case of GLV-0b347 has been interrupted with a vaccinia synthetic early/late promotor and TurboFP365. TurboFP365 does not naturally occur in vaccinia viruses. TurboFP365 is a far-red mutant of the red fluorescent protein (RFP) from the sea anemone *Entacmaea quadricolor* [128]. The incorporation of the gene into the viral genome leads to an expression of the fluorescent protein. The production of RFP within the infected cell facilitates cell imaging of the viral infection in addition to attenuating the virus. The remaining gene loci are the same as in the wild-type Western Reserve (Figure 1-4).

Research has investigated the use of Western Reserve vaccinia virus as an oncolytic virus. The distribution of vaccinia viruses differs between different strands of vaccinia virus. For instance, GLV-1h68, a vaccinia virus with LIVP backbone, hardly accumulates in the brain or ovaries yet results in an enlarged spleen. This enlargement is due to the immune response following the viral infection and not due to viral infection of the spleen [126, 127].

The genome of the Western Reserve vaccinia virus was only altered in the J2R gene locus for GLV-0b347. The aim is to monitor the infection and not genetically engineer tumour selectivity. Gene loci such A56R that encode proteins important for intracellular enveloping and mediation cell adhesion were not changed [129]. This can give an insight into the almost natural oncolytic properties of GLV-0b347.

1.5.3.3 GLV-1h94

GLV-1h94 is derived from GLV-1h68 and contains a LIVP backbone [126] (Figure 1-4). A56R is a non-essential gene encoding for haemagglutinin [127]. In GLV-1h94 the A56R gene has been disrupted by the insertion of the vaccinia synthetic early/late promoter and the suicide gene FCU1 (Figure 1-4). The inactivation of the A56R gene is part of the desired attenuation of the vaccinia virus to ensure patient safety [127].

Similar to oncolytic measles virus MeV-SCD, oncolytic vaccinia virus GLV-1h94 also encodes the FCU1 suicide fusion gene enabling enzymatic conversion of 5-FC to 5-FU and 5-FUMP [91]. The 5-FU produced with MeV-SCD and/or GLV-1h94 influences the host cell and neighbouring cells. The 5-FU can then enter the neighbouring cells by means of diffusion and interfere with the DNA and RNA. This effect on neighbouring uninfected cells is called a bystander effect [90, 130]. FCU1 does not naturally occur in vaccinia viruses.

GLV-1h94 expresses the Renilla luciferase - Aequorea green fluorescent protein (RUC-GFP) expression cassette in the gene locus of F14.5L, resulting in an inactivation of the F14.5L gene (Figure 1-4) and thereby attenuation of this recombinant virotherapeutic vector. In the wildtype context, the gene locus F14.5L encodes a protein important for cell adhesion and virulence [129]. RUC-GFP does not naturally occur in vaccinia viruses [126]. Furthermore, this insertion of the RUC-GFP cassette also allows the monitoring of viral infections not only *ex vivo*, but potentially also *in vivo* by simple detection of the respective GFP-based fluorescence signal.

The J2R gene locus encodes for thymidine kinase [127]. GLV-1h94, being a derivative of the Lister strain of vaccinia virus, has a disrupted J2R gene locus due to the insertion of an engineered lacZ gene, which encodes β-galactosidase. In a Western Reserve backbone this J2R negative phenotype results in a decreased neurovirulence [126]. Therefore GLV-1h94 is thought to have a beneficial patient safety profile as they are thymidine kinase negative.

1.6 Objective

In this study we set out to answer the question whether three-dimensional cell cultures are suitable for testing oncolytic virotherapeutic compounds.

We addressed this topic by developing a protocol in a stable three-dimensional organoid model derived from patients with primary breast cancer to determine the oncolytic effects of genetically engineered oncolytic viruses, encoding either marker genes for GFP (oncolytic measles virus MeV-GFP) and for red fluorescent protein (oncolytic vaccinia virus GLV-0b347), or the SCD/FCU1 suicide gene (oncolytic measles virus MeV-SCD, oncolytic vaccinia virus GLV-1h94) on breast cancer organoid cultures.

Our intention was to develop a personalized patient approach to screen and prioritize oncolytic virotherapeutic compounds before administered for the first time to a specific patient. We selected the oncolytic efficacy of each virotherapeutic compound to create novel “virograms” (in analogy to antibiograms for testing antibiotic compounds).

2 Materials and methods

2.1 Criteria implemented for tissue used in this project

All patients provided written informed consent and the study was approved by the local ethics committee (210/2019BO2).

2.1.1 *Criteria implemented for tissue from patients with breast cancer*

The criteria implemented for the breast cancer tissue used in this study were as follows: Female patients had been diagnosed with primary invasive breast cancer that was histopathologically confirmed. Patients diagnosed with recurrent breast cancer or metastases were excluded from the study. The original tumours had to be of a certain size (at least 1 cm^3) to allow sufficient tumour material for a full histopathological analysis without affecting the result of this analysis yet still allowing sufficient cells for cultivation.

2.1.2 *Criteria implemented for tissue from patients used in the control group*

Tissue was obtained within a period of four months in 2019 from ten female patients, at the Department of Women's Health of the University Hospital Tuebingen (Table 1) and obtained from reduction mammoplasties or mastectomies. Patients diagnosed with recurrent breast cancer or metastases were excluded from the study. Infiltration of tumour cells in lymph nodes was not defined as an exclusion criterion.

2.2 Establishment of organoid cultures derived from malignant and healthy tissue

2.2.1 *Processing patient tissue for establishing breast cancer organoid cultures*

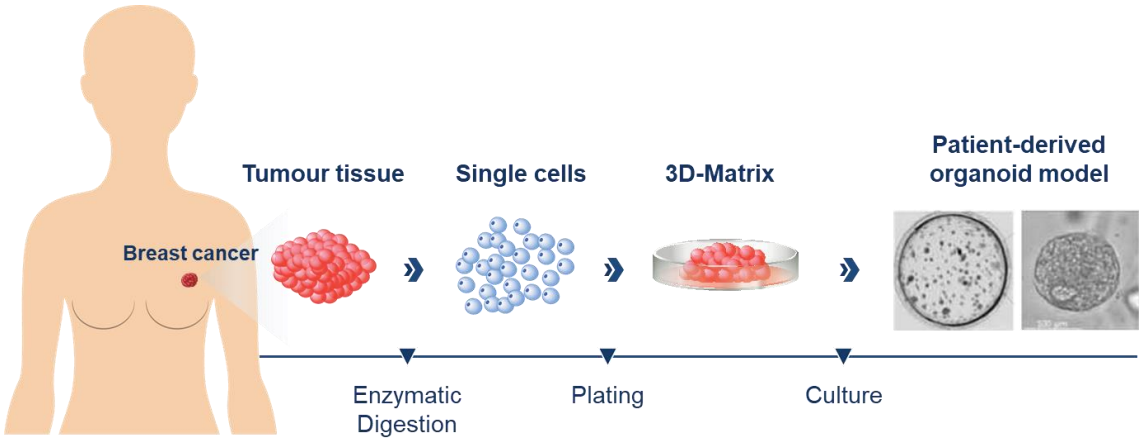

Figure 2-1 Deriving organoid cultures [121]

Figure 2-1 illustrates the overall process for preparing breast cancer patient-derived organoid cultures. Tumour tissues derived from each patient were cut into 1 mm^3 sized pieces and digested with a 1:1 mix of advDMEM/F12 +/+/+ (Gibco Advanced Dulbecco's Modified Eagle Medium/F-12 with the addition of 1% GlutaMAX, 1% 4-(2-hydroxyethyl)-1-piperazineethanesulfonic acid (HEPES) and 1% penicillin-streptomycin (all reagents from Thermo Fisher Scientific, Waltham, MA), collagenase (collagenase type IV 5 mg/mL, Sigma-Aldrich, Munich, Germany) and 10 µM Y-27632 (Hoelzel Diagnostika, Cologne, Germany) until sufficient digestion was achieved (about 1 – 3 hrs, visible clouding of the solution). The suspension was then transferred into a 15 mL tube containing 10 mL of advDMEM F12+/+/+ and centrifuged at 478 x g for 10 min. The supernatant was removed and the pellet was re-suspended in 1 mL of TrypLE Express (TrypLE™ Express Enzyme phenol red free from Thermo Fisher Scientific) and placed on the shaking table for another 15-30 min. The solution was filtered through a moist 100 µm filter into a 50 mL tube and washed with additional 10 mL advDMEM F12+/+/+. The remaining liquid was carefully removed from underneath the filter and added to the filtered suspension. The suspension was centrifuged for 478 x g for 10 min and the supernatant carefully

removed. Depending on the size of the remaining cell pellet it was re-suspended in 60-500 µL of advDMEM F12 +/+/+. For a standard organoid setup (6 wells in 48 well plate) an aliquot of 60 µL cell suspension was mixed with 70 µL of Corning Matrigel Membrane Matrix (Thermo Fisher Scientific), in a chilled 0.5 mL tube. Drops of 20 µL size were used for each well of a 48-well plate. Afterwards the culture plate was placed upside down in the incubator at 37°C and 5% CO_2. After 30 min 280 µL of breast cancer culture medium was added to each well and the surrounding wells filled with Dulbecco's phosphate-buffered saline (PBS) from Sigma-Aldrich. The medium was changed every four days.

The residual cell suspension not used for plating was re-suspended in 700 µL Gibco Recovery Cell Culture Medium (Thermo Fisher Scientific) per vial and frozen. The vials were then transferred to -80°C in Cell Coolers. For long-term storage the vials were transferred to liquid nitrogen.

2.2.2 *Passing of breast cancer organoids*

The cells were passaged after sufficient growth of the organoid cultures (ranging from 5 to 20 days). For this, the culture medium from the wells was transferred into a 15 mL tube. The wells were washed carefully (without removing or destroying the Matrigel dome) with 1 mL of Dulbecco's PBS (collected into the same 15 mL tube). The Matrigel domes were mechanically scraped of the bottom of the culture plate with a pipette tip and collected in TrypLE Express (1 mL for 6 wells). The solution was added to a 2 mL tube and placed on a shaking table for 5 min at 37°C and 1000 rpm. The solution was then triturated 5 times through a 27 ¾ G needle and 1 mL syringe and transferred to the 15 mL tube. After the addition of 10 mL of advDMEM/F12 +/+/+ the solution was centrifuged for 10 min at 478 x g. The supernatant was removed and the remaining cell pellet was re-suspended in advDMEM/F12 +/+/+. The amount of advDMEM/F12 +/+/+ needed was dependent on the number of wells that were plated and the number of vials that were frozen down. For a standard organoid setup (6 wells in 48-well plate) an aliquot of 60 µL cell suspension was mixed with 70 µL of Matrigel in a chilled 0.5 mL tube.

Drops of 20 µL size were used for each well of a 48well plate. Afterwards the culture plate was placed upside down in the incubator at 37°C and 5% CO_2. After 30 min 280 µL of breast cancer culture medium was added to each well and the surrounding wells filled with Dulbecco's PBS. The medium was changed every four days.

2.2.3 ***Breast cancer culture medium***

Table 5 Factors needed for the breast cancer culture medium (30 mL)

	Concentration needed	Concentration used	Amount used
L-WRN*	50%	100%	15 mL
Neuregulin (Peprotech, Rocky Hill, NJ)	5 nM	5 µM	30 µL
Fibroblast growth factor (FGF) 7 (Peprotech)	5 ng/mL	5 µg/mL	30 µL
FGF-10 (Peprotech)	20 ng/mL	20 µg/mL	30 µL
Epidermal growth factor (EGF) (Peprotech)	5 ng/mL	10 µg/mL	15 µL
A83-01 (Tocris, Wiesbaden, Germany)	500 nM	5 mM	3 µL
Y27632 (Hölzel)	5 µM	100 mM	1.5 µL
SB202190 (Sigma-Aldridge)	500 nM	5 mM	3 µL
Gibco B27 Supplement 2% (Thermo Fisher Scientific)	1x	50x	600 µL
N-Acetyl-Cysteine (Sigma-Aldrich)	1.25 mM	500 mM	75 µL
Nicotinamide (Sigma-Aldrich)	5 mM	1000 mM	150 µL
Primocin (InVivoGen, Toulouse, France)	50 µg/mL	50 mg/mL	30 µL
Gibco advDMEM/F12 50% (Thermo Fisher Scientific)			14 mL

*L-WRN: L cell line engineered to secrete Wnt3a, R spondin 3, and Noggin (L-WRN) conditioned medium

2.2.4 *Cryo-conservation of cells and organoids*

Cells or cell suspensions not used to plate into culture were re-suspended in Recovery Cell Culture Medium (700 µL per vial). The suspension was evenly distributed into the vials and placed in Cell Coolers at -80°C for at least 24 h before long-term storage in liquid nitrogen.

2.2.5 *Thawing of cells and organoids*

An aliquot of 10 mL of advDMEM/F12 +/+/+ was warmed to room temperature. Cells were thawed in a water bath (37°C, 2 min), added to the advDMEM/F12 +/+/+, and centrifuged at 478 x g for 10 min. The supernatant was removed and the cell pellet plated out as described above.

2.2.6 *Cultivation of breast cancer cell lines*

Breast cancer cell lines MCF7, T47D and MDA-MB-468 were grown in 2D in Dulbecco's modified Eagle's medium (DMEM, Gibco, with the addition of 1% GlutaMAX [Gibco], 1% penicillin-streptomycin [Gibco], and 10% foetal calf serum [Gibco] until 80% confluency. The medium was removed and washed with 5 mL of Dulbecco's PBS. The Dulbecco's PBS was then discarded and 1 mL of trypsin ethylenediaminetetraacetic acid (EDTA) was added to the cells. After an incubation of 5 min at 37°C 4 mL of advDMEM/F12 +/+/+ containing 10% FCS was added. 20 µL of suspension were then removed for cell counting. Then 20 µL of trypane blue were added to the 20 µL cell suspension. Cells were counted in a Neubauer counting chamber. The amount of cell suspension necessary for 8 wells containing 20,000 cells per well could then be determined. The necessary amount of cell suspension was then transferred into a 15 mL tube. To facilitate centrifugation 5 mL of Dulbecco's PBS were added to the tube. After 10 min of centrifugation at 478 x g the supernatant was removed and the remaining cell pellet was then re-suspended in advDMEM/F12 +/+/+. The subsequent steps were analogous to the passaging of organoids described above (2.2.2).

2.3 Characterization of organoid cultures derived from breast cancer tissue

2.3.1 *Preservation of breast cancer organoid cultures*

Firstly, the breast cancer culture medium was removed and the wells washed with Dulbecco's PBS. Then 250 µL of dispase II (1 mg/mL, Gibco™ Dispase II, Sigma)) were added to each well of a 48-well plate while scraping the Matrigel domes from the bottom of the well with the pipette tip. During the 15 min of incubation at 37°C a 15 mL tube was lined with 3 mL of Dulbecco's PBS with 1% bovine serum albumin (BSA) (Sigma-Aldridge) to reduce loss of organoids due to their adhesion to plastic surfaces. For all following steps pipette tips and tubes were treated with Dulbecco's PBS/1% BSA before use. The dispase II with the suspended organoids was transferred into the 15 mL tube using 1 mL of Dulbecco's PBS /1% BSA. After rinsing the wells with additional Dulbecco's PBS/1% BSA the suspension is centrifuged at 478 x g in a Multifuge 3 S-R for 10 min. The supernatant was carefully removed. A 1.5 mL tube was rinsed with 1.5 mL of Dulbecco's PBS/1% BSA and left to stand for 1-5 min. After emptying the tube, the cell pellet was re-suspended in 1 mL of 4% paraformaldehyde (Merck) and transferred into the tube. After a 30 min incubation period, 0.5 mL of Dulbecco's PBS/1% BSA was added and the tube was centrifuged at 250 x g in a Biofuge pico for 3 min. After removing the supernatant the cell pellet was re-suspended in 1.5 mL of Dulbecco's PBS/1% BSA. After another centrifugation at 250 x g in a Biofuge pico for 3 min the supernatant was removed and the cell pellet was re-suspended in 250 µL of 25% ethanol. After incubation for 10 min 300 µL of 50% ethanol were added. After letting the tube stand for an additional 10 min 600 µL of 96% ethanol were added. This procedure resulted in organoid cultures that could be stored at 4°C until further processing.

2.3.2 *Embedding of breast cancer organoid cultures in paraffin*

The organoid cultures that have been cryo-conserved according the protocol described above were stored in 70% ethanol. After removing the ethanol, organoids were resuspended in 65°C warm Thermo Scientific™ Richard-Allan

Scientific™ HistoGel™ (Thermo Fisher Scientific) and placed in a heating block at 65°C for 30 sec. The content was then transferred into forms and briefly frozen. Then it was frozen at -20°C for 5 min. The frozen material was scraped off and transferred into a plastic tray (IP ActivFlo Biopsy I Cassette, Leica Biosystems) and closed. It was then soaked twice in 70% ethanol for an hour and, subsequently twice in 96% ethanol for an hour at room temperature. Finally, it was placed for one hour in 100% ethanol and then incubated overnight in 100% ethanol. The cassette was then incubated in xylol (xylol, mix of isomers for analysis, ACS, ISO C, PanReac AppliChem ITW Reagents) twice for an hour. The next step included incubating the cassette three times for 45 min in paraffin (Leica Microsystems Paraplast™ X-tra, Thermo Scientific) at 65°C. Pre-heated metal forms were filled with paraffin and the cushions of Thermo Scientific™ Richard-Allan Scientific™ HistoGel™ were placed in the metal forms and pressed downwards. The plastic forms were then placed upon and filled with paraffin. The forms were then frozen at -20°C for 15 min and then gently warmed to remove from the forms.

2.3.3 *Sectioning of breast cancer organoid cultures*

FFPE-embedded organoid cultures were sectioned (4 µm) with a Microtome (Epredia™ HM 355S). The sections were put onto TOMO adhesion microscopy slides (Matsunami Glass) and dried at room temperature.

2.3.4 *Immunohistochemistry-staining of breast cancer organoid cultures*

Slides with organoid sections were transferred to the pathology department of the University of Tuebingen. Immunohistochemistry was performed on a Ventana Discovery automated immunostaining system (Ventana Medical Systems, Tucson, USA) using routine diagnostic antibodies targeting ER, PR, HER2-receptor and Mib1/Ki67.

2.4 Establishment and optimization of the assay necessary for viral infection of organoid cultures

2.4.1 *Protocol 1 – Infection with oncolytic viruses 24h after passaging*

Organoids were passaged according to the standard method described above. After centrifugation and removal of the supernatant the cell pellet is re-suspended in 260 µL of breast cancer culture medium. Aliquots of 60 µL were taken for plating out in 60% Matrigel according to the standard splitting protocol for further cultivating. For the remaining 200 µL of cell suspension 2,500 µL of breast cancer culture medium and 300 µL of Matrigel were added. This suspension was plated into 12 wells of an untreated 48-well cell culture plate with a 250 µL drop size and an estimated 2.5×10^4 cells per well.

After 24 h the amount of virus calculated for a certain viral concentration was suspended in breast cancer culture medium and 50 µL per well were added. This results in 2 wells per concentration. The plate was then left to keep warm in the incubator at 37°C and 5% CO_2. The infection state and viral distribution was monitored daily and documented photographically. After 96 h the Cell Titer-Blue Cell Viability Assay (Promega GmbH, Germany) was performed.

2.4.2 *Protocol 2 – Infection with oncolytic viruses while passaging*

Organoids were passaged according to the method described above. After centrifugation and removal of the supernatant the cell pellet was re-suspended in 300 µL of breast cancer culture medium. Aliquots of 90µL of this suspension were used for cultivation in 60% Matrigel according to the aforementioned method (passaging of organoids). Aliquots of 10 µL of suspension were used to count in an improved-Neubauer chamber. The remaining 200 µL of suspension was used for plating the cells in 10% Matrigel. Each well consisted of 225 µL of breast cancer culture medium with the cells/organoids, 25 µL of Matrigel and 50 µL of breast cancer culture medium with the virus (in case of the control wells additional breast cancer culture medium was used). A total of 18 wells were necessary for each infection (all calculations were made for 18.5 wells, to ensure sufficient material for all wells). The 200 µL cell suspension was re-suspended in breast cancer culture medium and Matrigel. From this suspension

500 µL were removed and 100 µL of the desired viral suspension added. Aliquots of 300 µL were plated out into one well at a time, resulting in the desired two wells for each viral concentration. This was repeated for all the desired viral concentrations. For the control wells breast cancer culture medium was added. An untreated 48-well culture plate was used. The plate was then placed in an incubator at 37°C with 5% CO_2. The viral distribution was monitored daily through microscopy and photographically documented each day. The Cell Titer-Blue Cell Viability Assay was performed 96h after the viral infection.

2.4.3 *Protocol 3 – Infection of organoid cultures with oncolytic viruses 7-10 days after passaging*

Organoid cultures were passaged according to the method described above and plated out in 6 wells of a treated 48-well culture plate in 60% Matrigel. The organoids were placed in an incubator at 37°C with 5% CO_2 for 7-10 days until the organoid cultures had reached a sufficient size and density for viral infection. Then aliquots of 100 µL of dispase II (1 mg/mL) were added to each well while mechanically scraping the Matrigel dome from the bottom of the well. The cell culture plate was returned to the incubator at 37°C with 5% CO_2 for 60 min. Then the contents of the wells were removed and transferred into a 15 mL tube. The wells were then washed with 1 mL of Dulbecco's PBS. This was also added to the 15 mL tube and centrifuged at 210 x g for 15 minutes. The supernatant was carefully removed with a pipette and discarded. The volume of the cell pellet was determined to enable future concentration calculations. Then 5 µL were pipetted into a 1.5 mL tube and digested with 45 µL of TrypLE Express (TrypLE™ Express Enzyme, no phenol red, Thermo Fisher) for 15 min to allow cell counting with an improved-Neubauer counting chamber. The cell pellet was re-suspended in 5,625 µL (25 x 225 µL) breast cancer culture medium. Aliquots of 625 µL (25 x 25 µL) of Matrigel were added. All calculations were performed for 25 wells to allow for sufficient cell suspension for each well. Subsequently, 520 µL of the suspension were pipetted into a 1.5 mL tube and 100 µL of the desired viral concentration was added. Then 300 µL of this suspension were transferred into a well of an untreated 48-well cell culture plate

thereby resulting in two wells with the same viral concentration and a total of 24 wells. The cell culture plate was then placed in an incubator at 37°C with 5% CO_2. The state of the viral infection was checked daily and documented photographically. The performance of the Cell Titer-Blue Cell Viability Assay was undertaken 96 h after infection of the organoid cultures with oncolytic viruses.

2.4.4 *Protocol 3 – Infection of organoid cultures with oncolytic viruses 7-10 days after passaging with staurosporine control*

Organoid cultures were passaged according to the method described above and plated out in 6 wells of a treated 48-well culture plate in 60% Matrigel. The organoid cultures were placed in an incubator at 37°C with 5% CO_2 for 7-10 days until the organoid cultures had grown and reached a sufficient size and density for viral infection. Then 100 µL of dispase II (1mg/mL) was added to each well while gently scraping of the Matrigel dome from the bottom of the well. The cell culture plate was returned to the incubator for 60 min. Then the contents of the wells were removed and transferred into a 15 mL tube. The wells were then washed with 1 mL of Dulbecco's PBS. The Dulbecco's PBS was also added to the 15 mL tube. To inactivate the dispase II an additional 5 mL of Dulbecco's PBS were added to the 15 mL tube. The 15 mL tube was centrifuged at 210 x g for 15 min. The supernatant was carefully removed with a pipette and transferred to a different 15 mL tube to discard. The volume of the cell pellet was determined to enable future concentration calculations. Then 5 µL were pipetted into a 1.5 mL tube and digested with 45 µL of TrypLE Express (TrypLE™ Express Enzyme, no phenol red, Thermo Fisher) for 15 min to allow cell counting with an improved-Neubauer counting chamber. The remaining cell pellet was re-suspended in 6,075 µL (27 x 225 µL) breast cancer culture medium. Aliquots of 675 µL (27 x 25 µL) of Matrigel were added. All calculations were performed for 27 wells to allow for sufficient cell suspension for each well. Aliquots of 520 µL cell suspension were pipetted into a 1.5 mL tube and 100 µL of the desired viral concentration or staurosporine was added. The final concentration of staurosporine was 1 µM for each of the two wells. For control wells additional breast cancer culture medium was added instead of viral

suspension. Then 300 µL of this suspension were transferred into one well of an untreated 48-well cell culture plate resulting in two wells with the same viral concentration and a total of 26 wells. The cell culture plate was then placed in the incubator with 5% CO_2 and at 37°C. The state of the viral infection was checked daily and documented photographically. The performance of the Cell Titer-Blue Cell Viability Assay was undertaken 96 h after infection of the organoid cultures with oncolytic viruses.

2.5 Viral infection of organoid cultures

2.5.1 *Cell counting*

To quantify the number of cells being cultured and contained in organoid cultures we used an improved-Neubauer cell counting chamber. The 10 µL of organoid suspension obtained from the pre-steps of a viral infection were incubated with TrypLE Express for 15-30 min to ensure all organoids had been digested to single cells. An aliquot of 20 µL of this solution was removed and used for cell counting.

The cover glass was moistened and placed vertically on the counting chamber. An aliquot of 10 µL the above solution was added from the top of the cover slip and the lower end of the cover slip. The four large squares contained in the Neubauer counting chamber were counted from both grids. This was also done for 20 µL of the remaining 30 µL suspension. The average count of all four grids was taken to ascertain the correct number of cells per µL using the following equation. The remaining 10 µL of suspension were discarded.

$$cells\ per\ \mu L\ of\ original\ sample = \frac{number\ of\ cells\ counted}{surface\ area\ counted\ (mm^2) \times depth\ of\ the\ chamber\ (mm) \times dilution\ factor}$$

Equation 1: http://www.zaehlkammer.de/pdf/info_zaehlkammern.pdf

2.5.2 *Viral titration*

In order to ensure reliable results a cell density of approximately 25,000 cells per well was defined. The viruses used included the MeV-GFP, MeV-SCD, GLV-0b347 and GLV-1h94 (Table 6). The vaccinia viruses used in the

experiment are attenuated vaccinia viruses. Sufficient 5-FC was added to the infection with MeV-SCD and GLV-1h94 to achieve a concentration of 1 mmol/L of 5-FC. Additionally, the following controls were measured for each organoid line: 1 mmol/L 5-FC, MeV-SCD/GLV-1h94 without the prodrug 5-FC and 1 mmol/L 5-FU as well as two wells containing breast cancer culture medium only.

Table 6 Viruses used for experiments (MOI = multiplicity of infection)

Virus	Viral titer or stock concentration	Concentration used
MeV-GFP p3	$\frac{2 \times 10^7\ PFU}{ml}$	MOI 1 and MOI 10
MeV-SCD	$\frac{2.4 \times 10^7}{ml}$	MOI 10
GLV-0b347	$\frac{1.6 \times 10^9}{ml}$	MOI 0.1, MOI 1 and MOI 10
GLV-1h94	$\frac{1.1 \times 10^8}{ml}$	MOI 10
5-FC	$\frac{50\ mmol}{l}$	$\frac{1\ mmol}{l}$
5-FU	$\frac{384\ mmol}{l}$	$\frac{1\ mmol}{l}$

All calculations were done for an additional half of a well to ensure sufficient material for the infection of organoids.

2.5.3 *Fluorescence microscopy of infected organoids*

Starting 24 h after the infection, imaging was performed on all organoid cultures every 24 h to depict viral spread in the breast cancer cells. The microscope (Olympus IX50 inverted fluorescence phase-contrast microscope) used, was permanently connected to an F-view camera system (Soft Imaging System GmbH, Muenster Germany). Pictures taken with phase contrast (100 ms exposure time) and fluorescence (150 ms to 5 s exposure time) were processed

using AnalySIS version 3.1 software (Soft Imaging System GmbH, Muenster, Germany).

2.6 Cell Titer-Blue Cell Viability Assay

We used the CellTiter-Blue® Assay (Promega, Walldorf, Germany) to measure the viability of organoids after infection. An aliquot of 60 µL was added per well. The plate was then placed back in the incubator for 90 min and measured using a Synergy HT microplate reader and Gen5.11 software (BioTek Instruments, Winooski, VT).

2.7 Statistical analysis

To determine the percentage of surviving cells with the CellTiter-Blue Viability Assay we divided the read out of organoids treated with virus, 5-FC or 5-FU by the read out of untreated organoids (no virus, 5-FC or 5-FU). As Matrigel alone exhibits a small signal with the assay, this control value was deducted from all original values before calculating the percentage of surviving cells. All data are expressed as mean ± standard deviation of ten independent experiments performed in duplicate. Statistical analyses were performed using GraphPad Prism software (GraphPad Holdings, LLC, San Diego, CA, USA). A one-way analysis of variance (ANOVA) was performed to determine whether there were any significant differences between the groups or between the different MOI of 10, 1 and 0.1. Subsequent post-hoc Tukey's multiple comparisons tests were performed to determine statistical significance between any two groups. A significance level of $p < 0.05$ was used to reject the null hypothesis that there was no difference between the groups tested. We expressed the level of significance with the following annotations in the figures: *$p < 0.05$, **$p < 0.01$, ***$p < 0.001$, and ****$p < 0.0001$.

3 Results

The subsequent data have been published in part in the journal *Frontiers in Molecular Biosciences* in the *Research Topic Oncolytic Virotherapy* [121].

3.1 Establishing 20 patient-derived breast cancer and 10 patient-derived healthy organoid cell cultures

3.1.1 *Characteristics of the patients used for the project*

3.1.1.1 Tumour characteristics

Table 7 Tumour characteristics [121]

Study ID	Age	Diagnosis	Grading	ER		PR		Her2	Her2-IHC-Score	Ki67-Index
BC-ORG 1	37	Invasive ductal carcinoma	G1	Pos.	ER-IRS:12 90% ER-staining	Pos.	PR-IRS:12 90%	Neg.	1+	10%
BC-ORG 2	49	Invasive lobular carcinoma	G2	Pos.	ER-IRS:12 90% ER-staining	Pos.	PR-IRS:4 90%	Neg.	1+	5%
BC-ORG 3	52	Invasive ductal carcinoma	G3	Neg.	ER-IRS:0 0% ER staining	Neg.	PR-IRS:0 2%	Neg.	1+	60%

Study ID	Age	Diagnosis	Grading	ER		PR		Her2		Ki67-Index
BC-ORG 4	42	Mucinous with associated ductal carcinoma in situ	G2	Pos.	ER-IRS:9 80% ER staining	Pos.	PR-IRS:6 40%	Pos.	2+ FISH pos.	15%
BC-ORG 5	59	Invasive lobular carcinoma with associated lobular carcinoma in situ	G2	Pos.	ER-IRS:12 100% ER staining	Pos.	PR-IRS:1 1-9%	Neg.	1+	10%
BC-ORG 6	67	Invasive lobular carcinoma	G2	Pos.	ER-IRS:12 100% ER staining	Pos.	PR-IRS:6 n.d.	Neg.	0	10-15%
BC-ORG 7	56	Invasive ductal carcinoma	G2	Pos.	ER-IRS:12 100% ER staining	Pos.	PR-IRS:12 100%	Neg.	1+	5%

Study ID	Age	Diagnosis	Grading	ER		PR		Her2		Ki67-Index
BC-ORG 8	52	Tubular carcinoma	G1	Pos.	ER-IRS:12 90% ER-staining	Pos.	PR-IRS:6 60%	Neg.	1+	5%
BC-ORG 9	51	Invasive ductal carcinoma	G3	Pos.	ER-IRS:12 100% ER-staining	Pos.	PR-IRS:1 2%	Pos.	3+	10-15%
BC-ORG 10	62	Invasive ductal carcinoma	G2	Pos.	ER-IRS:12 100% ER-staining	Pos.	PR-IRS:12 100%	Neg.	1+	10-15%

3.1.1.2 Control patient characteristics

Table 8 Control patient characteristics

Study ID	Age	Type of operation	Matching tumour tissue
C-ORG 1 (C1)	34	Nipple-sparing mastectomy	-
C-ORG 2 (C3)	50	Reduction mammaplasty	-
C-ORG 3 (C7)	59	Nipple-sparing mastectomy	-
C-ORG 4 (C25)	49	Nipple-sparing mastectomy	BC-ORG 2
C-ORG 5 (C26)	30	Reduction mammaplasty	-
C-ORG 6 (C27)	62	Breast-conserving surgery	BC-ORG 9

3.1.2 *Establishing organoid cultures from patient tissue samples*

At the Department of Women's Health of the University Hospital Tübingen breast cancer tissue undergoing pathological analysis was screened and when possible obtained for cultivation. The pieces of tissue received typically looked like the tissue samples shown in (Figure 3-1).

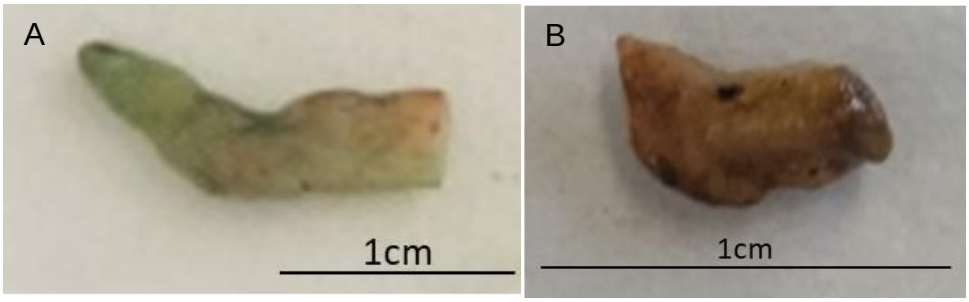

Figure 3-1 Tissue samples of tumour BC-ORG 3 (A) and tumour BC-ORG 6 (B)

Breast cancer tissue was obtained from breast-conserving surgeries and mastectomies from a total of 10 breast cancer patients. In two patients, the tissue obtained from the surgery also included healthy tissue which was cultivated separately as seen in Figure 3-2.

The tissue samples exhibited a green or blue colour in addition to normal yellow to red colour due to staining in the pathology department depending on the positioning of the tissue sample within the tumour. Although the tissue samples only differed slightly in their physical appearance, larger differences in their texture were observed. Breast cancer tissue was found to be denser/harder and more difficult to cut than control tissue. The control tissue was softer and included more adipose tissue. Whenever possible, the adipose tissue was mechanically removed from the control tissue to facilitate enzymatic digestion.

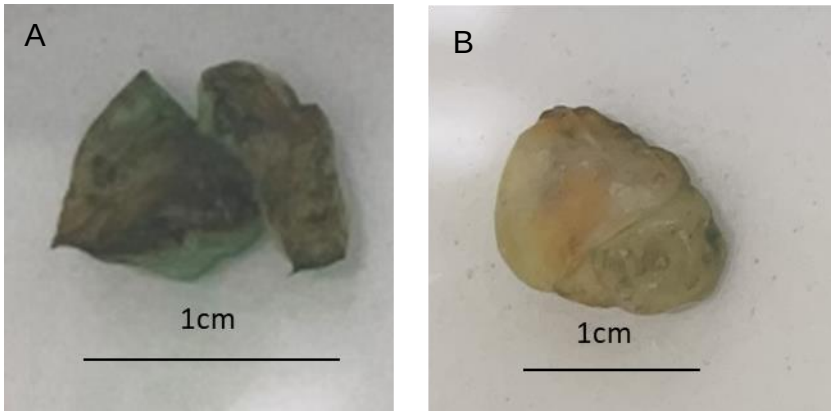

Figure 3-2 Tissue samples of tumour 161 (A) and control 25 (B)

In addition to the two patient-matched control tissue samples, another four control tissue samples were obtained from patients undergoing breast surgery with no malignant indication for surgery. To obtain single breast cancer cells, a combination of mechanical and enzymatic techniques (collagenase IV) was used. The time for enzymatic digestion varied from between 30 min to 4 h. This was independent of whether control tissue or breast cancer tissue was used, but was dependent on the size of the tissue sample.

After enzymatic digestion and filtration, the cell suspension was plated in Matrigel domes. Initially, single cells could be identified (A→ in Figure 3-3) which then grew into organoids (B→ in Figure 3-3). Even after one day, small organoids could be identified, which increased in size during the following days (□ in Figure 3-3). Organoids derived from breast tissue exhibited a round shape and appeared to have a smooth edge (Figure 3-4).

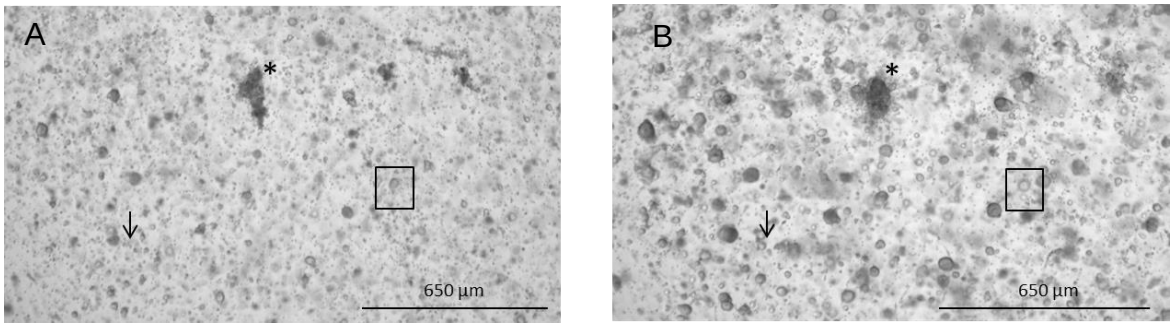

Figure 3-3 Breast cancer organoid line (BC-ORG) 3: Original tumour digest 1 day after digestion (A) and original tumour digest 4 days after digestion (B)

Figure 3-4 BC-ORG 3

The passaging time varied depending on the initial cell density seeded in the Matrigel. BC-ORG 2 displayed a high density seen as many single cells which subsequently grew into organoids (Figure 3-5). Between clusters of organoids some areas were not as densely populated with organoids (* in Figure 3-5 B).

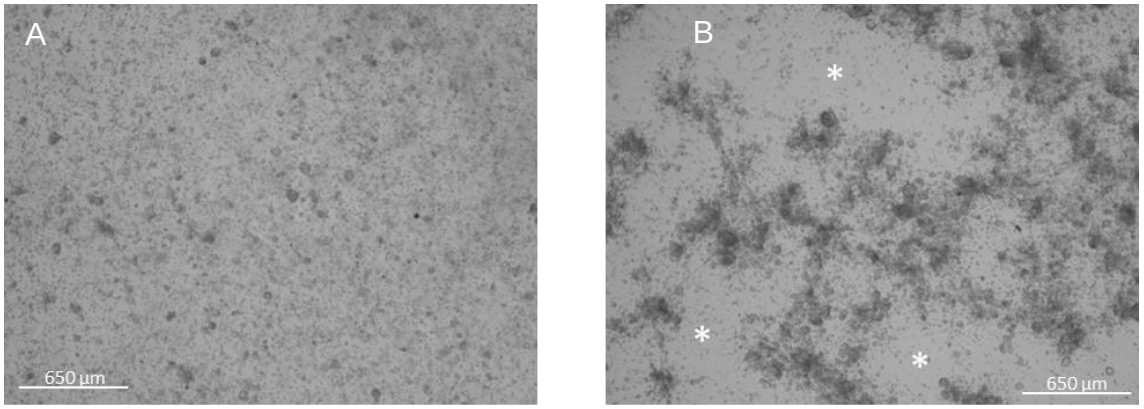

Figure 3-5 BC-ORG 2: Original tumour digest 1 d after digestion (A) and 4 d after digestion (B)

C-ORG 4 was derived from the same patient as BC-ORG 2. As seen in Figure 3-2, the tissue sample of C-ORG 4 was larger than the tissue sample of BC-ORG 2. However, the sample size did not always correlate with the density of single cells (cell density of C-ORG 4 seen in Figure 3-6).

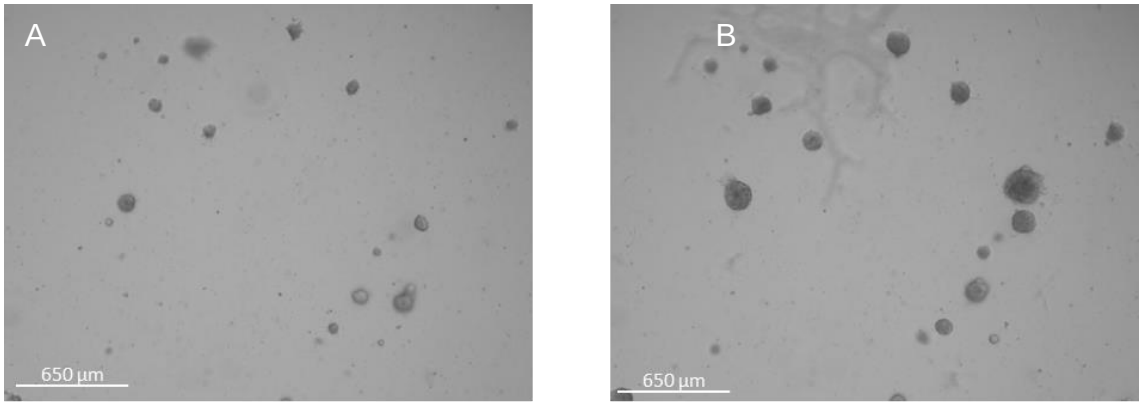

Figure 3-6 C-ORG 4: Original tissue digest 1 d after digestion (A) and 4 d after digestion (B)

Organoid cultures were grown for between 5 and 20 days and passaged according to the protocol described in Section 2.2.2. The passaging resulted in the breakdown of the organoids into single cells, thereby allowing the single cells to grow into organoids.

To achieve a consistent organoid density, cells were frozen at the time of passaging. For example, the growth of BC-ORG 3 is depicted in Figure 3-7. The cell density was similar on day 1 of each passage. Some organoids were not completely dissociated into single cells while passaging and could be recognized as organoids as early as day 1 (* in Figure 3-7). However, many single cells could be seen that appeared to grow into organoids (→ in Figure 3-7). Organoids were mainly observed as being circular and dark coloured (→ in Figure 3-8). In some cases organoids were paler and appeared as a cystic structure (* in Figure 3-8, Figure 3-9, Figure 3-10). This pale, cystic architecture was not limited to control tissue organoids, but could also be seen in organoid lines derived from breast cancer tissue (* in Figure 3-8).

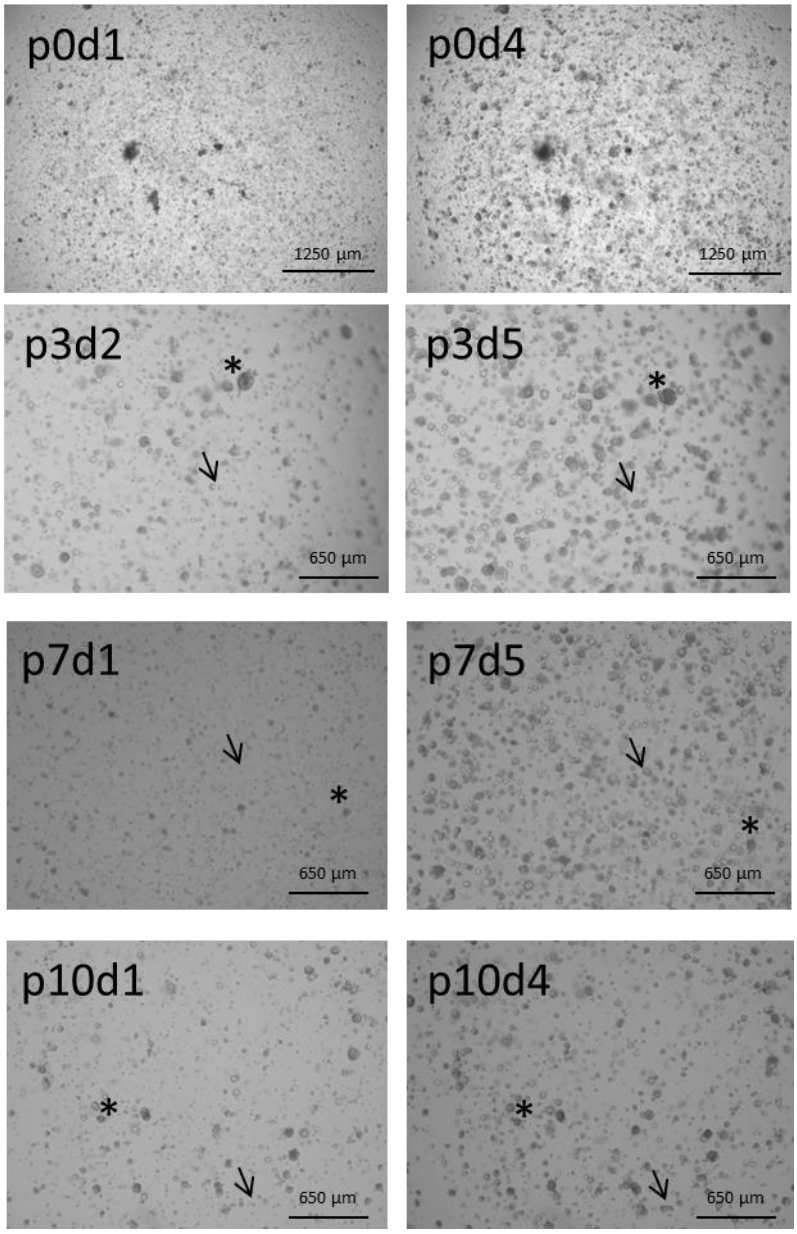

Figure 3-7 BC-ORG 3 growth overview: Pictures were taken at different passages (p) and on different days (d)

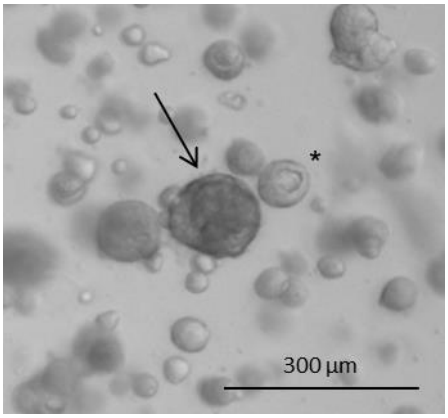

Figure 3-8 BC-ORG 3 p3 [121]

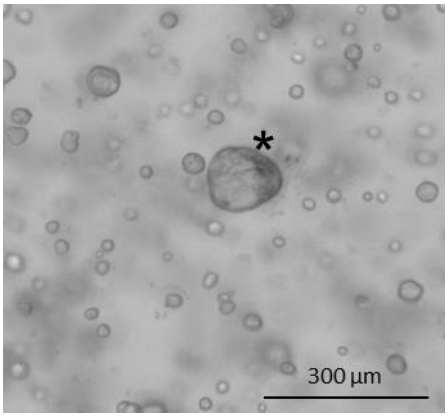

Figure 3-9 C-ORG 3 p2 [121]

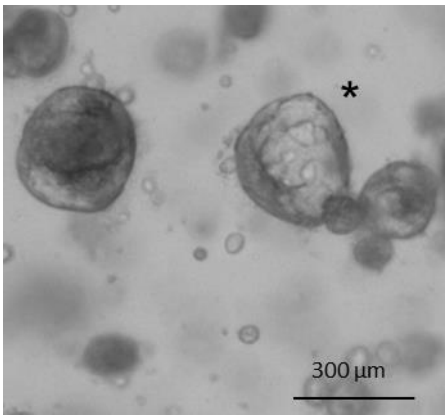

Figure 3-10 C-ORG 4 p7

The growth pattern of breast cancer-derived organoid lines and control tissue-derived organoid lines was found to be similar. As demonstrated in Figure 3-11 and Figure 3-12, the initial organoid samples differed in cell density. There were fewer single cells in p0 of C-ORG 4. In contrast, there were more single cells in p0 of BC-ORG 2. After 4 days, as an exception the growth pattern initially appeared to differ between these two lines. In line C-ORG 4 organoid-like

structures existed on day 1 that grew to form organoids (* in Figure 3-11). In BC-ORG 2, a greater number of single cells could be found on day 1, which grew into clusters and formed organoids (▭ in Figure 3-12). However, as of passage 2 or 3 and as seen in passage 7, the growth pattern was very similar for both organoid lines. The single cells visible on day 1 grew into organoids during the subsequent days of comparable size and density. Therefore, it is concluded that control and breast cancer organoid cultures demonstrated similar growth patterns.

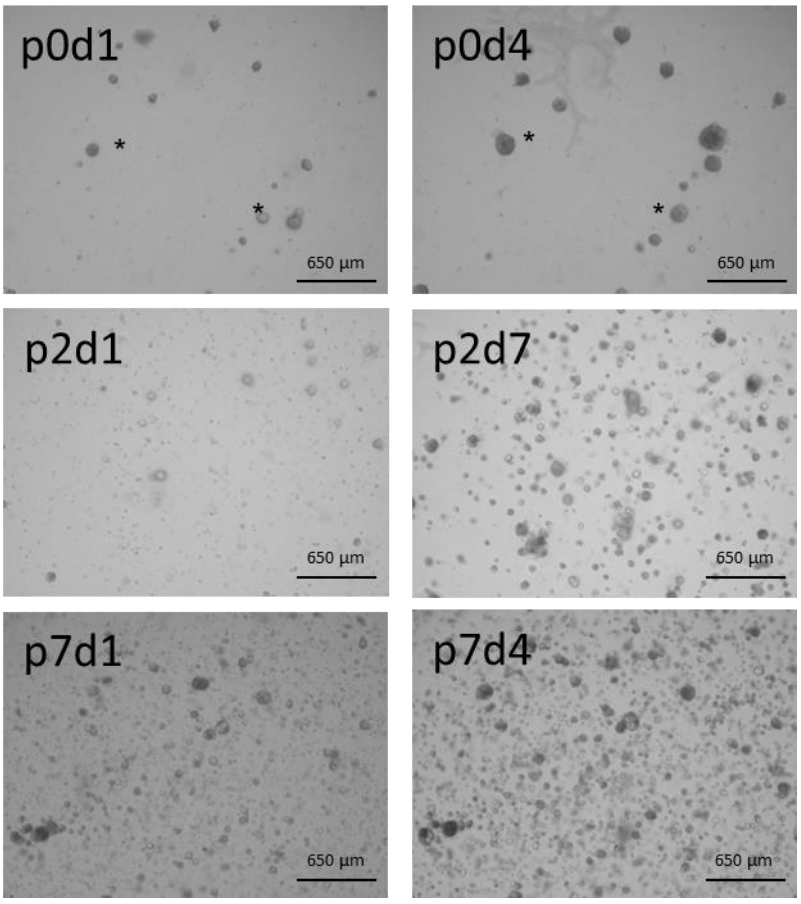

Figure 3-11 C-ORG 4 derived from control tissue; growth overview: Pictures were taken in different passages (p) and on different days (d)

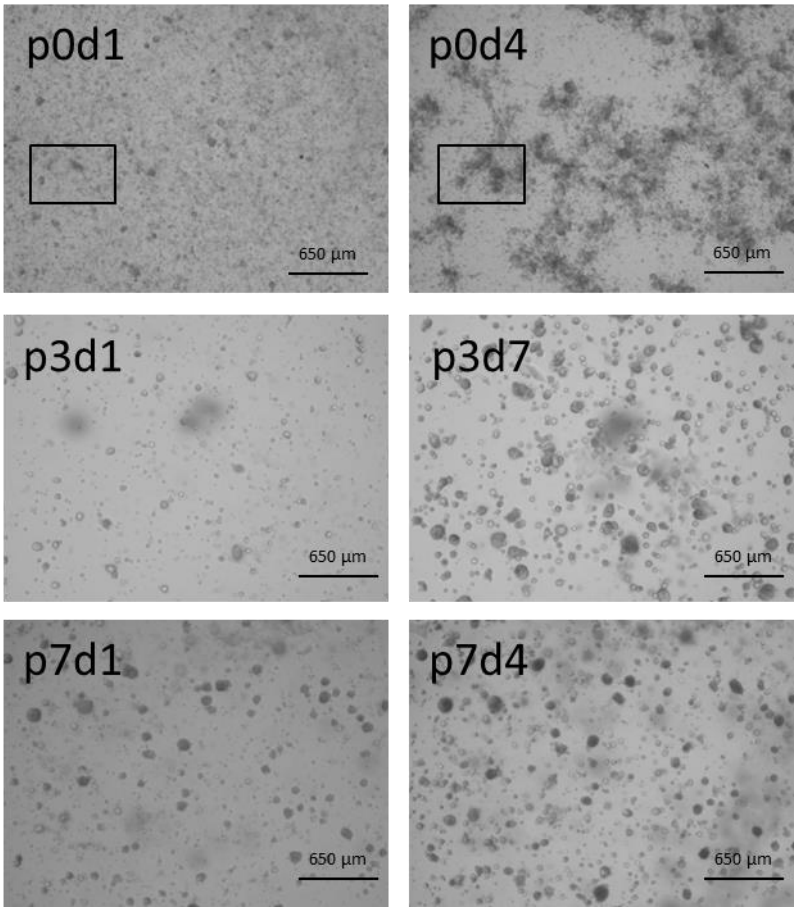

Figure 3-12 BC-ORG 2 growth overview: Pictures were taken in different passages (p) and on different days (d) [121]

The tumour grading varied in different breast cancer tissue samples. This had an influence on the growth of organoids as seen in Figure 3-13. The initial culture sample of G1 (BC-ORG 1) and G2 (BC-ORG 2) breast cancer samples appeared similar and showed growth in clusters. G3 (BC-ORG 3) breast cancer samples displayed a more evenly distributed growth of organoids to begin with. Over the course of different passages G1 organoid lines seemed to display smaller organoids.

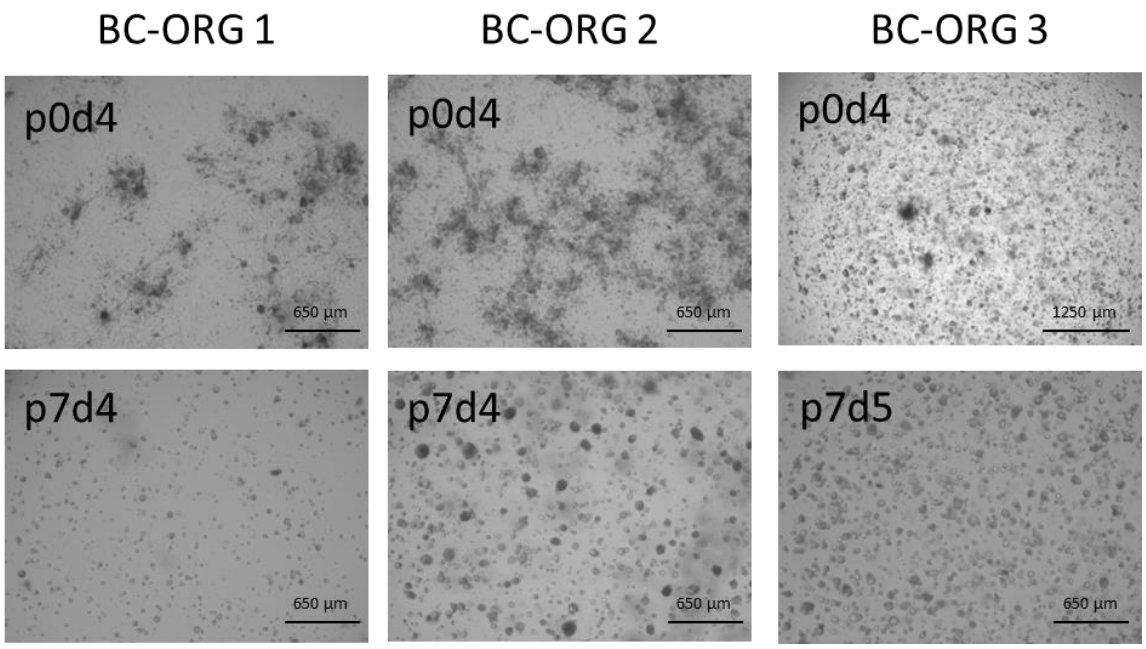

Figure 3-13 Comparison of growth rates between organoid lines of different grading types. BC-ORG 1 was graded as G1, BC-ORG 2 as G2 and BC-ORG 3 as G3.

A wide variety of tumour grades ranging from G1 to G3, and different expression rates of ER, PR and Her2 were covered whilst establishing the breast cancer organoids. Therefore, the established organoid cultures could be used as a resource for later testing of oncolytic virotherapy as they represented the heterogeneity of the underlying disease. Histological classification of organoids was necessary to ensure applicability of future test results.

3.1.3 *Histological comparison of the breast cancer organoid cultures*

All 10 organoid cultures derived from breast cancer and the 6 organoid cultures derived from healthy tissue underwent histological staining for ER, PR and Ki67. Some lines were also stained for Her2.

The staining of organoid lines (breast cancer and control organoid lines) was negative for ER, PR and Her2. The organoid lines were positive for Ki67 with a variable expression rate. BC-ORG 3 and C-ORG 2 are shown as examples for the histological staining (Figure 3-14, Figure 3-15).

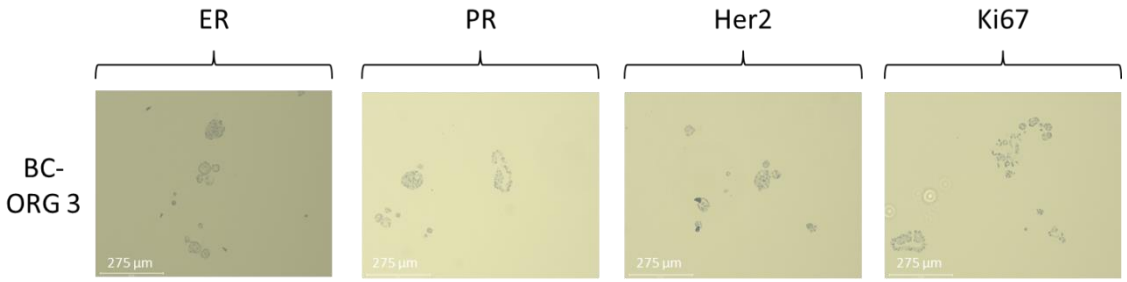

Figure 3-14 Staining of BC-ORG 3 for ER, PR, Her2 and Ki67

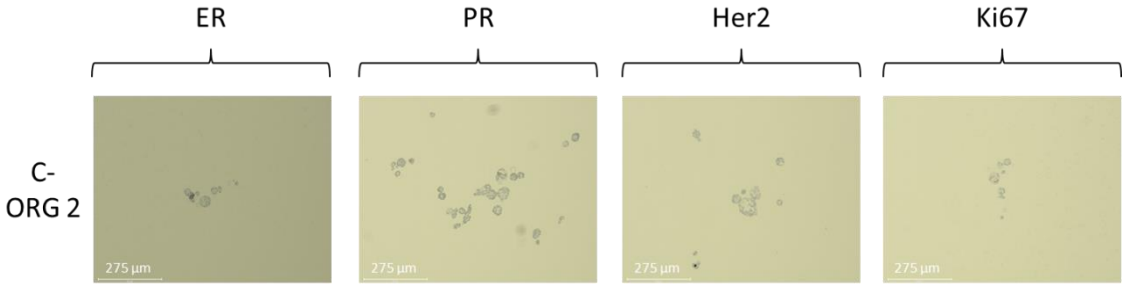

Figure 3-15 Staining of C-ORG 2 for ER, PR, Her2 and Ki67

BC-ORG 2 and matched control organoid line C-ORG 4 were derived from the same patient. The ER, PR and Her2 staining of both lines was, as previously mentioned, negative (Figure 3-16). However, the staining for Ki67 was positive. The breast cancer organoid lines BC-ORG 2 displayed a higher Ki67 proliferation index than the control organoid lines C-ORG 4 (Figure 3-16).

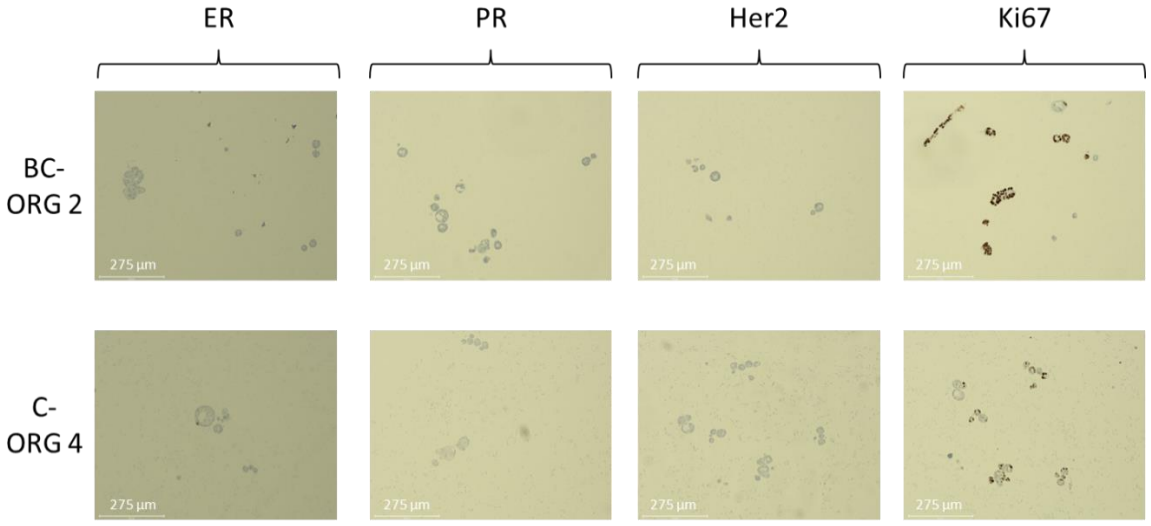

Figure 3-16 Staining of organoid lines BC-ORG 2 and C-ORG 4 for ER, PR, Her2 and Ki67

3.2 Viral infection of organoid cultures derived from breast cancer tissue and healthy breast tissue

3.2.1 *Development of the method for viral infection of breast tissue organoid cultures*

In Protocol 1 we first tested the infection of breast cancer tissue organoids based on established methods for testing oncolytic virotherapy in two-dimensional cell culture models. Here the organoids were plated out in 10% Matrigel after regular passaging and infected 24 h later with GLV-0b347 (Figure 3-17) and MeV-GFP (data not shown). The distribution of the resulting fluorescence was used as an indicator for the distribution of viral spread throughout the organoids. Following infections with oncolytic vaccinia virus GLV-0b347, red fluorescent organoids could be seen first at 48 hours post infection (hpi) (Figure 3-17, Protocol 1, upper panels) and even more fluorescent organoids could be observed at 72 hpi and 96 hpi (Figure 3-17, Protocol 1, middle and lower panels). However, even at 96 hpi some organoid clusters still were not found to be infected (Figure 3-17, Protocol 1, lower panels). Beyond that infections did not appear to be distributed homogeneously throughout the wells.

The first protocol showed an important result that oncolytic virotherapy in an organoid model is indeed possible.

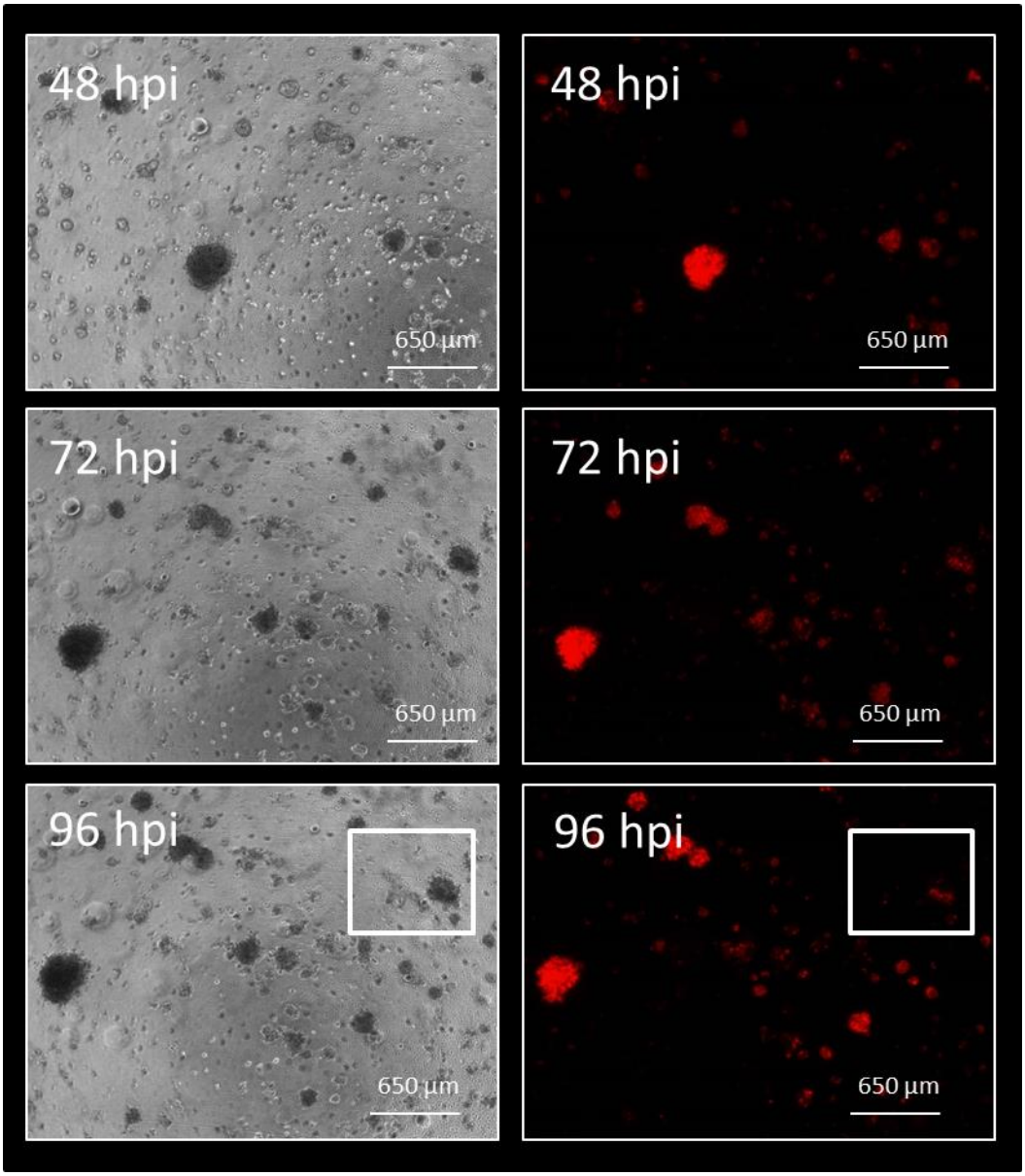

Figure 3-17 BC-ORG 3 GLV-0b347 MOI 10 protocol 1 [121]

The next goal was to improve the protocol to enable evenly distributed viral infection of the organoid model. Therefore, in protocol 2 the timing of the infection was changed as this was thought to be the reason for uneven viral infection. Instead of infecting the organoids 24 h after passaging, the viruses were directly added to the organoid culture suspension containing Matrigel and breast cancer culture medium.

The viral infection is shown representatively for GLV-0b347 MOI 10. After 24 h, more organoids were infected as demonstrated by the red fluorescence (white

arrows in Figure 3-18) in comparison to protocol 1. The viral distribution was seen to be more even over the course of 96 h. However, a different problem arose with this protocol. The cells which were plated out did not form the large number of organoids seen in protocol 1. Figure 3-17 shows multiple organoids of various sizes. However, Figure 3-18 shows no larger organoids (marked in white box) and only few organoids were found in the well (highlighted by * in Figure 3-18). Generally, more organoids were infected during the infection with the second protocol in comparison to the first protocol as indicated by the increased detection of fluorescence.

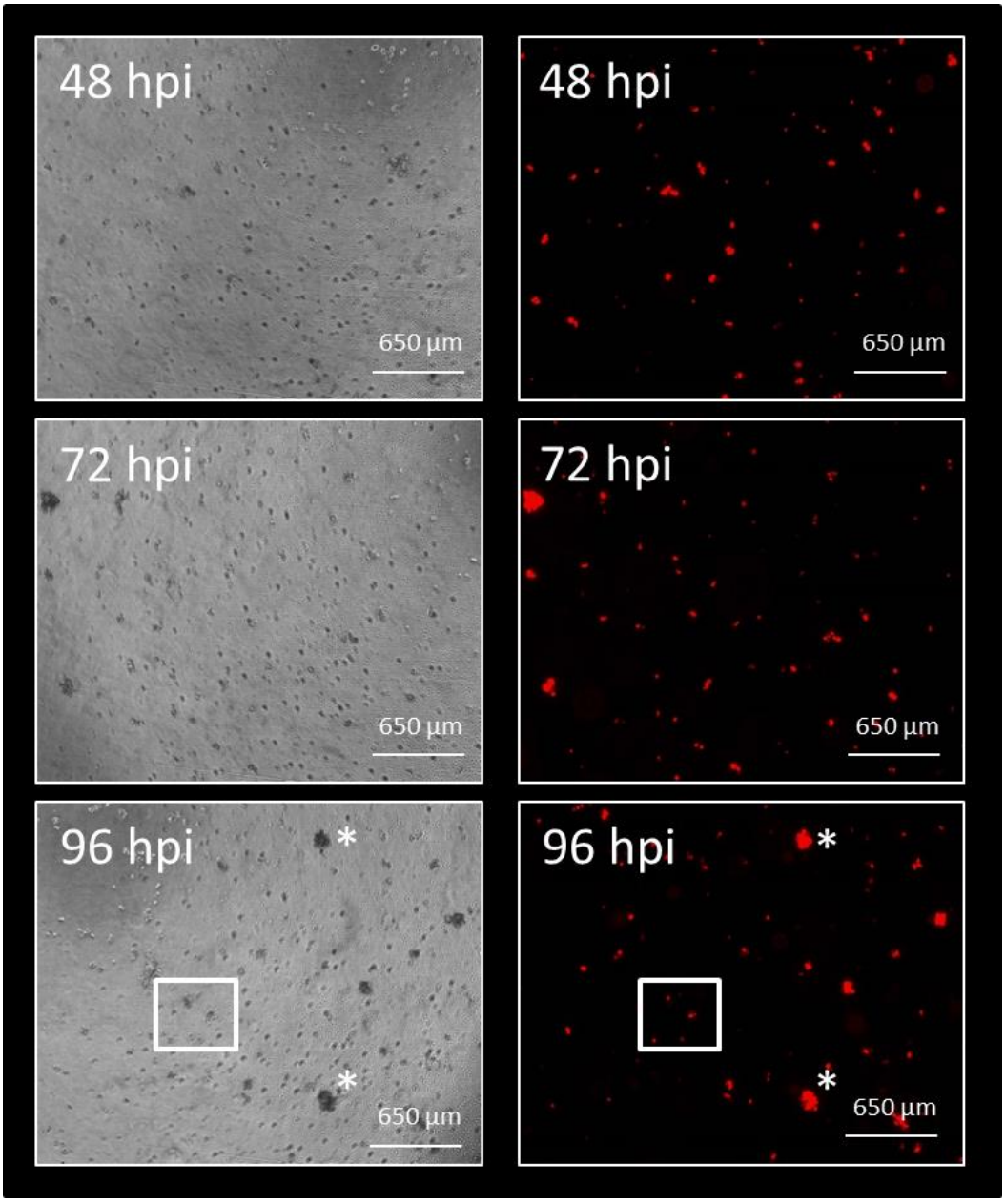

Figure 3-18 Infection of breast cancer organoid line BC-ORG 5 with GLV-0b347 MOI 10 according to protocol 2 [121]

Protocol 3 aimed to allow growth of organoids and even distribution of oncolytic viruses throughout the organoids (aiming to achieve cell density of 25.000 cells per well). Organoids were harvested using 100 µL of 1 mg/mL dispase II rather than TrypLE after being cultivated in normal growth environment without addition of oncolytic viruses. The oncolytic viruses were then added to the cell suspension and seeded into Matrigel. After 48 h, a greater number of large organoids (* in Figure 3-19) could be seen during the infection with protocol 3 in

comparison to protocol 2 (Figure 3-18). This trend could also be seen and was clearer at 96 hpi (white boxes in Figure 3-18 and Figure 3-19). 96 hpi also showed a larger amount of red fluorescence as seen in Figure 3-19. The following results in chapter 3 were all based on experiments with protocol 3.

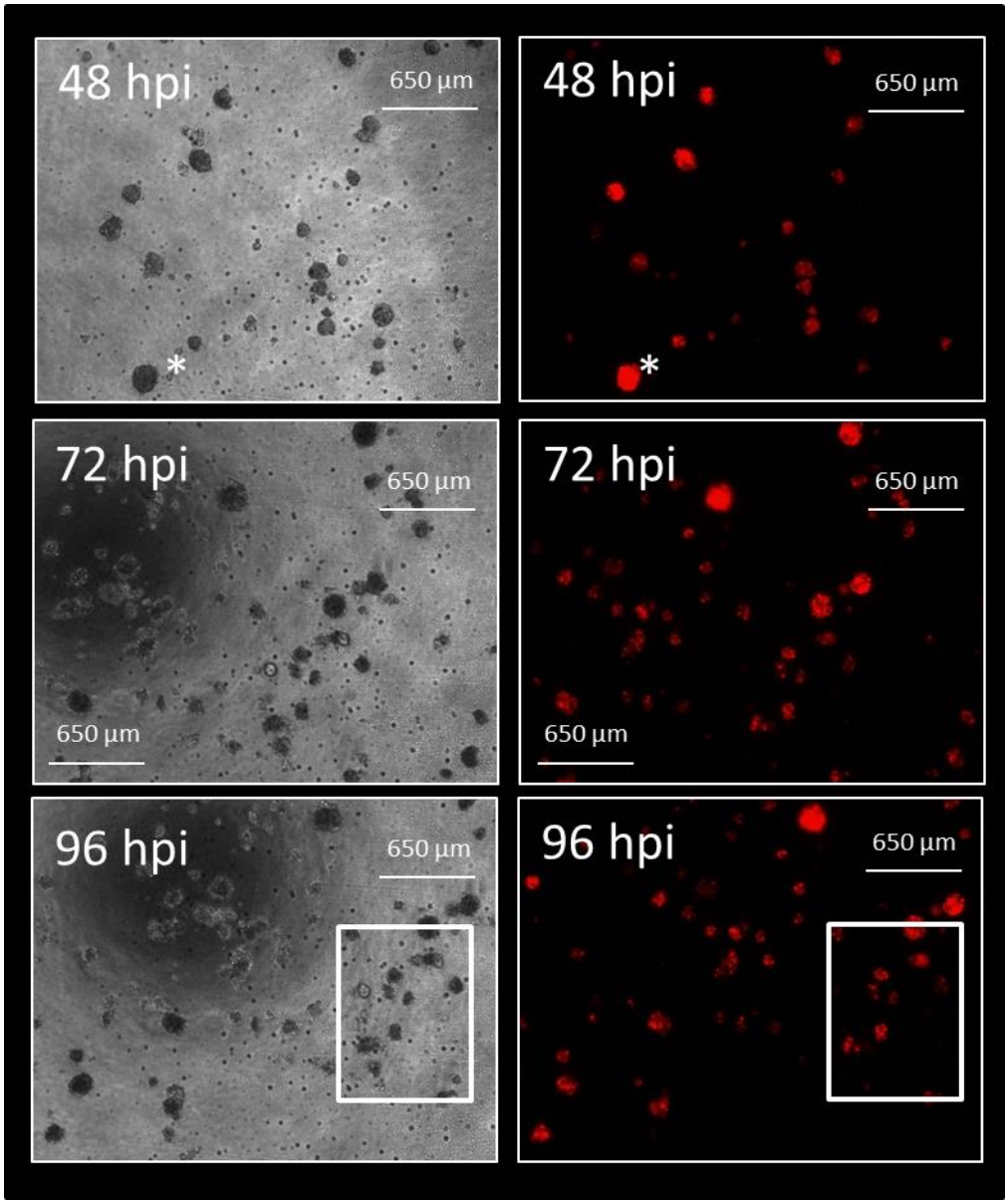

Figure 3-19 Infection of breast cancer organoid line BC-ORG 5 with GLV 0b347 MOI 10 according to protocol 3 [121]

Matrigel interferes with the baseline viability measurements. Therefore, for each experiment a Matrigel control was measured.

Oncolytic viruses have the potential to lyse all cells they come in contact with. Therefore, to test the organoid model and experimental setup, staurosporine, an agent that induced apoptosis, was added to some wells instead of oncolytic viruses. The aim was to determine the lowest possible viability with the Cell Titer-Blue Cell Viability Assay to measure the viability of the organoids. As seen in Table 9 the viability measurement varied mainly between 0 and 20%. The organoid lines with higher viability measurements were organoid lines with either very large organoids or very small organoids (Figure 3-20) and partially subject to measurement errors.

Table 9 Viability measurement for staurosporine treated organoids after 96 h incubation

Organoid line	Viability measurement in %
BC-ORG 1	34%
BC-ORG 2	53%
BC-ORG 3	17%
BC-ORG 4	9%
C-ORG 1	0%
C-ORG 2	11%
C-ORG 5	17%
T47D	measurement error
MCF7	measurement error
MDA-MB-468	0%

In Figure 3-20 the treatment of breast cancer organoids with staurosporine can be seen. In the first 48h of incubation with staurosporine the organoids remained intact with a smooth surface. After 48h the organoid contained small cells creating the impression of rough-edged organoids. This development can be seen in Figure 3-20 for different organoid lines. For each line one organoid

has been highlighted (→ or *) to trace this evolution. In Figure 3-21 the growth pattern of untreated organoids (MOCK) and staurosporine-treated organoids can be seen. The MOCK organoids displayed a smooth growth pattern as seen previously. The treatment of staurosporine resulted in rough-edged organoids. However, this transformation in breast cancer organoid line BC-ORG 4 could be already seen at 24 h after the incubation began. This resulted in a lower viability (9%) in comparison to the two organoid lines in Figure 3-20 (breast cancer organoid line BC-ORG 1 with 34% viability; breast cancer organoid line BC-ORG 2 with 53%). The staurosporine control therefore allowed the evaluation of the lowest cell viability measurement possible for treated organoid lines.

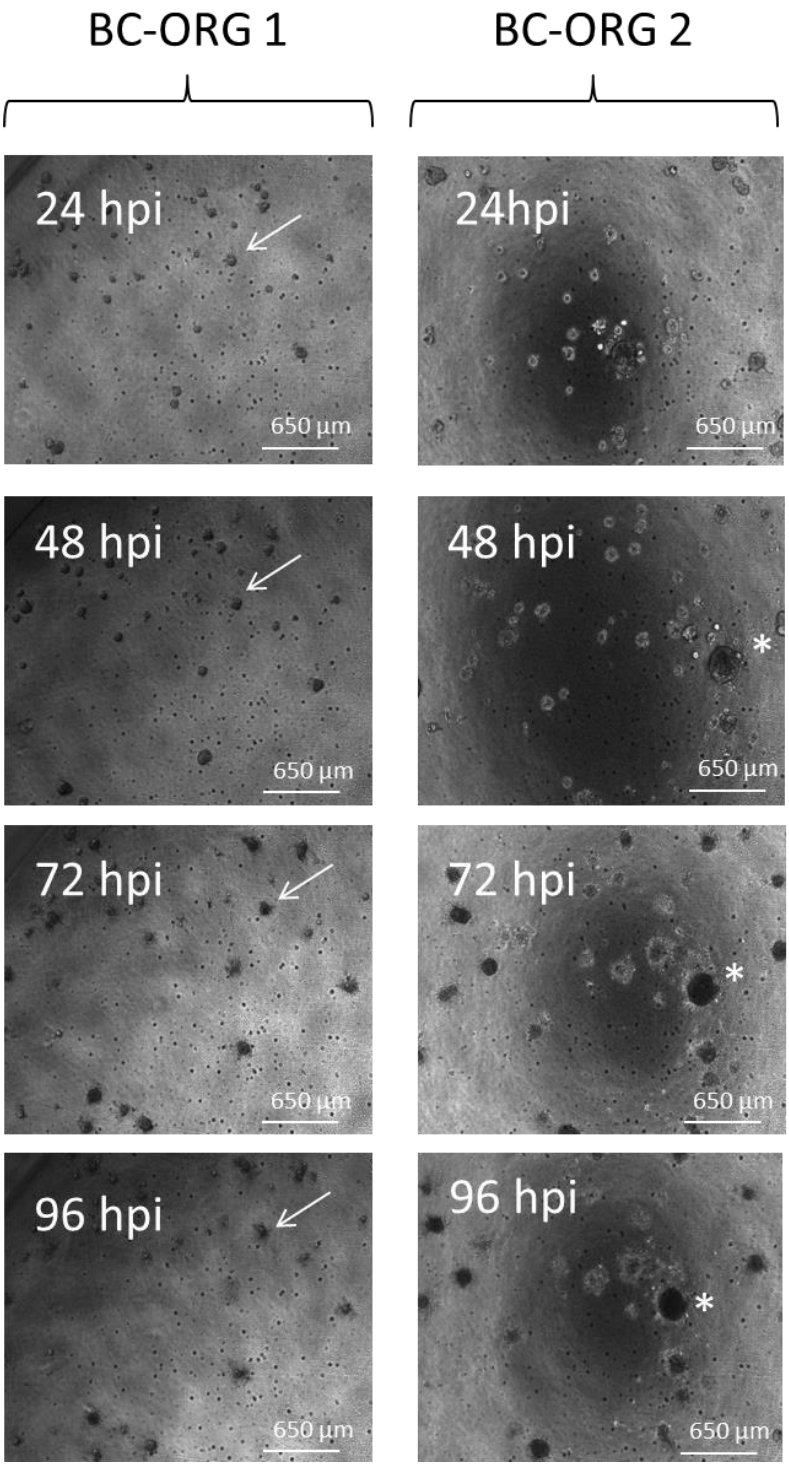

Figure 3-20 Staurosporine-treated breast cancer organoid lines BC-ORG 1 and BC-ORG 2

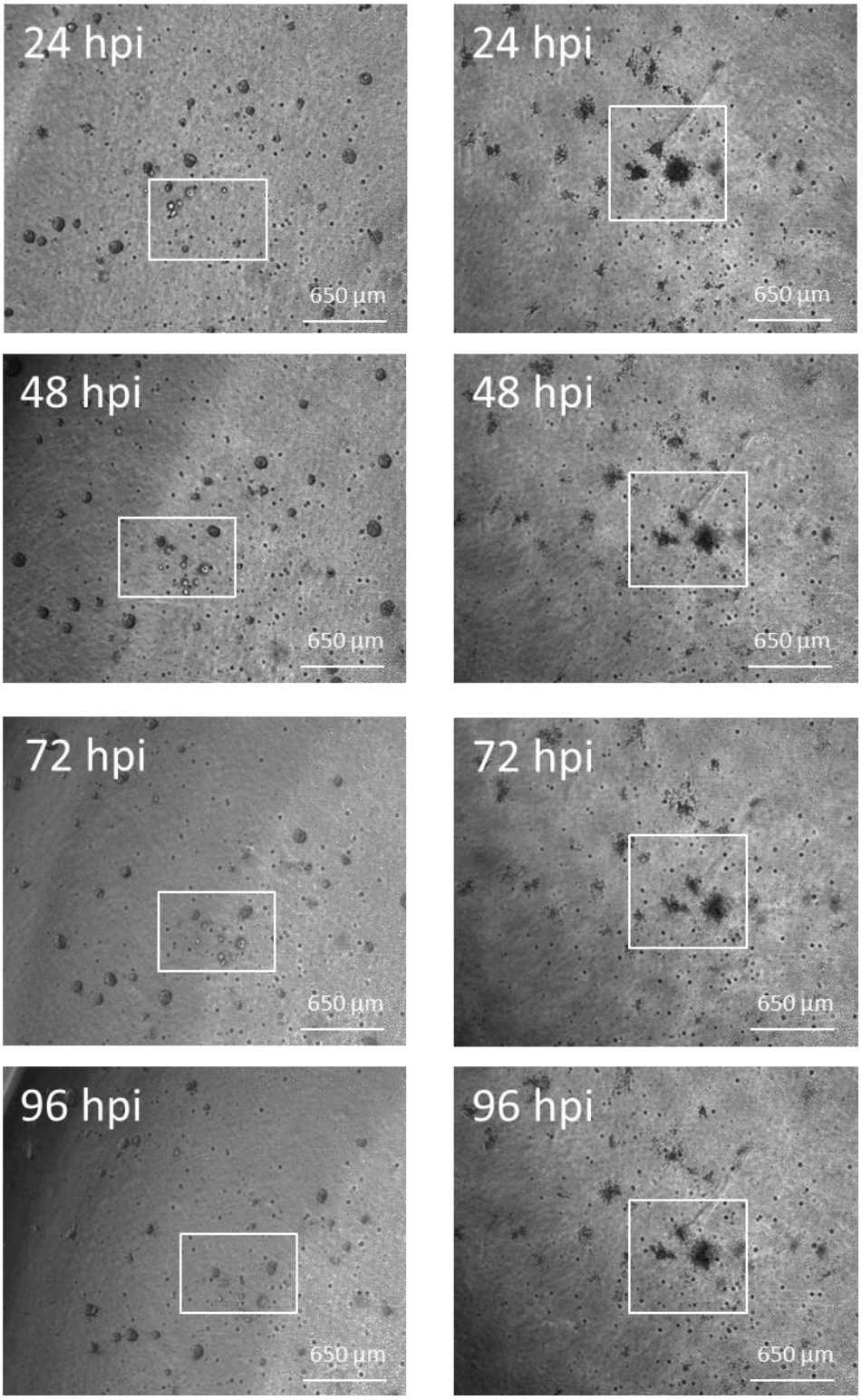

Figure 3-21 MOCK (left) and staurosporine (right) treated breast cancer organoid line BC-ORG 4

Additionally, to facilitate the interpretation and comparability of the subsequent viability measurements the numbers of cells were counted for each line. This was done as part of the infection process to quantify the number of cells contained in each well (Table 10). All concentration calculations for the subsequent virotherapy were done with 25,000 cells per well.

Table 10 Number of cells per well for used for oncolytic virotherapy

Organoid line	Number of cells per well (approximately)
BC-ORG 1	23,000
BC-ORG 2	30,000
BC-ORG 3	37,000
BC-ORG 4	21,000
C-ORG 1	1,300
C-ORG 2	25,000
C-ORG 4	30,000
T47D	41,000
MCF7	25,000
MDA MB 468	10,000

3.2.2 *Treatment of organoid cultures with oncolytic measles viruses*

3.2.2.1 Response of breast cancer organoid cultures

We derived ten organoid lines from different breast cancer tumours. Figure 3-22 shows the effect of oncolytic viruses on the viability of organoid lines (n=10). Viability was measured 96 h after the addition of (= infection with) oncolytic viruses.

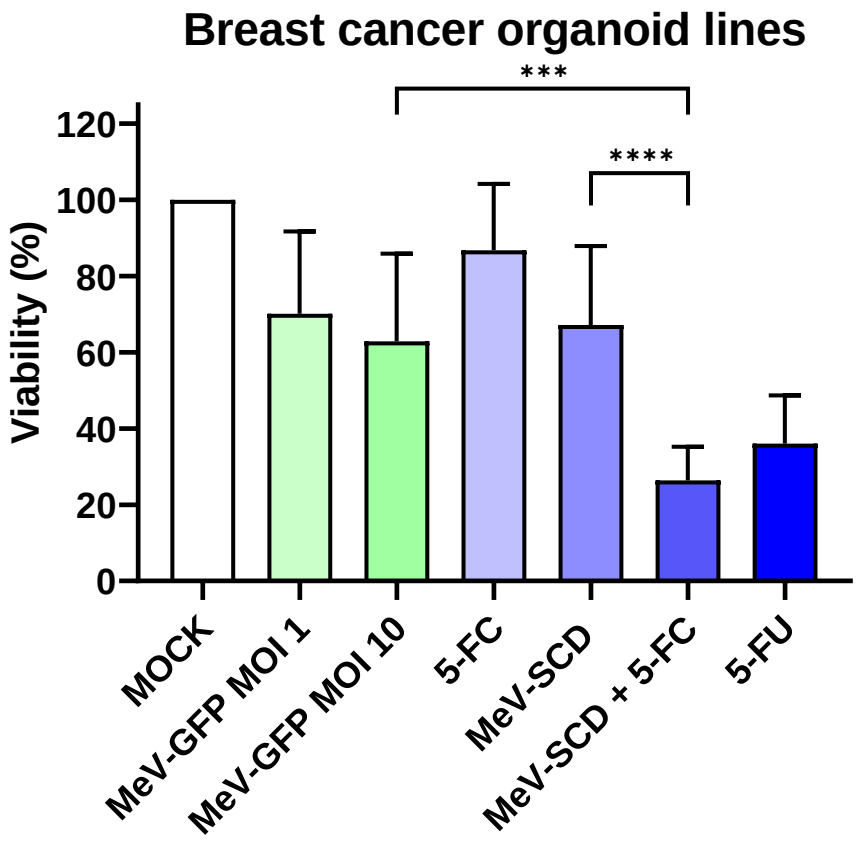

Figure 3-22 The effects of oncolytic measles viruses on organoids derived from breast cancer tissue [121]
***p < 0.001, ****p < 0.0001 with post-hoc Tukey's multiple comparisons tests, n=10.

In Figure 3-22 we compared the effects of a measles virus expressing GFP (MeV-GFP) and a measles virus expressing a suicide gene (MeV-SCD) in organoid cultures (Figure 3-22). When we compared the mean effects for all ten breast cancer organoid lines measured with the CellTiter-Blue Viability Assay, a one-way ANOVA was statistically significant ($p < 0.0001$; $F(5, 53) = 15.18$). Post-hoc analysis revealed no significant difference between two different titres of MeV-GFP (MOI 1 and MOI 10) (Figure 3-22). Moreover, MeV-SCD without the prodrug 5-FC showed no significant difference from the same titre MeV-GFP (MOI 10) (Figure 3-22). The combination of MeV-SCD and the prodrug 5-FC resulted in a significantly greater inhibition of viability ($p < 0.0001$) compared to MeV-SCD without 5-FC (Figure 3-22). Furthermore, there was no significant difference between the MeV-SCD with the prodrug 5-FC in comparison to its

active metabolite 5-FU (Figure 3-22). We observed a significant reduction of cell viability when breast cancer organoids were infected with MeV-SCD compared to the corresponding measles virus lacking the suicide gene (MeV-GFP), provided that the prodrug 5-FC was present ($p < 0.001$) (Figure 3-22).

Organoid lines BC-ORG 1, 2, 3 and 4 were selected for in-depth analysis of oncolytic infection of breast cancer organoids. These organoid lines were chosen because they reflected the heterogeneous entities of breast cancer. The four organoid lines include different gradings, hormone receptor status and HER2 status of the original tissue sample in order to ensure a representative sample.

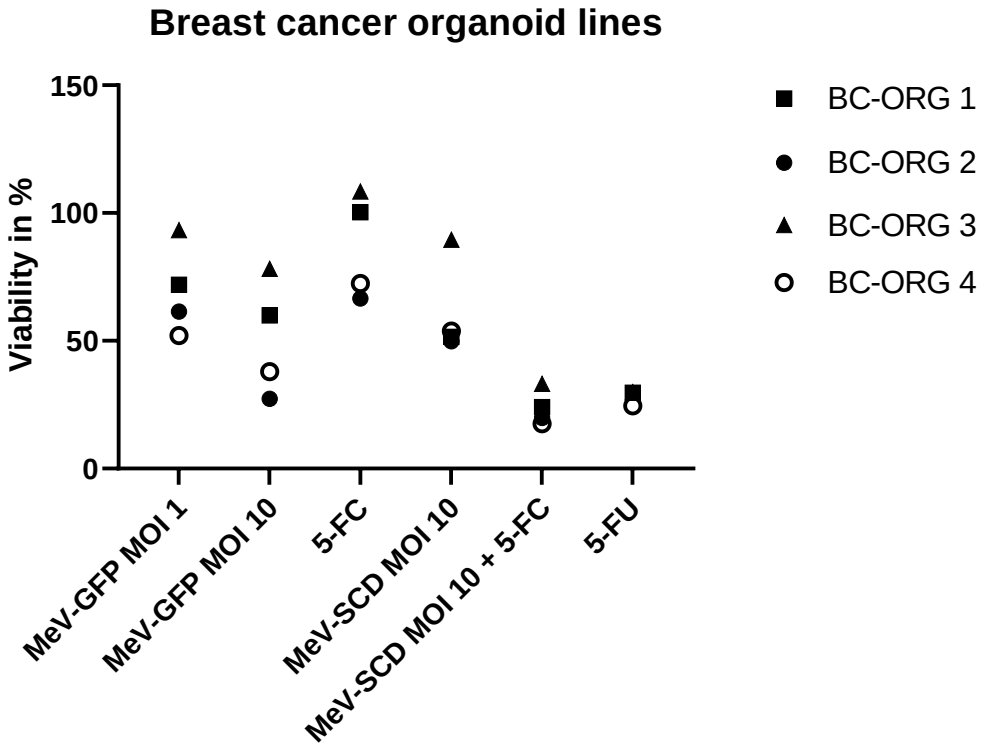

Figure 3-23 The effects of oncolytic measles viruses on breast cancer organoid lines BC-ORG 1, 2, 3 and 4

Figure 3-23 shows the viability measurements seen in Table 11. The increase of the viral titre when adding MeV-GFP from MOI 1 to MOI 10 results in a reduction of cell viability of about 20%. The addition of 5-FC and no oncolytic viruses to the organoid lines has the least impact of the treatments used in

Figure 3-23. MeV-SCD MOI 10 treatment resulted in a loss of viability in comparison to the prodrug 5-FC. The addition of the prodrug 5-FC to the infection with MeV-SCD MOI 10 led to a further reduction of organoid viability. The treatment of organoids with 5-FU resulted in a similar viability to the co-treatment of organoids with MeV-SCD MOI 10 and 5-FC. Staurosporine treatment of organoids led to a similar or lower viability than the treatment with MeV-SCD MOI 10 and 5-FC or 5-FU (Table 11).

Table 11 Viability measurements for organoid lines BC-ORG 1, 2, 3 and 4

Organoid line	MeV-GFP MOI 1	MeV-GFP MOI 10	5-FC	MeV-SCD MOI 10	MeV-SCD MOI 10 + 5-FC	5-FU	Stauro-sporine
BC-ORG 1	72%	60%	100%	52%	24%	30%	34%
BC-ORG 2	61%	27%	67%	50%	20%		53%
BC-ORG 3	93%	78%	108%	90%	33%	30%	17%
BC-ORG 4	52%	38%	72%	54%	18%	25%	9%

The organoid line BC-ORG 4 is used representatively for the organoid lines used for experiments to portray the results. It was derived from oestrogen positive, progesterone positive and HER2 positive breast cancer. The spread of oncolytic viruses can be seen by the expression of GFP (Figure 3-24).

The detection of green fluorescence in MeV-GFP MOI 1 and MeV-GFP MOI 10 infected breast cancer derived organoid lines increased over 96 hpi (* in Figure 3-24). Initially at 24 hpi no green fluorescence could be detected. Organoids infected with MeV-GFP MOI 1 did not seem to spread the viral infection to neighbouring organoids. However, organoids infected with MeV-GFP MOI 10 developed multiple sites of oncolytic viral infection represented by the green fluorescence. The viral infection spread to neighbouring organoids, thereby resulting in different clusters of viral infection. These findings correlated with the viability measurements done at 96 hpi. The viability measured for MeV-GFP

MOI 10 (38%) was lower than the viability measured for MeV-GFP MOI 1 (52%) (Table 11).

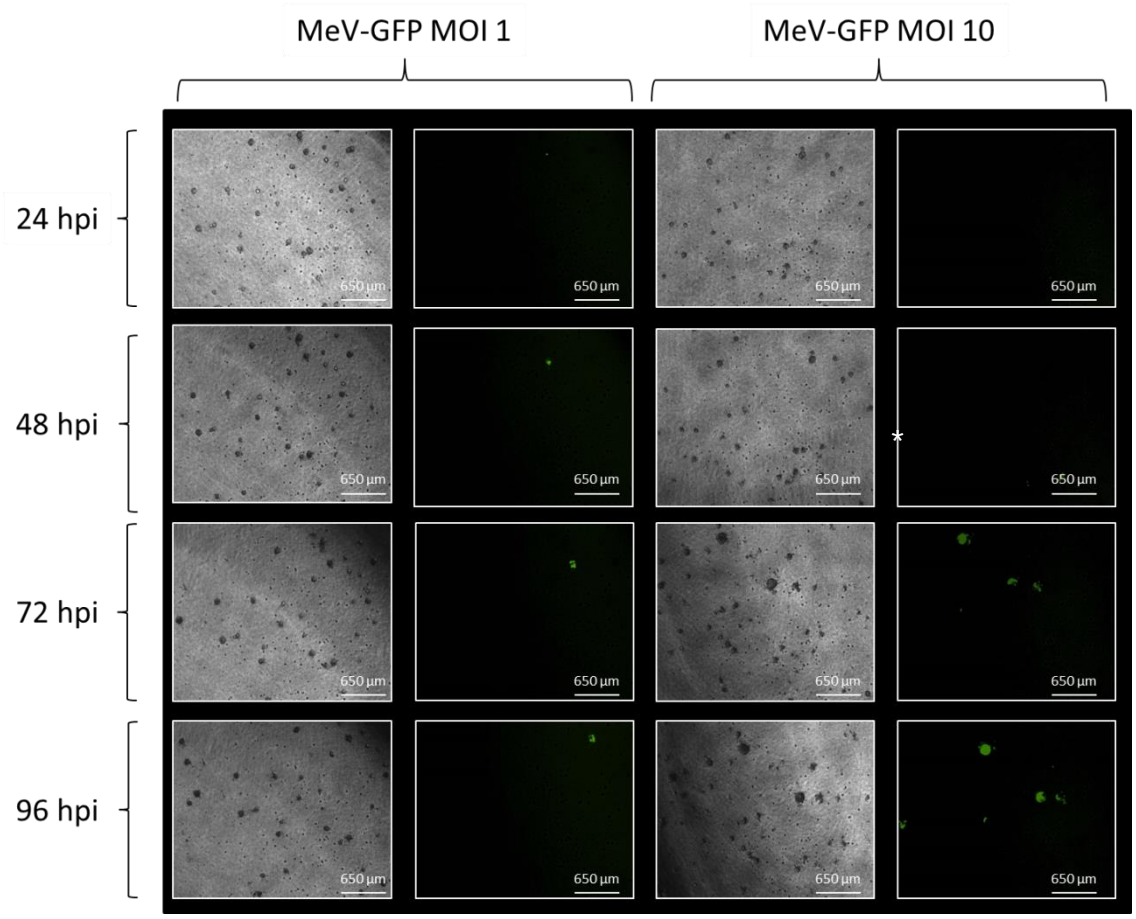

Figure 3-24 Infection of breast cancer organoid line BC-ORG 4 with MeV-GFP MOI 1 and MOI 10

As there are currently many ongoing clinical trials for breast cancer using oncolytic virotherapy including genetically engineered oncolytic viruses, the next step was to use a genetically engineered oncolytic virus for enhanced cell killing. All breast cancer organoid lines were treated with MeV-SCD and organoid line BC-ORG 4 is shown representatively. In order to assess the effect of the oncolytic virus MeV-SCD the prodrug needed to be assessed individually. Therefore, organoid lines were treated for 96 h with 5-FC (1 mmol/L). The viability was reduced in comparison to untreated organoids (72%; Table 11). The organoids which underwent this treatment showed no change in shape. Over the time period of 96 h the organoids grew (Figure 3-25). The treatment of

organoids with MeV-SCD MOI 10 resulted in a reduction of viability (54%; Table 11). The organoids were round and smooth at 24 hpi. However, in the following 72 h the shape of the organoids changed and the edges became rougher. The treatment of organoids with MeV-SCD MOI 10 and the prodrug 5-FC resulted in higher loss of viability (18%; Table 11) than MeV-SCD MOI 10 alone. Generally, more dispersed organoids with dark halos could be found in the wells containing the organoids treated with MeV-SCD MOI 10 and 5-FC (Figure 3-25). This treatment scheme resulted in a comparable viability to treatment with 5-FU (25%, Table 11). The lowest viability was achieved with the staurosporine control (9%, Table 11).

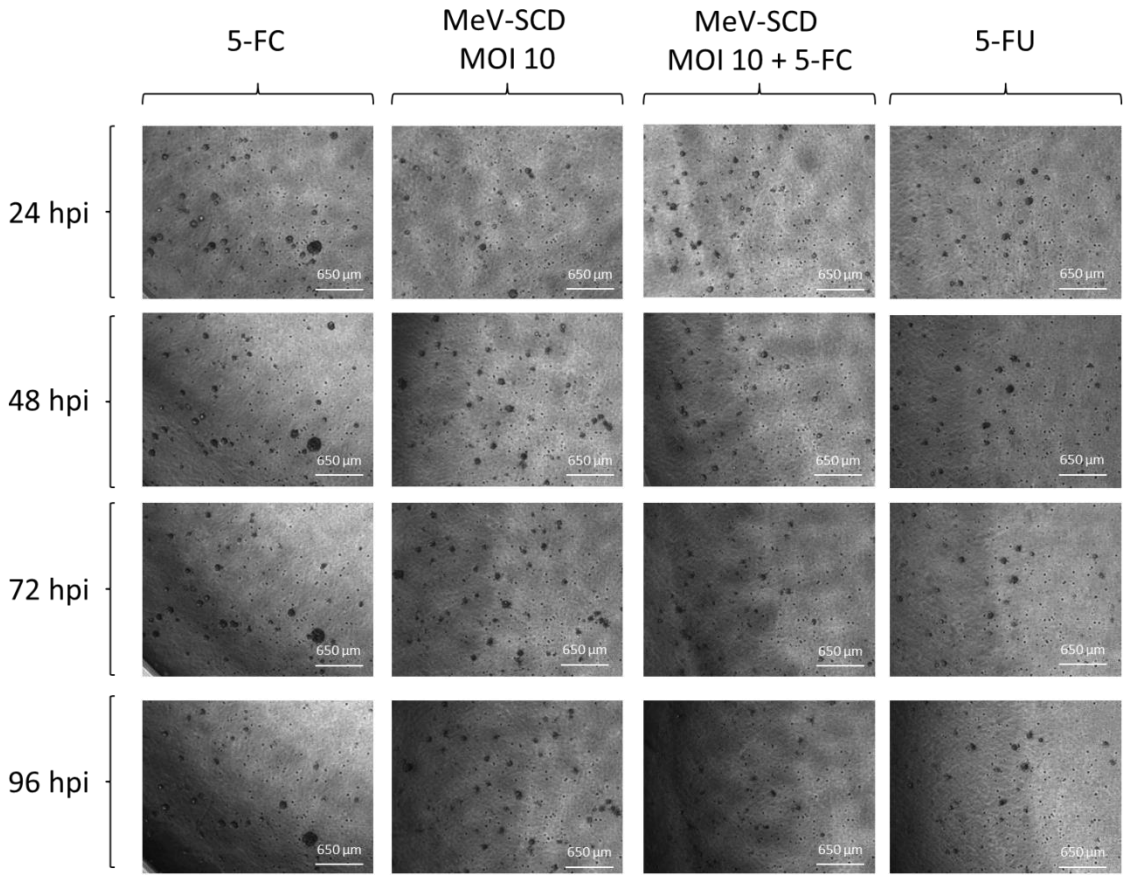

Figure 3-25 Infection of breast organoid line BC-ORG 4 with MeV-SCD MOI 10 and MeV-SCD MOI 10 + 5-FC and treatment of organoid line BC-ORG 4 with 5-FC and 5-FU

The organoid lines BC-ORG 1, 2 and 3 were chosen to depict all three grading types (G1-3, from left to right in Figure 3-26) and different hormone receptor status (Table 7). The organoids of line BC-ORG 2 appeared larger than BC-

ORG 1 and BC-ORG 3. BC-ORG 1 and BC-ORG 3 appeared to be of comparable size (Figure 3-26).

The infection of all three organoid lines with MeV-GFP MOI was successful as seen by the detected green fluorescence after 48/96 hpi. The least green fluorescence could be seen for organoid line BC-ORG 1 (Figure 3-26). This correlated with the viability measurement of 60% (Table 11). Organoid line BC-ORG 2 showed a higher expression of GFP as more green fluorescence was detected. The wider spread of oncolytic viral infection for line BC-ORG 2 was reflected in the lower viability measurement in comparison to BC-ORG 1 (Table 11). Figure 3-27 showed infected and uninfected organoids. The organoid highlighted with an arrow has been infected with oncolytic viruses. The neighbouring organoid highlighted with a square was not infected and expressed no GFP. Organoid line BC-ORG 3 showed a similar expression of green fluorescence as organoid line BC-ORG 2 in Figure 3-26. However, the measured viability was higher than with the other two organoid lines (78%), an observation that indicates a smaller spread of oncolytic viral infection.

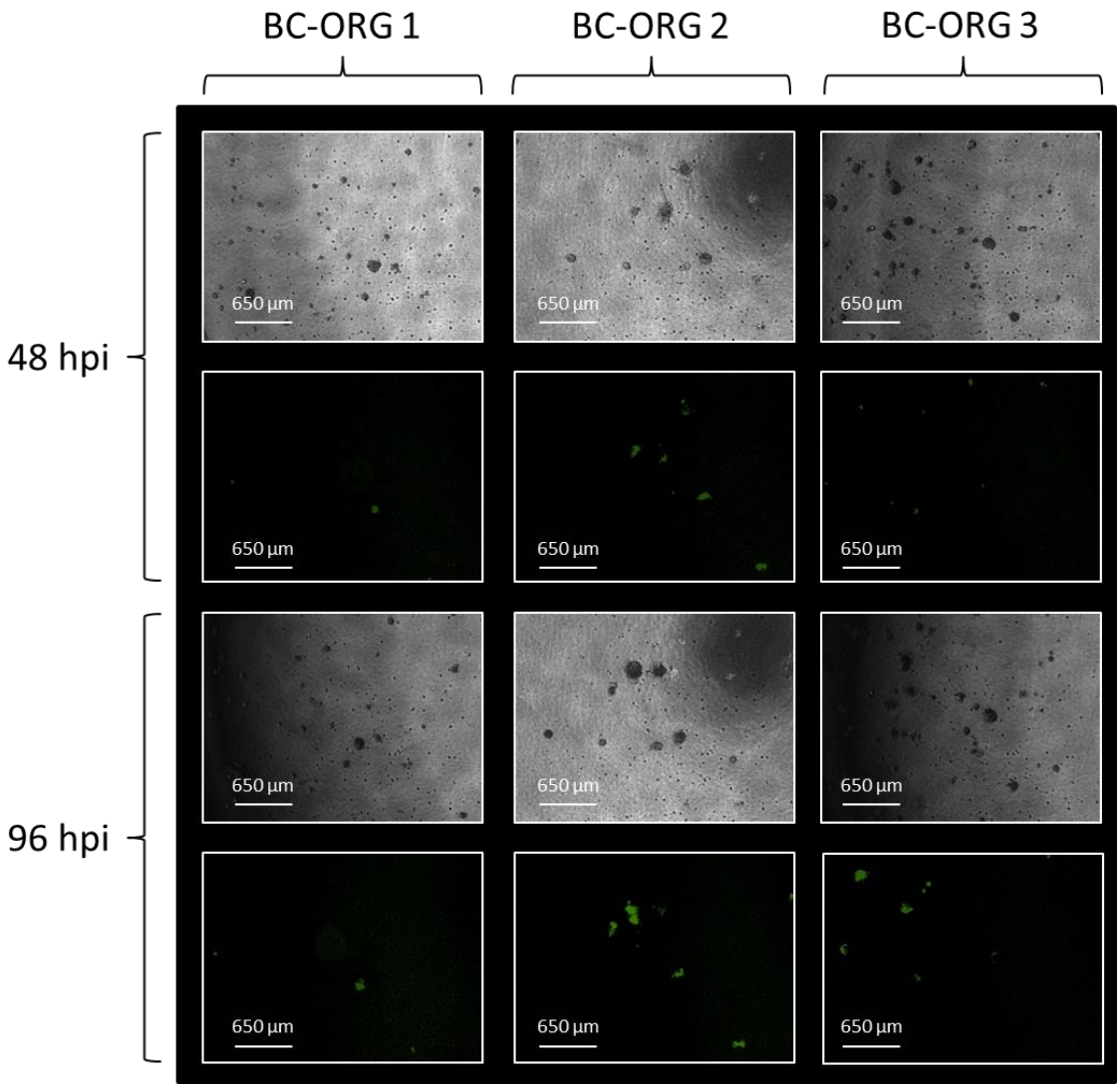

Figure 3-26 Infection of breast cancer organoid line BC-ORG 1, 2 and 3 with MeV-GFP MOI 10 48 hpi and 96 hpi [121]

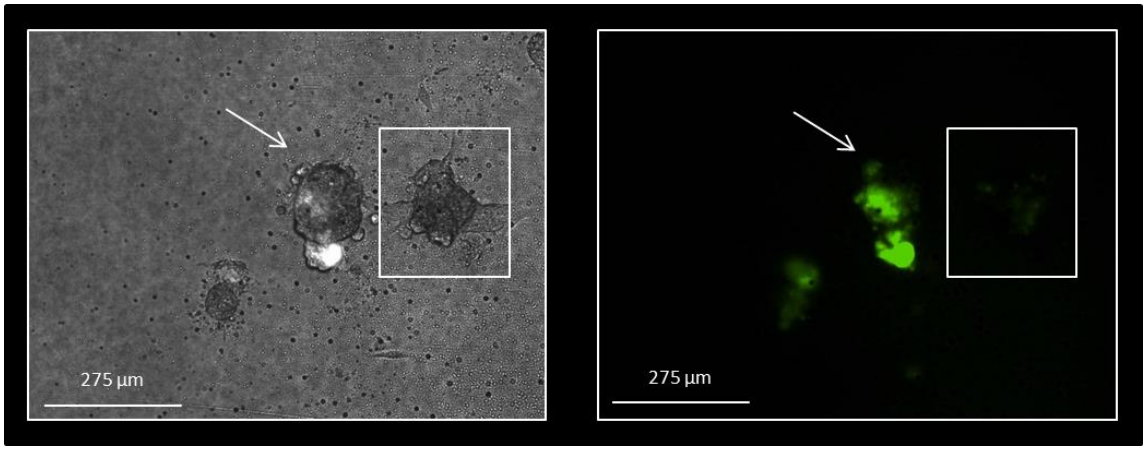

Figure 3-27 Infection of breast cancer organoid line BC-ORG 2 with MeV-GFP MOI 10 96 hpi [121]

Breast cancer organoid line BC-ORG 1 was treated with MeV-SCD MOI 10 with and without the prodrug 5-FC. The addition of 5-FC resulted in a lower organoid viability (24. %) than the treatment with MeV-SCD MOI 10 alone (5%; Table 11). This trend could be seen in all lines. The addition of the prodrug resulted in a greater number of rough-edged organoids with a dark halo, containing single cells dispersed from the organoid (Figure 3-28). Additionally, in some cases the smooth organoids fully dispersed into individual cells (Figure 3-29).

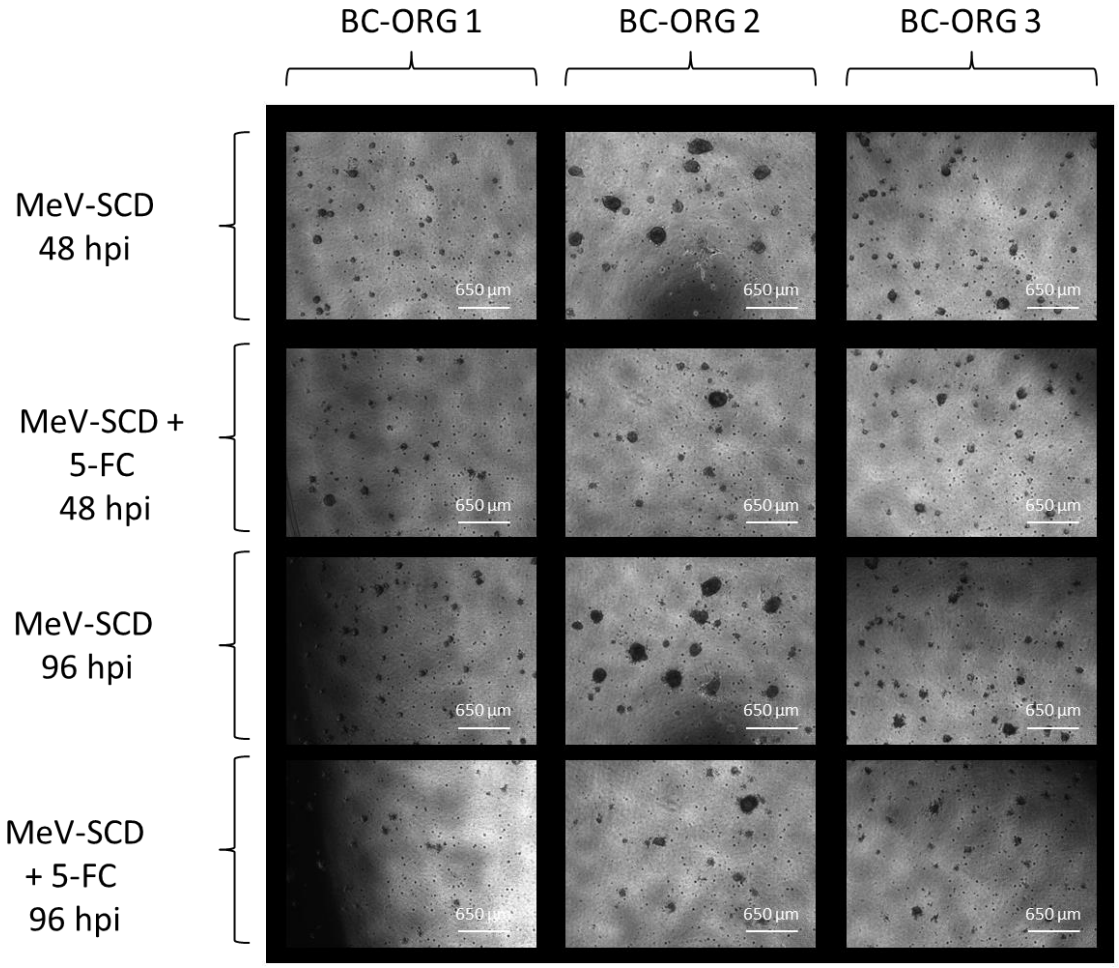

Figure 3-28 Infection of breast cancer organoid line BC-ORG 1, 2 and 3 with MeV-SCD MOI 10 and MeV-SCD MOI 10 with and without 5-FC 48 hpi and 96 hpi [121]

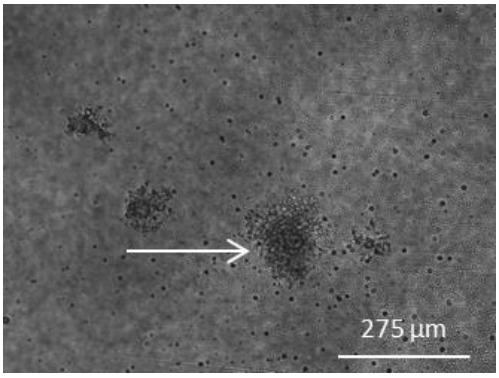

Figure 3-29 Infection of breast cancer organoid line BC-ORG 4 with MeV-SCD MOI 10 + 5-FC 96 hpi

Organoid line BC-ORG 2 and control organoid line C-ORG 4 were derived from the same patient, and thus the two organoid lines could be compared. The organoid viabilities measured for the different measles virus treatment schemes were compared, the main difference being higher organoid viability for C-ORG 4 organoids when treated with MeV-GFP MOI 10 in comparison to organoid line BC-ORG 2 (Figure 3-30, Table 12).

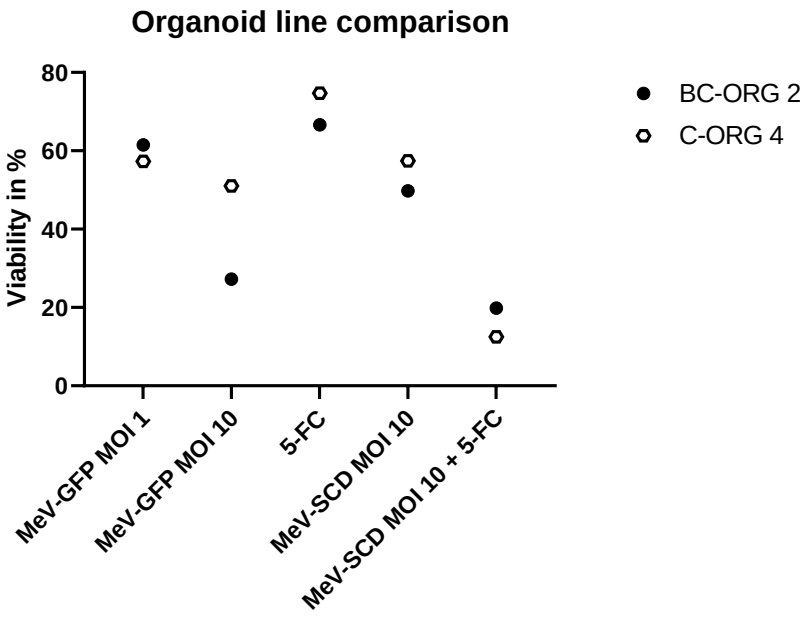

Figure 3-30 The effects of oncolytic measles viruses on breast cancer organoid line BC-ORG 2 and control organoid line C-ORG 4

Table 12 Viability measurements for organoid lines BC-ORG 2 and C-ORG 4 for treatments with different measles viruses

Organoid line	MeV-GFP MOI 1	MeV-GFP MOI 10	5-FC	MeV-SCD MOI 10	MeV-SCD MOI 10 + 5-FC
BC-ORG 2	61%	27%	67%	50%	20%
C-ORG 4	57%	51%	75%	58%	13%

3.2.2.2 Response of control organoid cultures

Six organoid cultures were established from control breast tissue. These organoid cultures were used to test the effects of oncolytic virotherapy. In these experiments, we compared the response to a measles virus expressing GFP (MeV-GFP) and a measles virus expressing a suicide gene (MeV-SCD) in organoid cultures (Figure 3-31).

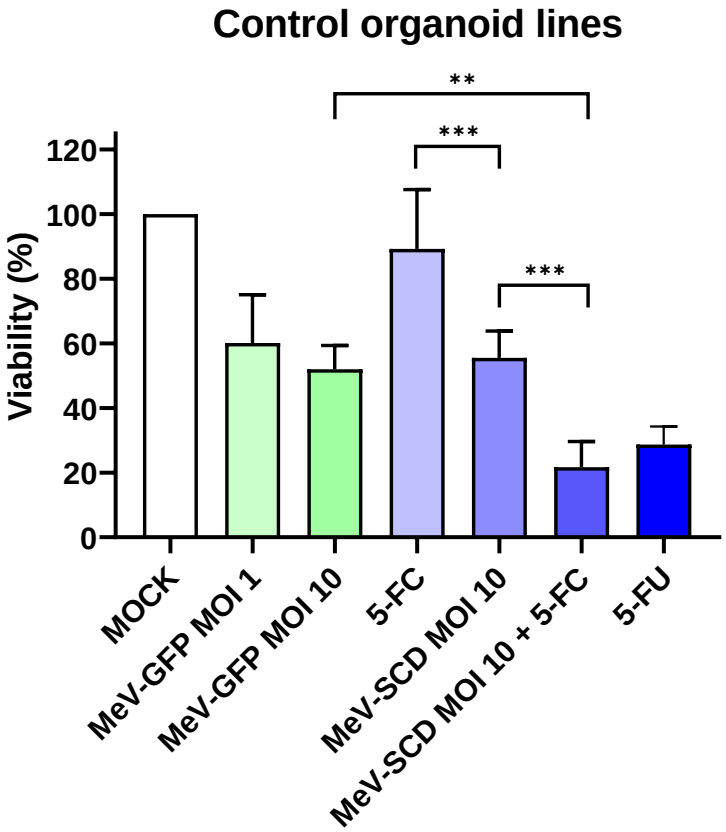

Figure 3-31 The effects of oncolytic measles viruses on organoids derived from control breast tissue

**p < 0.01, ***p < 0.001 with post-hoc Tukey's multiple comparisons tests, n=6.

When we compared the mean effects for all 6 control organoid lines measured with the CellTiter-Blue Viability Assay, a one-way ANOVA was statistically significant ($p < 0.0001$; $F(5, 29) = 25.56$). No statistically significant difference could be seen between two different titres of MeV-GFP (MOI 1 and MOI 10; Figure 3-31). When using a virus titre of MOI 10, no significant difference could be found between MeV-GFP and MeV-SCD (when no prodrug was added; Figure 3-31). MeV-SCD without the addition of the prodrug, however, significantly reduced the viability in the organoid cultures ($p < 0.001$) in comparison to the prodrug 5-FC alone (Figure 3-31). The addition of the prodrug 5-FC to MeV-SCD resulted in a significantly greater reduction of viability than MeV-SCD without the prodrug 5-FC ($p < 0.001$; Figure 3-31). There was no significant difference between the MeV-SCD in combination with the prodrug 5-FC in comparison to the active metabolite 5-FU (Figure 3-31). We observed a significantly greater reduction of cell viability when control organoids were infected with MeV-SCD compared to the corresponding measles virus expressing GFP but lacking the suicide gene (MeV-GFP), provided that the necessary prodrug 5-FC was present for the suicide gene ($p < 0.01$; Figure 3-31).

Organoid lines C-ORG 1, 2 and 4 were selected as a representative group of control organoid lines. The infection of control organoid lines was successful and spread over time as seen by the different infected areas in Figure 3-33 (white squares in Figure 3-33). After 96 h of incubation the infection had spread within the organoid and to neighbouring organoids (arrow in Figure 3-33). The viability measurements for all three organoid lines are similar for the infection with MeV-GFP MOI 10 (Table 13; Figure 3-32). Organoid line C-ORG 2 visually does not show a wide spread oncolytic infection, seen by the small amounts of green fluorescence. Organoid line C-ORG 4 shows a homogenous spread of oncolytic viral infection and spread of green fluorescence over time (Figure 3-33).

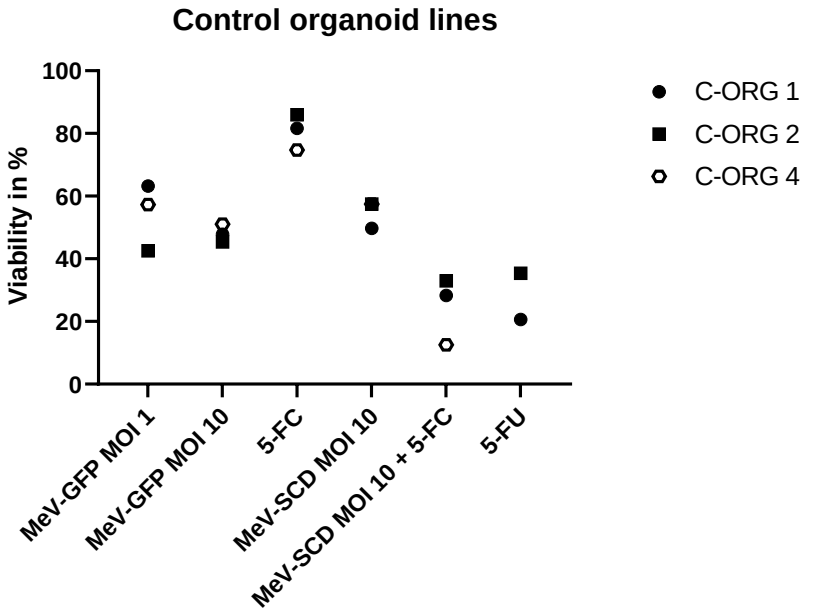

Figure 3-32 Effects of oncolytic measles viruses on control organoid lines C-ORG 1, 2 and 4

Table 13 Viability measurement of organoid lines C-ORG 1, and 4 for infection with MeV-GFP MOI 10, MeV-SCD MOI 10 and MeV-SCD MOI 10 with 5-FC 96 hpi

Organoid line	Viability measurement MeV-GFP MOI 10 96 hpi	Viability measurement MeV-SCD MOI 10 96 hpi	Viability measurement MeV-SCD MOI 10 + 5-FC 96 hpi
C-ORG 1	48%	50 %	28%
C-ORG 2	45%	57%	33%
C-ORG 4	51%	57%	13%

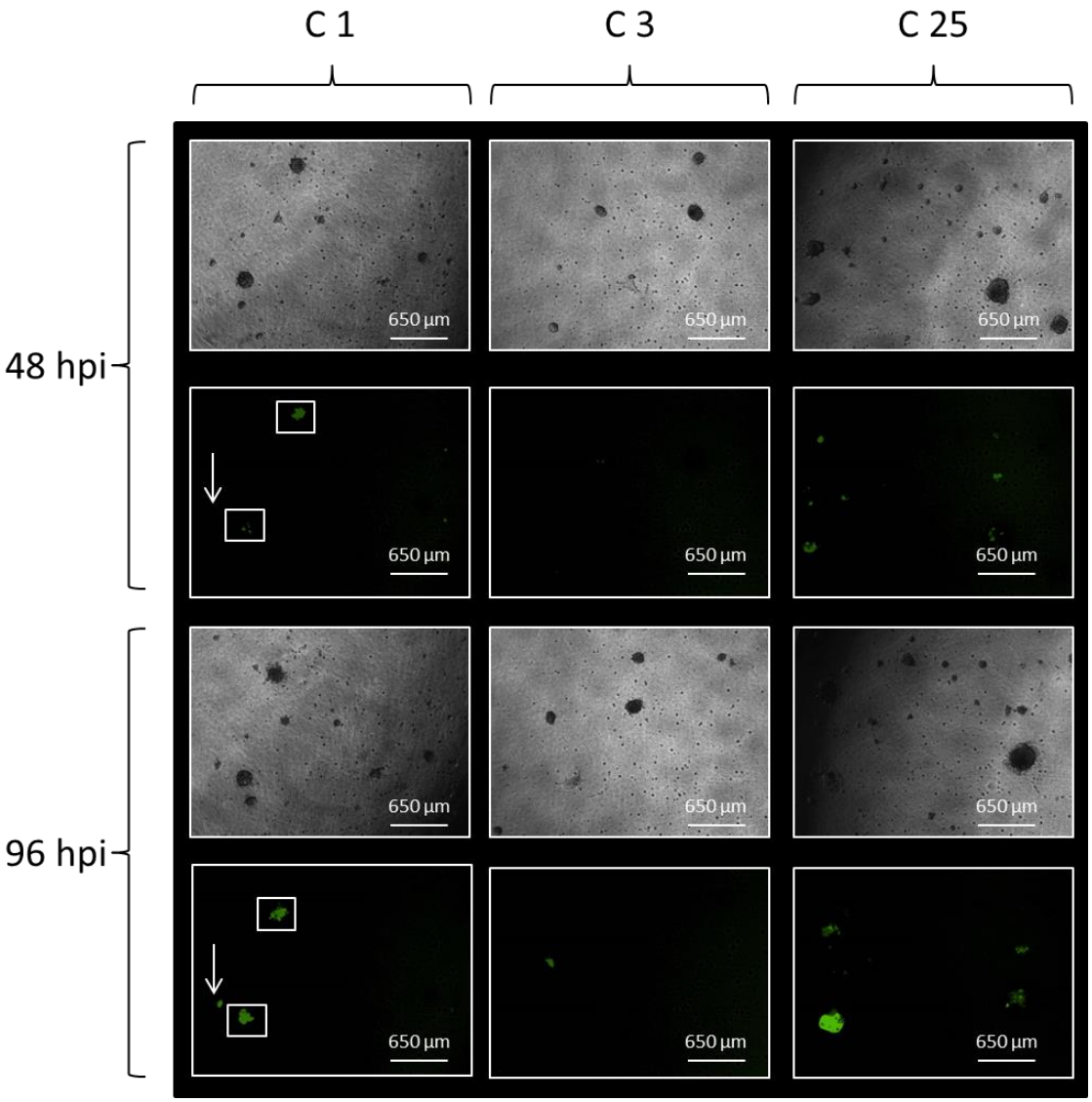

Figure 3-33 Infection of control organoid line C-ORG 1, 2 and 4 with MeV-GFP MOI 10 48 hpi and 96 hpi

The treatment of control organoid lines C-ORG 1, 2 and 4 showed comparable viability measurements for the infection of organoids with MeV-SCD MOI 10 (Table 13). The addition of the prodrug 5-FC resulted in a further reduction of organoid viability (Table 13). However, the organoid viability was lower for organoid line C-ORG 4 (13%) than the organoid lines C-ORG 1 (28%) and C-ORG 2 (33%) (Table 13). C-ORG 4 contains a greater number of large organoids in comparison to organoid lines C-ORG 1 and C-ORG 2 (Figure 3-34). The response of control organoid lines to infection with MeV-SCD MOI 10

and MeV-SCD MOI 10 with 5-FC was comparable to breast cancer organoid lines (Figure 3-34,Figure 3-28).

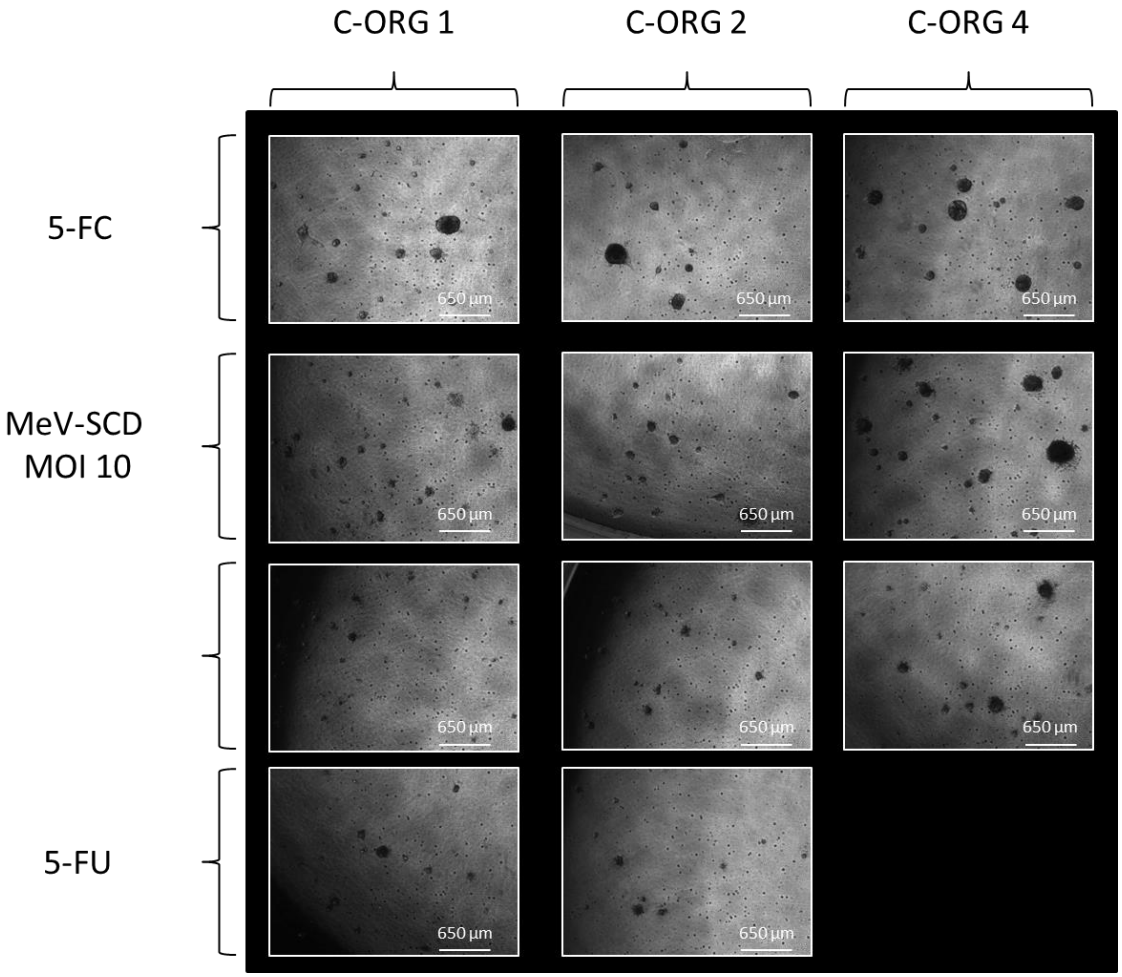

Figure 3-34 Treatment of control organoid line C-ORG 1, 2 and 4 with 5-FC, MeV-SCD MOI 10, MeV-SCD MOI 10 + 5-FC and 5-FU 96 hpi

3.2.2.3 Response of organoid cultures derived from breast cancer cell lines

The effects of a measles virus expressing GFP (MeV-GFP) and a measles virus expressing a suicide gene (MeV-SCD) were compared in organoid cultures derived from breast cancer cell lines T47D, MCF7 and MDA-MB-468 (Figure 3-35).

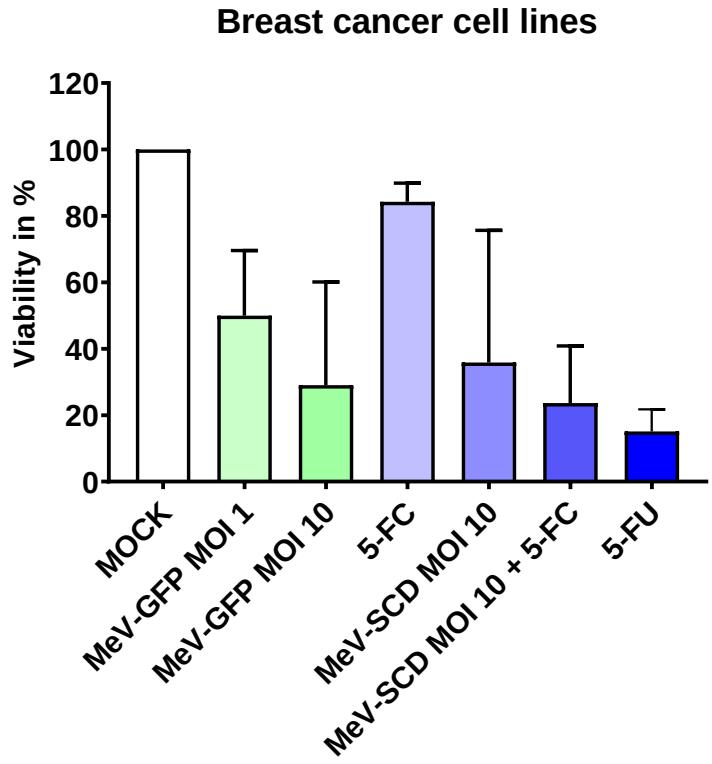

Figure 3-35 The effects of oncolytic measles viruses on organoids derived from breast cancer cell lines (n=3)

There was little difference between the viral titres MOI 1 and MOI 10 for MeV-GFP (Figure 3-35). However, the addition of the oncolytic viruses to the organoid culture resulted in a decrease of viability in compared to the prodrug alone (Figure 3-35). The addition of 5-FC to the MeV-SCD resulted in an additional loss of viability (Figure 3-35). The viability was comparable between the MeV-SCD with 5-FC and the application of 5-FU alone (Figure 3-35). The viability for staurosporine-treated organoids measured 0% (Table 9). The number of experiments (n) was too low to perform any meaningful statistical tests.

Table 14 The effects of oncolytic measles viruses on viability of organoid lines derived from breast cancer tumour cell lines T47D, MCF7 and MDA MB 468 96 hpi

Cell line	MeV-GFP MOI 1	MeV-GFP MOI 10	5-FC	MeV-SCD MOI 10	MeV-SCD MOI 10 + 5-FC	5-FU
T47D	63%	49%	83%	76%	36%	19%
MCF7	60%	45%	90%	35%	30%	20%
MDA-MB-468	27%	0.00%	79%	15%	4%	7%

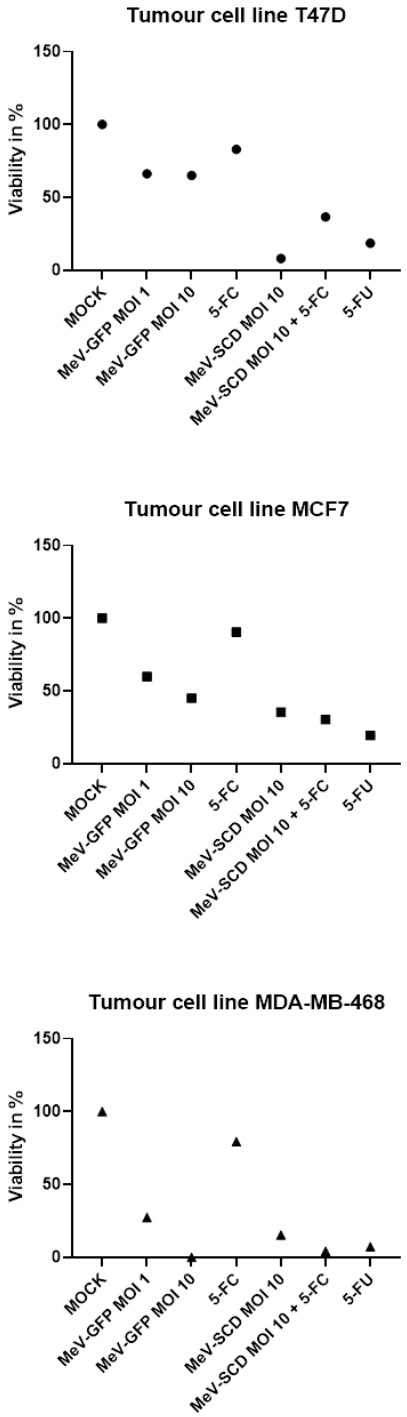

Figure 3-36 The effects of oncolytic measles viruses on organoid lines derived from breast cancer tumour cell line T47D, MCF7 and MDA-MB-468

The organoid lines derived from tumour cell lines T47D, MCF7 and MDA-MB-468 were cultivated in the same media used for the organoid lines derived directly from breast cancer tumours or control tissue. The size of the organoids varied between the tumour cell lines. The organoids derived from MCF7 were

large whereas the organoids derived from MDA-MB-468 cell lines were smaller in size (Figure 3-37). Moreover, the viability measurements after infection with MeV-GFP MOI 1 and MOI 10 varied between the three organoid lines. The greatest effect on organoid viability was seen with MDA-MB-468 (Table 14). The effect of 5-FC alone was comparable for all three organoid lines (90-79%; Table 14). The treatment with MeV-SCD led to different reductions of organoid viability. The highest reduction in organoid viability after treatment with MeV-SCD could be seen with MDA-MB-468 (15%; Table 14). The effect of MeV-SCD MOI 10 on organoid viability remained the greatest with the addition of the prodrug 5-FC, and resulted in complete dissolution of the organoids (4%; Table 14, Figure 3-38). MCF7 and T47D had a similar response on organoid viability (37% and 30%, respectively; Table 14). The MCF7 organoids completely dissipated into single cells but clusters still remained, which made the outline of the original organoids traceable (Figure 3-38). 5-FU had the greatest effect on organoid viability for MDA-MB-468 (77%; Table 14).

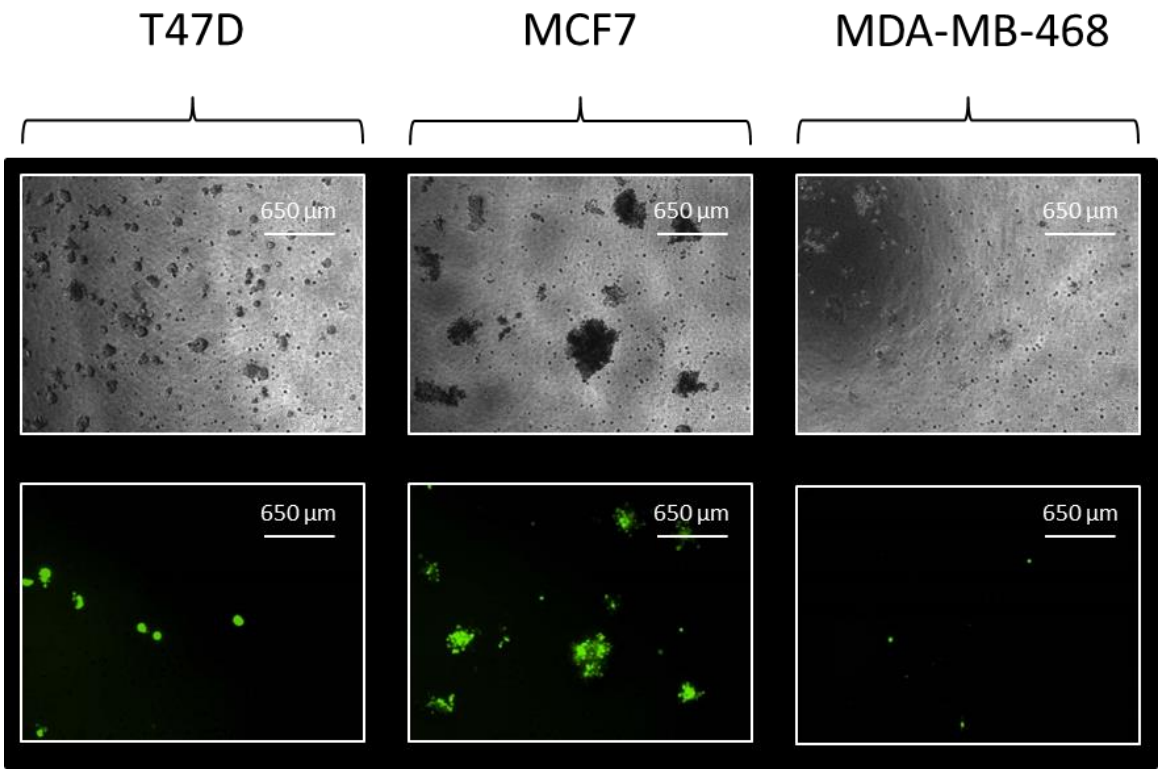

Figure 3-37 The effect of oncolytic measles virus MeV-GFP MOI 10 on organoid lines T47D, MCF7 and MDA-MB-468 96 hpi

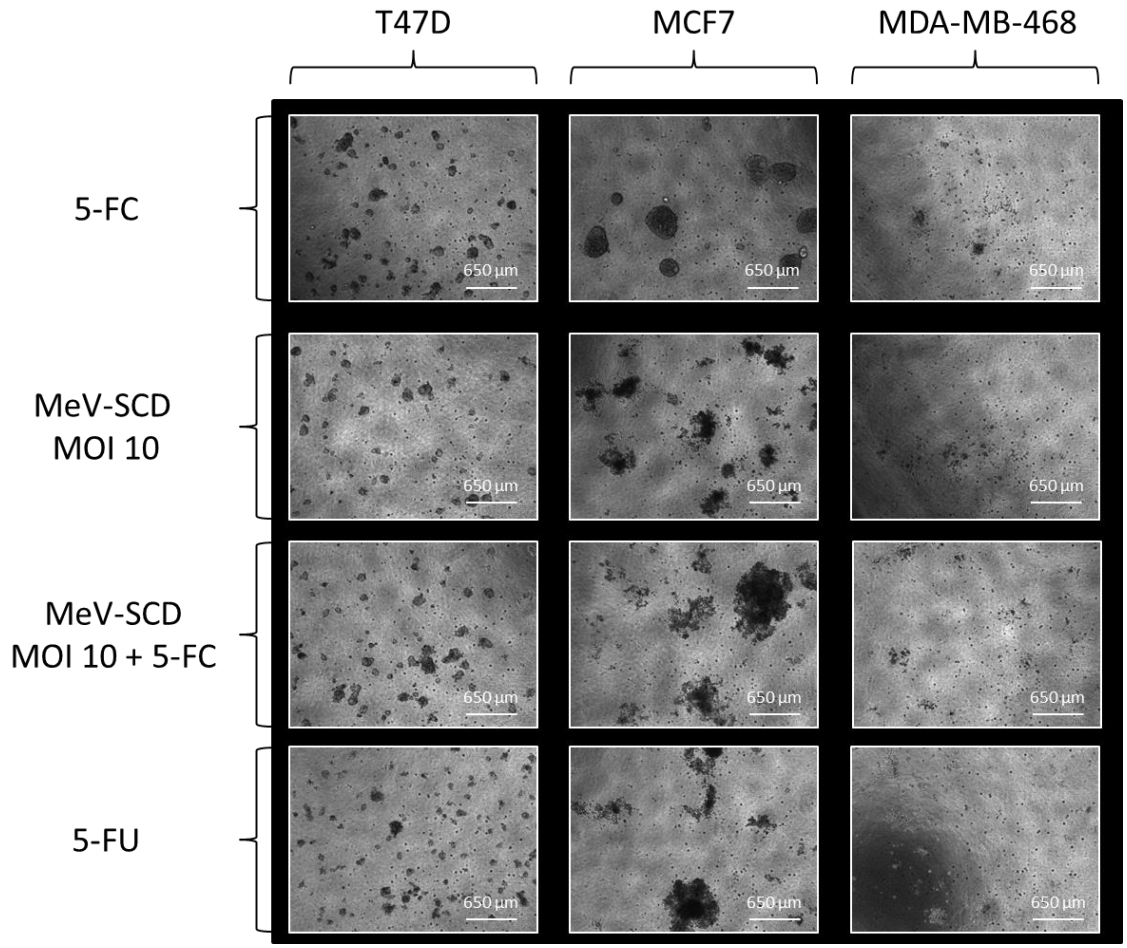

Figure 3-38 Treatment of organoid lines T47D, MCF7 and MDA-MB-468 with 5-FC, MeV-SCD MOI 10, MeV-SCD MOI 10 + 5-FC and 5-FU 96 hpi

3.2.3 *Treatment of organoid cultures with oncolytic vaccinia viruses*

3.2.3.1 Response of breast cancer organoid cultures

We compared the effects of a vaccinia virus expressing a red fluorescent protein (RFP) (GLV-0b347) and a vaccinia virus expressing a suicide gene (GLV-1h94) in organoid cultures derived from breast cancer tissue (Figure 3-39).

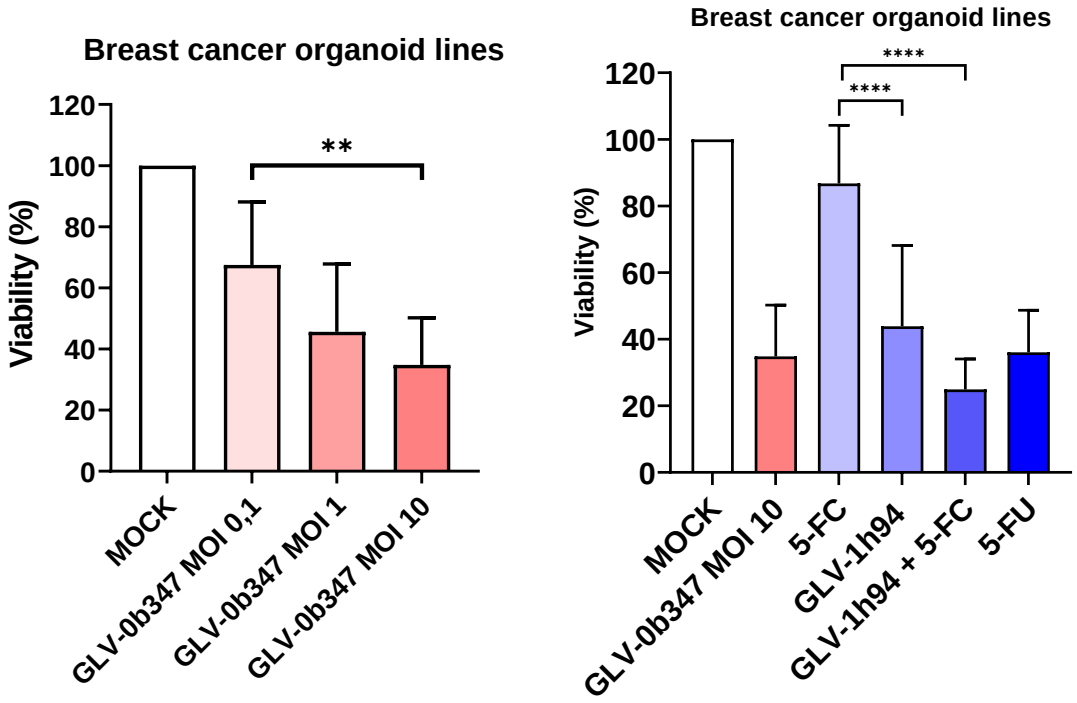

Figure 3-39 The effects of oncolytic vaccinia viruses on organoids derived from breast cancer tissue [121]

*p < 0.05, **p < 0.01, ***p < 0.001, ****p < 0.0001 with t-test, n=10.

When we compared the mean effects for all ten breast cancer organoid lines measured with the CellTiter-Blue Viability Assay, a one-way ANOVA demonstrated statistical significance ($p < 0.0001$; $F(6, 62) = 13.84$) between all groups. In addition, a statistically significant difference was also observed with a one-way ANOVA ($p < 0.0031$; $F(2, 27) = 7.226$) between the three titers of GLV-0b347 (MOI 0.1., MOI 1, MOI 10), thereby indicating titer-dependent effects of the GLV-0b347 (Figure 3-39). The greater the concentration of GLV-0b347, the greater was the reduction of viability (MOI 0.1 vs MOI 10 $p < 0.001$;

Figure 3-39). There was no statistically significant difference in viability between the vaccinia virus expressing RFP (GLV-0b347) and the vaccinia virus expressing the suicide gene (GLV-1h94) with the same viral titre (MOI 10; Figure 3-39). GLV-1h94 without the addition of the prodrug 5-FC reduced the viability in a statistically significant manner in comparison to the prodrug 5-FC alone ($p < 0.0001$; Figure 3-39). GLV-1h94 with the addition of the prodrug 5-FC resulted in a statistically significant reduction if viability in comparison to 5-FC alone ($p < 0.0001$; Figure 3-39). Interestingly, there was no significant difference between the viability of the organoid cultures treated with GLV-0b347 compared to GLV-1h94 with the addition of the prodrug 5-FC (Figure 3-39).

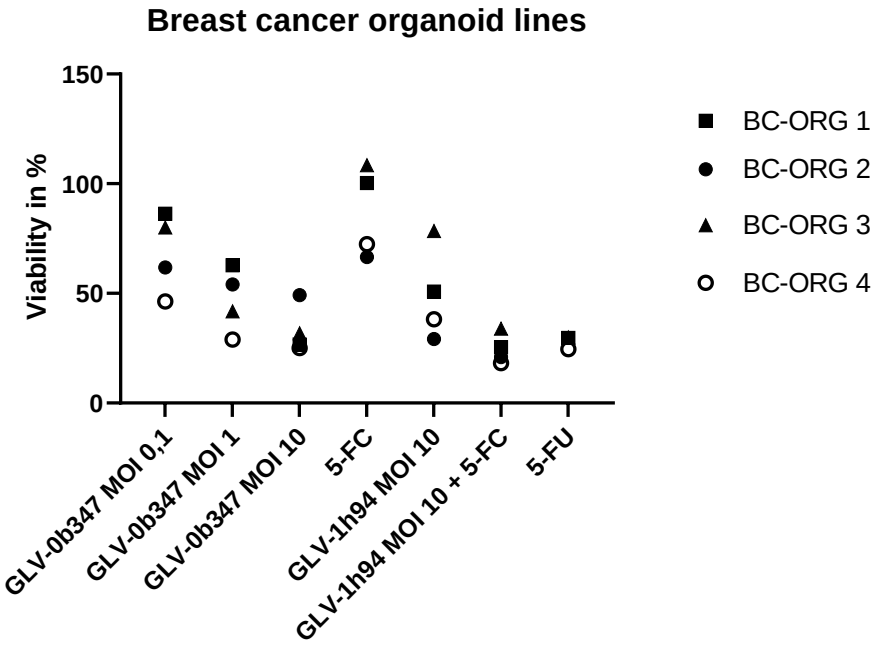

Figure 3-40 The effects of oncolytic vaccinia viruses on breast cancer organoid lines BC-ORG 1, 2 3, and 4

Figure 3-40 and Table 15 offer a more in-depth view of the oncolytic virotherapy for breast cancer organoids with vaccinia viruses.

Table 15 Viability measurements of breast cancer organoid lines BC-ORG 1, 2 3, and 4 treated with oncolytic vaccinia viruses, 5-FC and 5-FU

Organoid line	GLV-0b347 MOI 0.1	GLV-0b347 MOI 1	GLV-0b347 MOI 10	5-FC	GLV-1h94 MOI 10	GLV-1h94 MOI 10 + 5-FC	5-FU
BC-ORG 1	86%	63%	27%	100%	51%	25%	30%
BC-ORG 2	62%	54%	49%	67%	29%	21%	
BC-ORG 3	80%	42%	37%	108%	78%	34%	30%
BC-ORG 4	46%	29%	25%	72%	38%	18%	25%

Organoid line BC-ORG 4 was infected with different titres of GLV-0b347. In Figure 3-41 the infection can be seen by the increasing red fluorescence over 96 h. The distribution of the infection throughout the well appeared to be similar. However, the viability measurement indicated that the infection with GLV-0b347 led to a larger decrease of organoid viability with a greater viral titre such as MOI 10 (46% for MOI 1 and 25% for MOI 10, Table 15). Figure 3-42 shows an infected organoid (with full red fluorescence) and a partially infected organoid (with partial red fluorescence).

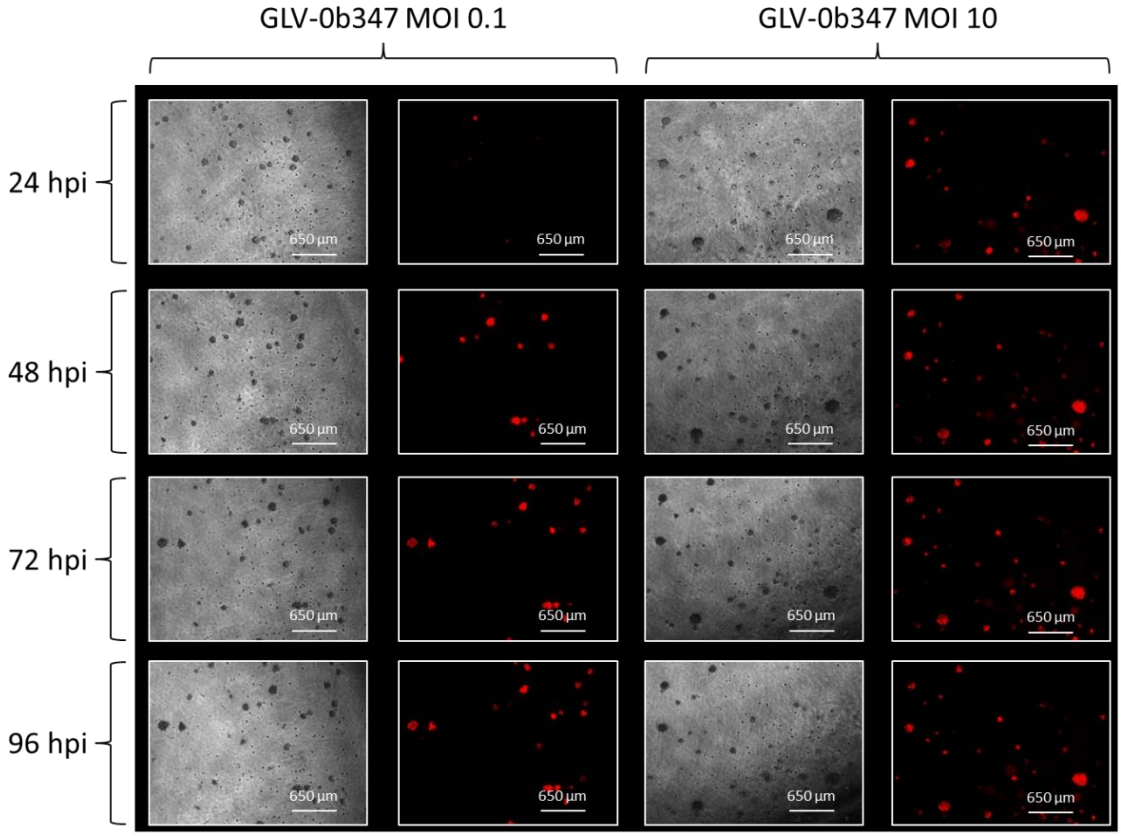

Figure 3-41 Infection of breast cancer organoid line BC-ORG 4 with GLV-0b347 MOI 0.1 and MOI 10 [121]

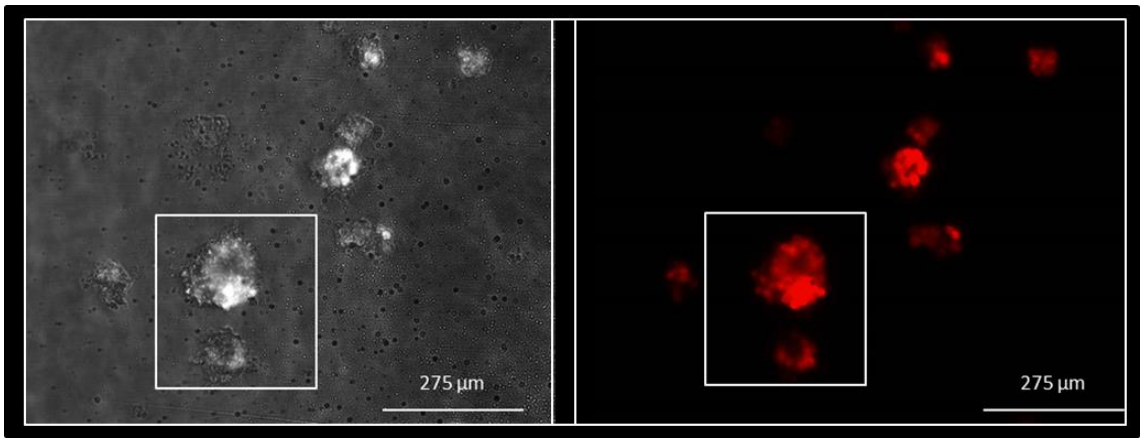

Figure 3-42 Treatment of breast cancer organoid line BC-ORG 4 with GLV-0b347 MOI 1 96 hpi [121]

Organoid lines BC-ORG 1, 2 and 3 showed a greater distribution of red fluorescence 96 hpi when using a higher GLV-0b347 titre (MOI 10) than a lower viral titre (GLV-0b347 MOI 0.1) (Figure 3-41). This can also be seen in the decrease of organoid viability ranging between 20 and 60% (Table 15).

The lowest organoid viability was 27% with GLV-0b347 MOI 10 in breast cancer organoid line BC-ORG 1 (Table 15). All three organoid lines showed a comparable distribution of red fluorescence (Figure 3-43). Large organoids were not uniformly infected after viral administration. Some cells of the same organoid appeared brighter through the greater production of RFP than other neighbouring cells of the organoids (Box in Figure 3-44). This showed the spread of infection throughout the organoid. The infection of neighbouring organoids can be seen as a lighter red fluorescence (arrow in Figure 3-44).

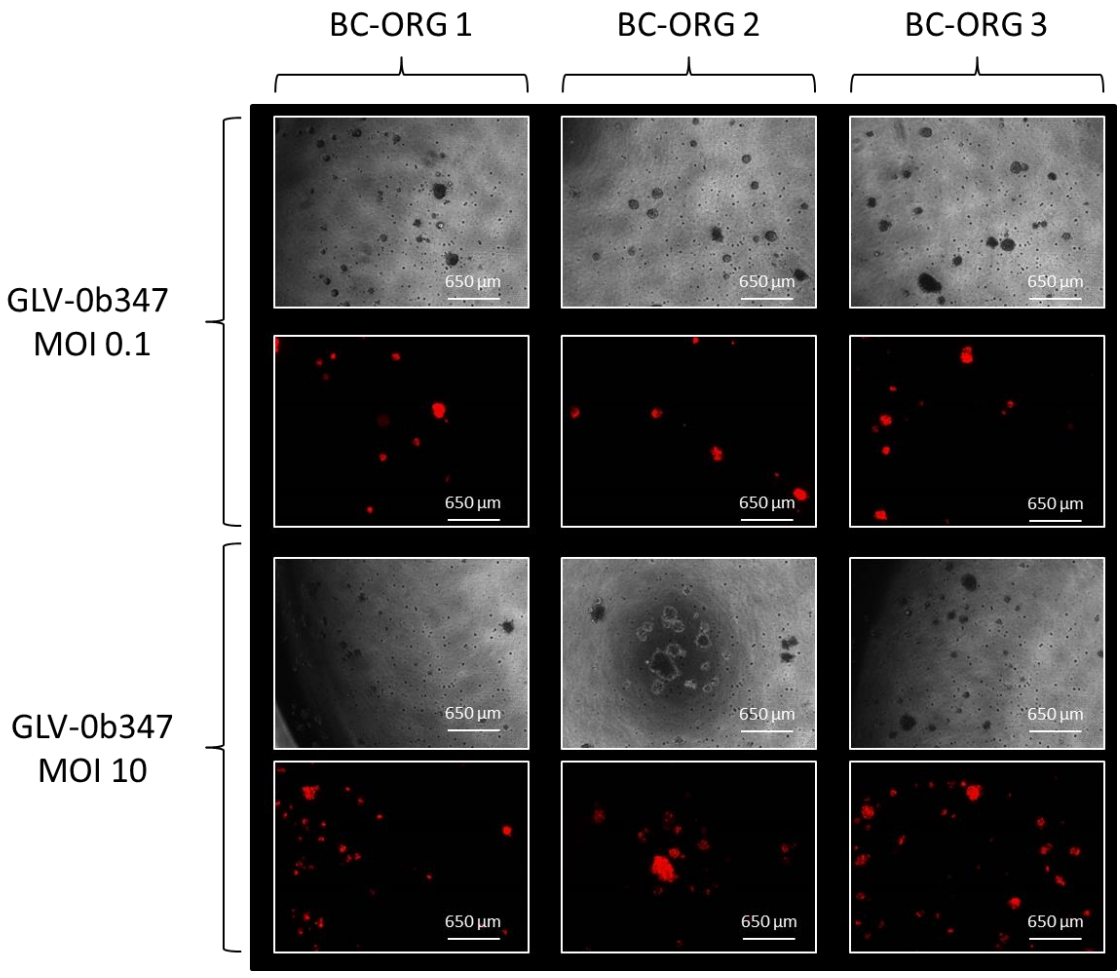

Figure 3-43 Treatment of breast cancer organoid lines BC-ORG 1, 2 and 3 with GLV-0b347 MOI 0.1 and MOI 10 96 hpi

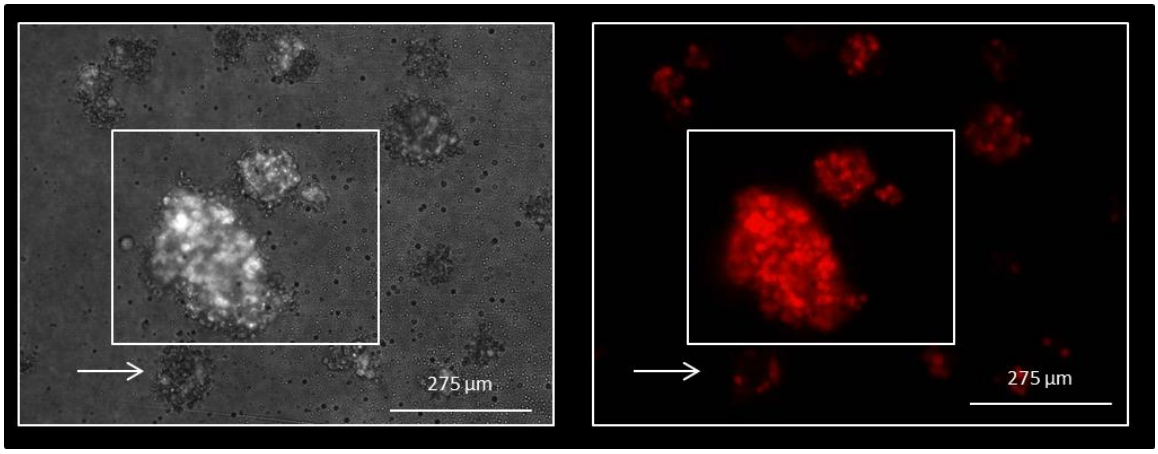

Figure 3-44 Treatment of breast cancer organoid line BC-ORG 2 with GLV-0b347 MOI 10 96 hpi

The infection of breast cancer organoid line BC-ORG 4 with GLV-1h94 MOI 10 resulted in lower viability (37%) than the treatment with 5-FC (72%; Table 15). The viability was further reduced (to 18%) through the addition of 5-FC to GLV-1h94 (Table 15). However, the spread of oncolytic viruses seemed greater without the addition of 5-FC as the green fluorescence was less in GLV-1h94 MOI 10 than it is in GLV-1h94 with 5-FC (Figure 3-45). Figure 3-46 shows that organoids infected with GLV-1h94, seen by the green fluorescence, displayed an uneven morphology. This shape can also be seen on some organoids which were not fully green fluorescent, thereby indicating a previous infection in the last 96 hours or a beginning of an infection (GLV-1h94 MOI and 5-FC in Figure 3-46). Organoids with no green fluorescence appeared smooth edged and indicated a viable uninfected organoid (box in Figure 3-46).

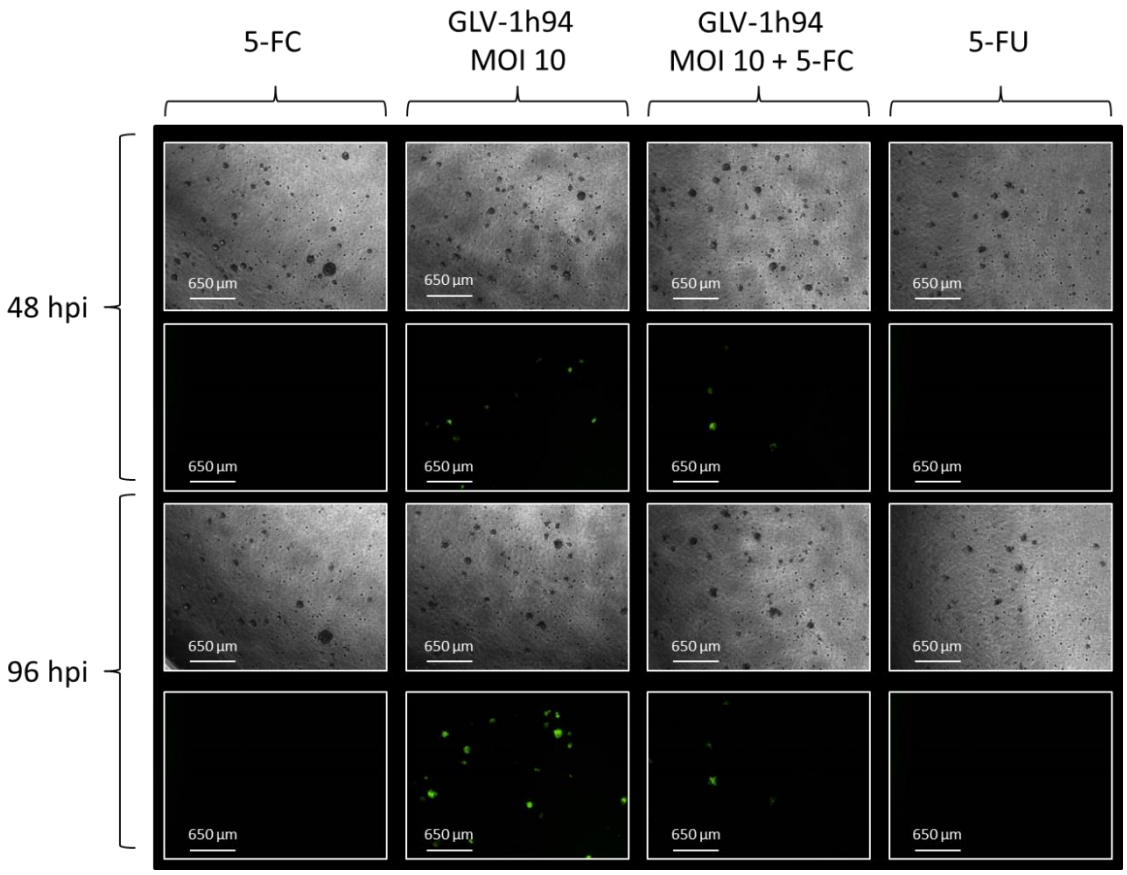

Figure 3-45 Treatment of breast cancer organoid line BC-ORG 4 with 5-FC, GLV-1h94 MOI 10, GLV-1h94 MOI 10 + 5-FC and 5-FU 48 hpi and 96 hpi

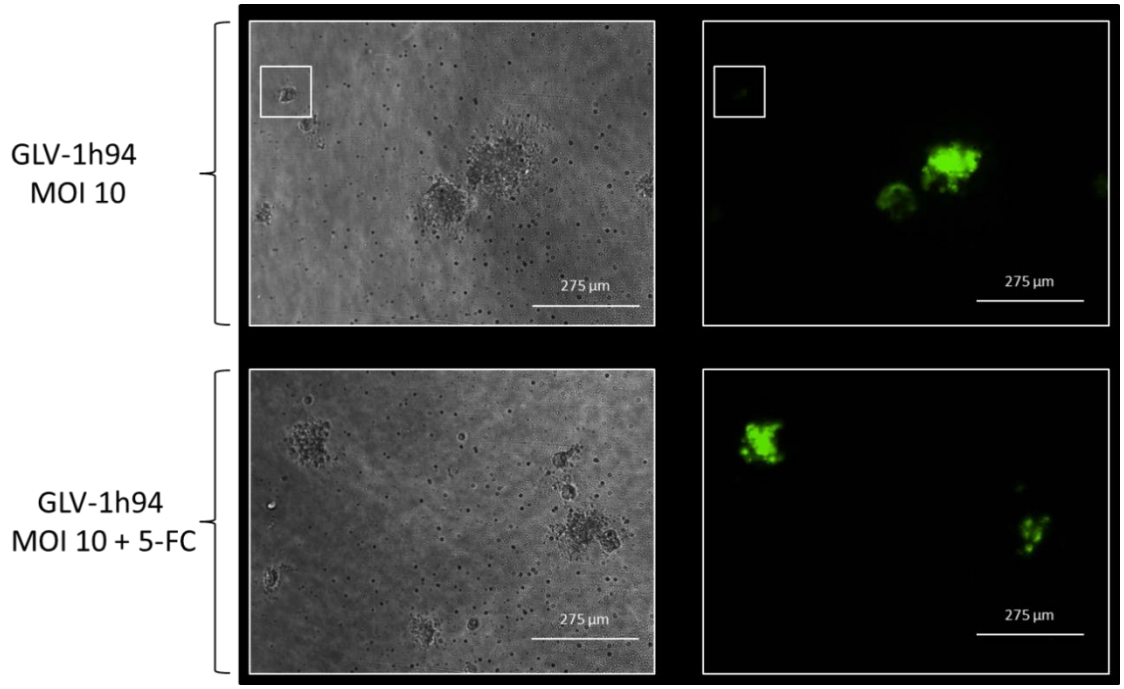

Figure 3-46 Treatment of breast cancer organoid line BC-ORG 4 with GLV-1h94 MOI 10 and GLV-1h94 MOI 10 + 5-FC 96 hpi

Organoids infected with GLV-1h94 without 5-FC produce more green fluorescence than the organoids infected with GLV-1h94 and 5-FC (Figure 3-47). Over 48 hours the viral infection spread throughout the well of GLV-1h94 as indicated by the increase of green fluorescence (Figure 3-47). The addition of 5-FC inhibited the production of green fluorescence after 48 hours (Figure 3-47). The addition of 5-FC to the infection with GLV-1h94 resulted in approximately half the viability measurement for organoid line BC-ORG 1 (25% instead of 51%; Table 15). In organoid line BC-ORG 3 the addition of 5-FC resulted in reduction of viability of 45% (from 78% to 34%; Table 15). This trend was not seen in organoid line BC-ORG 2, the addition of 5-FC to GLV-1h94 resulted in a similarly low viability (from 29% to 21%; Table 15). The treatment of organoid lines with 5-FU resulted in comparable organoid viability to the treatment of organoid lines with GLV-1h94 + 5-FC (Table 15).

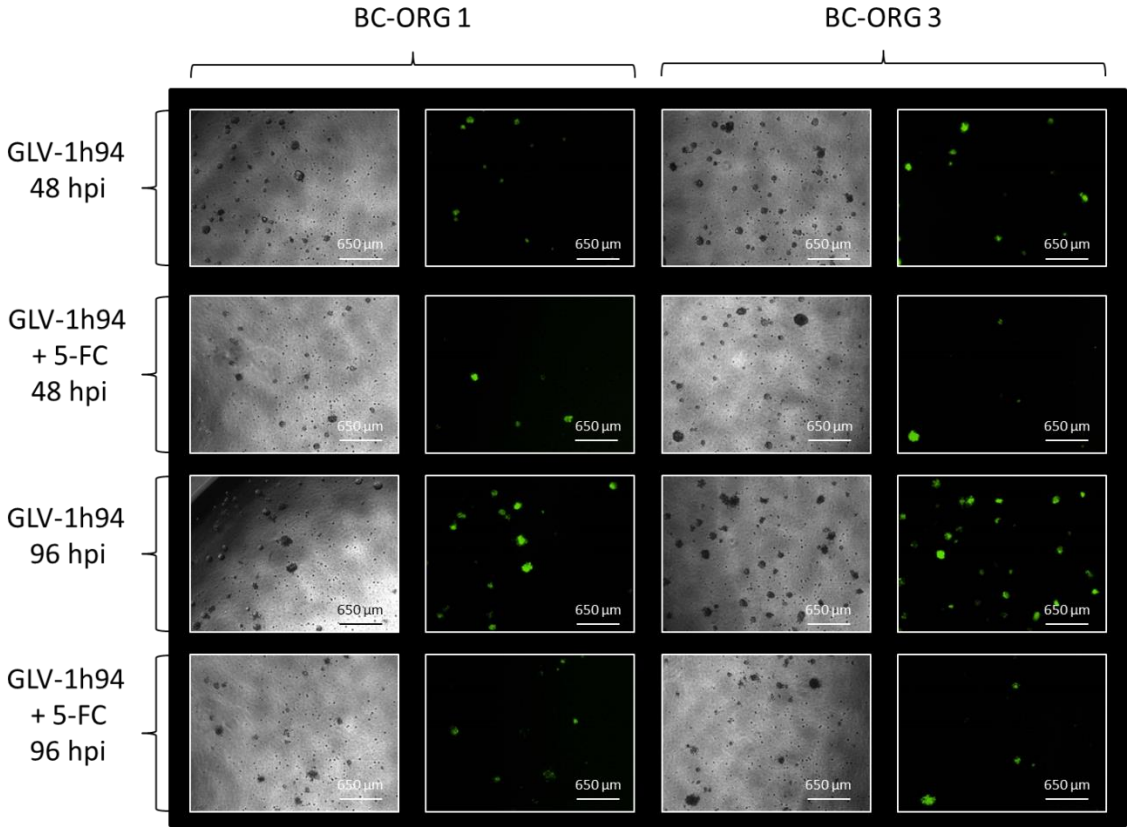

Figure 3-47 Treatment of breast cancer organoid lines BC-ORG 1 and 3 with GLV-1h94 MOI 10 and GLV-1h94 MOI 10 + 5-FC 48 hpi and 96 hpi [121]

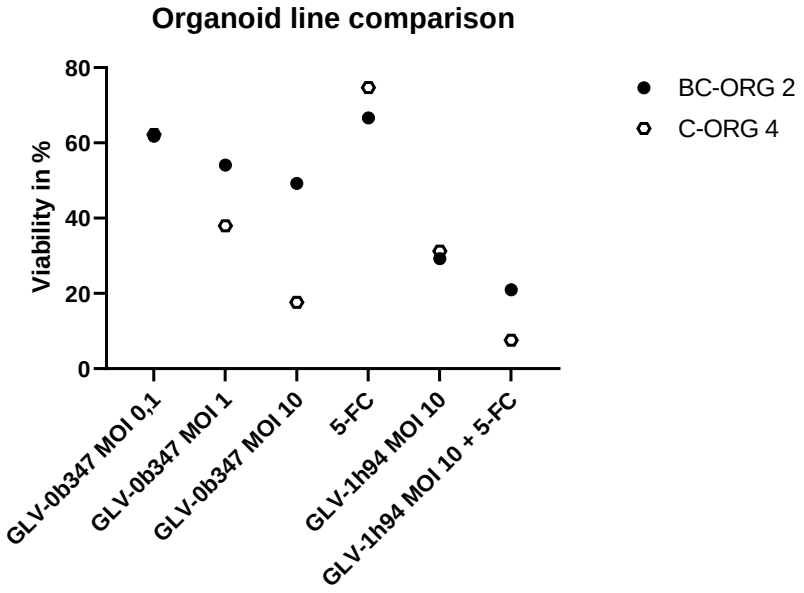

Figure 3-48 The effects of oncolytic vaccinia viruses on breast cancer organoid line BC-ORG 2 and control organoid line C-ORG 4

Breast cancer organoid line BC-ORG 2 and control organoid line C-ORG 4 derived from the same patient displayed a similar response to GLV-1h94 and the addition of 5-FC (Figure 3-48, Table 16). The response to GLV-0b347 was different between breast cancer organoid line BC-ORG 2 and control organoid line C-ORG 4. A greater reduction of the organoid viability measurement can be seen with the increase in viral titre of GLV-0b347 (from MOI 0.1 to MOI 10) of GLV-0b347 (reduction of organoid viability from 62% to 18%; Table 16). The reduction of organoid viability was less in breast cancer organoid line BC-ORG 2 (from 62% to 49%; Table 16).

Table 16 Viability measurements of organoid line BC-ORG 2 and C-ORG 4 treated with oncolytic vaccinia viruses, 5-FC and 5-FU

Organoid line	GLV-0b347 MOI 0.1	GLV-0b347 MOI 1	GLV-0b347 MOI 10	5-FC	GLV-1h94 MOI 10	GLV-1h94 MOI 10 + 5-FC
BC-ORG 2	62%	54%	49%	67%	29%	21%
C-ORG 4	62%	38%	18%	75%	31%	8%

3.2.3.2 Response of control organoid cultures

We compared the effects of a vaccinia virus expressing a red fluorescent protein (RFP) (GLV-0b347) and a vaccinia virus expressing a suicide gene (GLV-1h94) in six organoid cultures derived from control breast tissue.

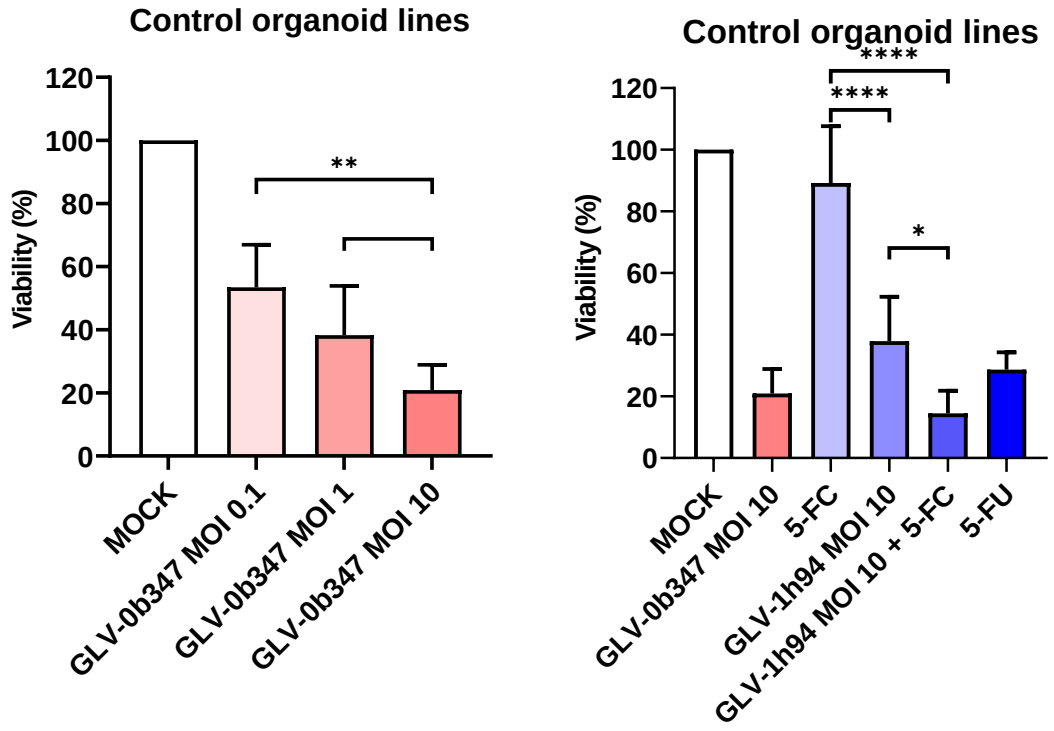

Figure 3-49 The effects of oncolytic vaccinia viruses on organoids derived from control breast tissue

*p < 0.05, **p < 0.01, ***p < 0.001, ****p < 0.0001 with t-test, n=6.

When we compared the mean effects for all 6 control organoid lines measured with the CellTiter-Blue Viability Assay, a one-way ANOVA demonstrated statistical significance ($p < 0.0001$; $F(6, 34) = 22.78$) between all groups. In addition, a statistically significant difference was also observed with a one-way ANOVA ($p < 0.002$; $F(2, 15) = 9.724$) between the three titres of GLV-0b347 (MOI 0.1., MOI 1, MOI 10), thereby indicating titre-dependent effects of the GLV-0b347 (Figure 3-49). The greater the concentration of GLV-0b347, the greater was the reduction of viability (MOI 0.1 vs. MOI 10, $p < 0.01$, Figure 3-49). The reduction in viability of the organoid cultures was not statistically

significant between GLV-0b347 and GLV-1h94 without the addition of the prodrug 5-FC (Figure 3-49). GLV-1h94 without the prodrug 5-FC resulted in a greater reduction of cell viability in comparison to the prodrug 5-FC alone ($p < 0.0001$; Figure 3-49). The addition of 5-FC to GLV-1h94 led to a statistically significant reduction in viability in comparison to GLV-h94 alone ($p < 0.05$; Figure 3-49). The addition of 5-FC to GLV-1h94 also led to a statistically significant reduction in viability in comparison to 5-FC ($p < 0.0001$; Figure 3-49). There was no significant difference between the viability of organoid cultures treated with GLV-0b347 compared to GLV-1h94 without the addition of the prodrug 5-FC (Figure 3-49).

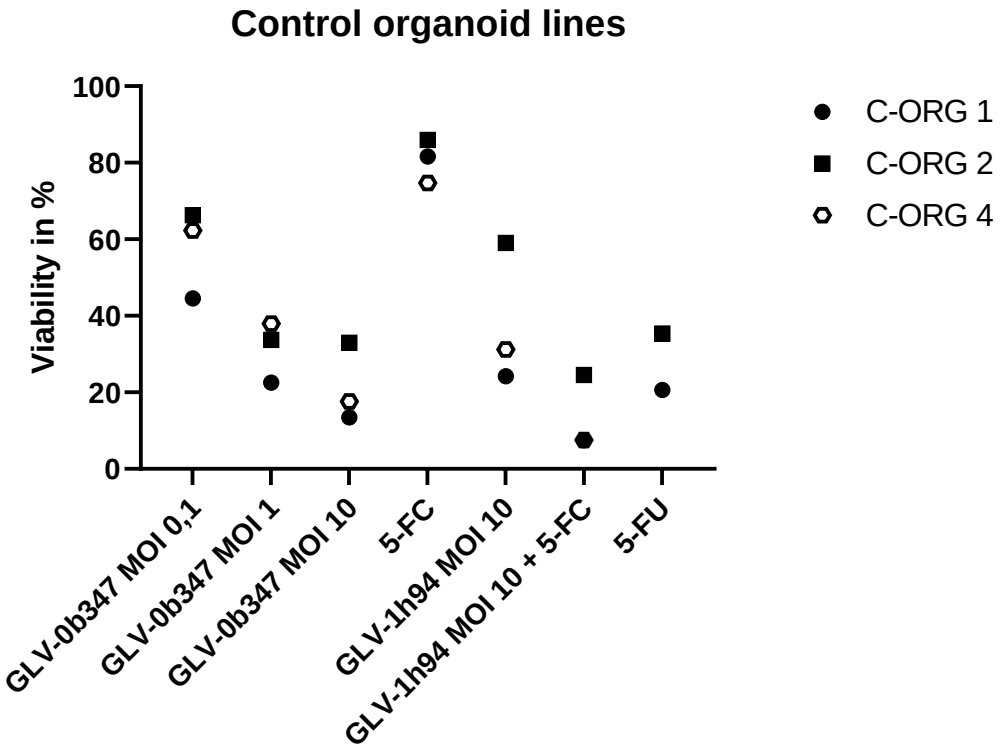

Figure 3-50 The effects of oncolytic vaccinia viruses on control organoid lines C-ORG 1, 2 and 4

Table 17 Viability measurements of organoid lines 1, 2 and 4 treated with oncolytic vaccinia viruses, 5-FC and 5-FU

Organoid line	GLV-0b347 MOI 0.1	GLV-0b347 MOI 1	GLV-0b347 MOI 10	5-FC	GLV-1h94 MOI 10	GLV-1h94 MOI 10 + 5-FC	5-FU
C-ORG 1	45%	23%	13%	82%	24%	7%	21%
C-ORG 2	66%	34%	33%	86%	59%	25%	35%
C-ORG 4	62%	38%	18%	75%	31%	8%	

The control organoid lines were successfully infected with oncolytic viruses. GLV-0b347 caused a viral titre dependent decrease of organoid viability. The decrease was largest in organoid line C-ORG 4 and smallest in organoid line C-ORG 2 (Table 17; Figure 3-50). Organoid line C-ORG 4 displayed the reddest fluorescing organoids in MOI 10. In lower viral concentrations the production of red fluorescent was comparable between the three organoid lines (MOI 0.1 in Figure 3-51). Interestingly, the sizes of organoids can vary within an organoid line as highlighted by the small white box in C-ORG 4 in Figure 3-51.

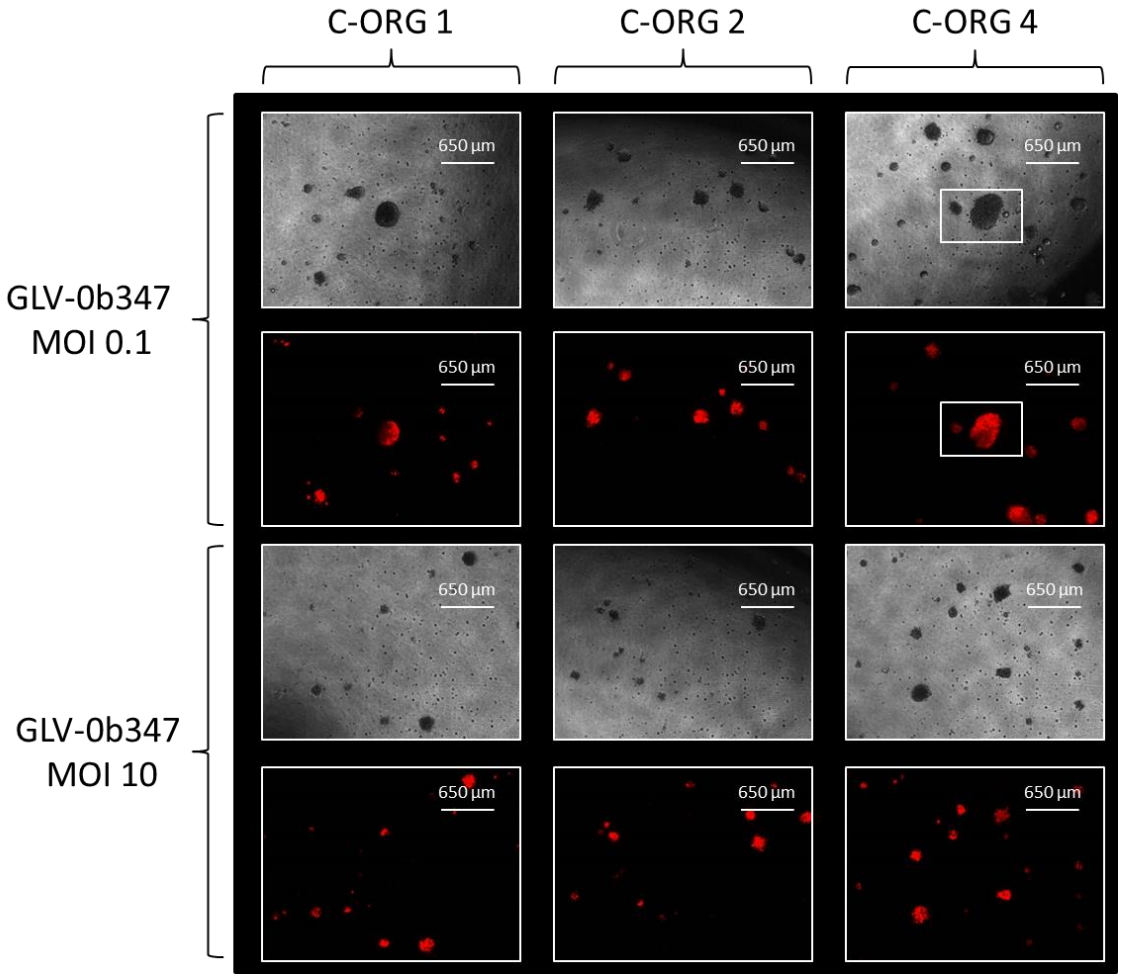

Figure 3-51 Treatment of control organoid lines C-ORG 1, 2 and 4 with GLV 0b347 MOI 0,1 and MOI 10 96 hpi

The infection of neighbouring organoids cannot be visualized directly but indirectly. The arrow in Figure 3-52 shows an initially uninfected organoid which after 48 hours produced red fluorescence indicating an infection with GLV-0b347. The neighbouring organoid (marked with a small white box in Figure 3-52) was already partially infected 48 hpi and the viral infection spread over the subsequent 48 h. However, not all neighbouring organoids were infected as seen in Figure 3-53.

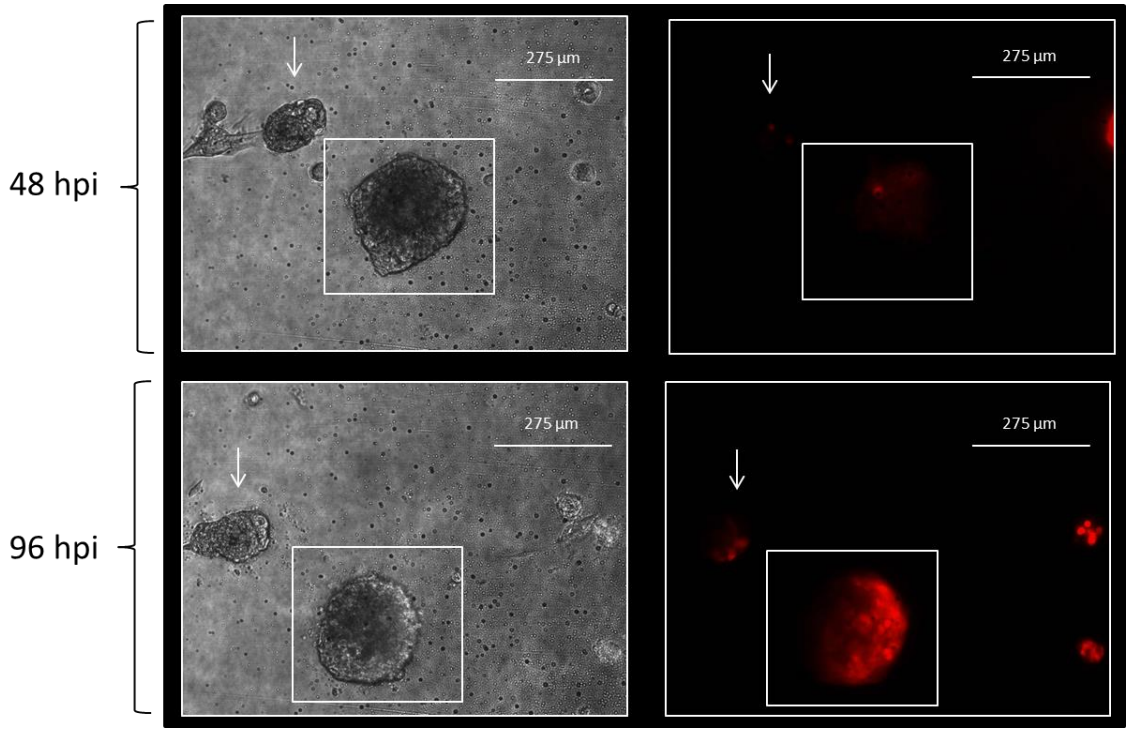

Figure 3-52 Treatment of control organoid line C-ORG 1 with GLV-0b347 MOI 0.1 48 hpi and 96 hpi

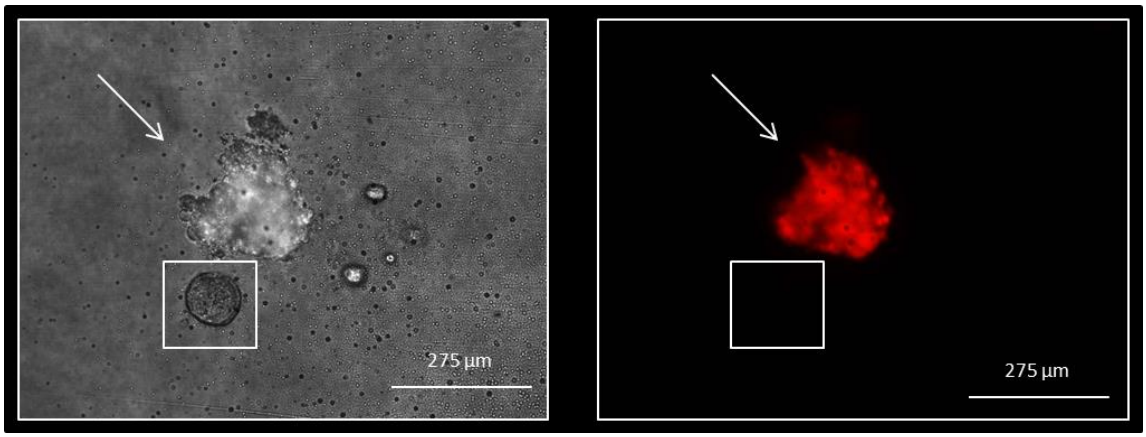

Figure 3-53 Treatment of control organoid line C-ORG 4 with GLV-0b347 MOI 1 96 hpi

The addition of GLV-1h94 resulted in a successful infection as seen by the green fluorescence (Figure 3-54). The production of green fluorescence appeared greater in the infection with GLV-1h94 without the addition of 5-FC (Figure 3-54). However, as seen with the breast cancer organoid lines, the reduction of organoid viability was greater when 5-FC was added to the infection with GLV-1h94 (Table 17).

The largest reduction in organoid viability was seen in control organoid line C-ORG 2 (reduction from 59% to 25%). Control organoid lines C-ORG 4 and C-ORG 1 showed a similar reduction of organoid viability (Table 17). The organoid viability for infections with GLV-1h94 + 5-FC were lower than the organoid viability for treatment with 5-FU alone (Table 17).

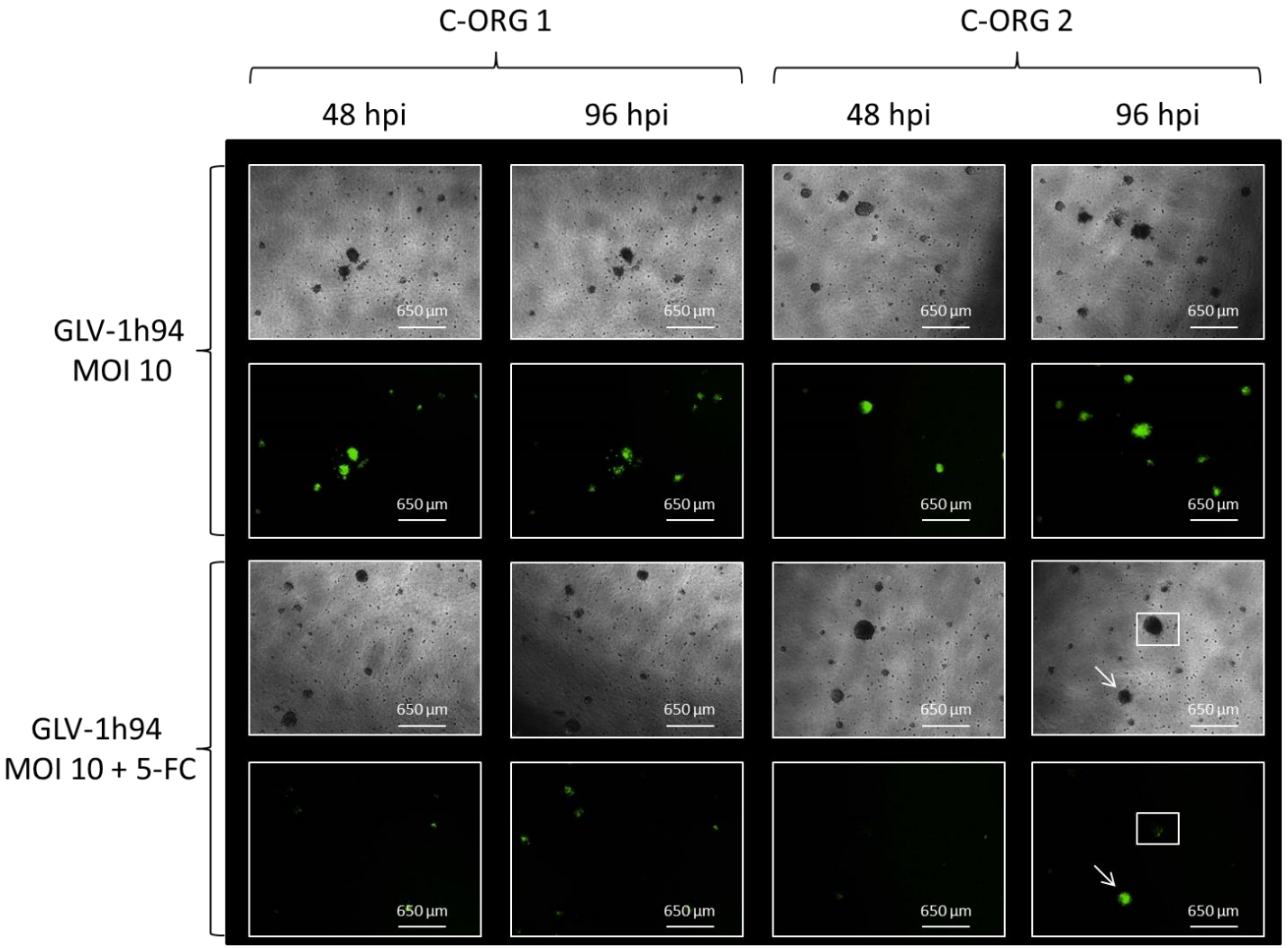

Figure 3-54 Treatment of organoid lines C-ORG 1 and 2 with GLV-1h94 MOI 10 and GLV-1h94 MOI 10 + 5-FC 48 hpi and 96 hpi

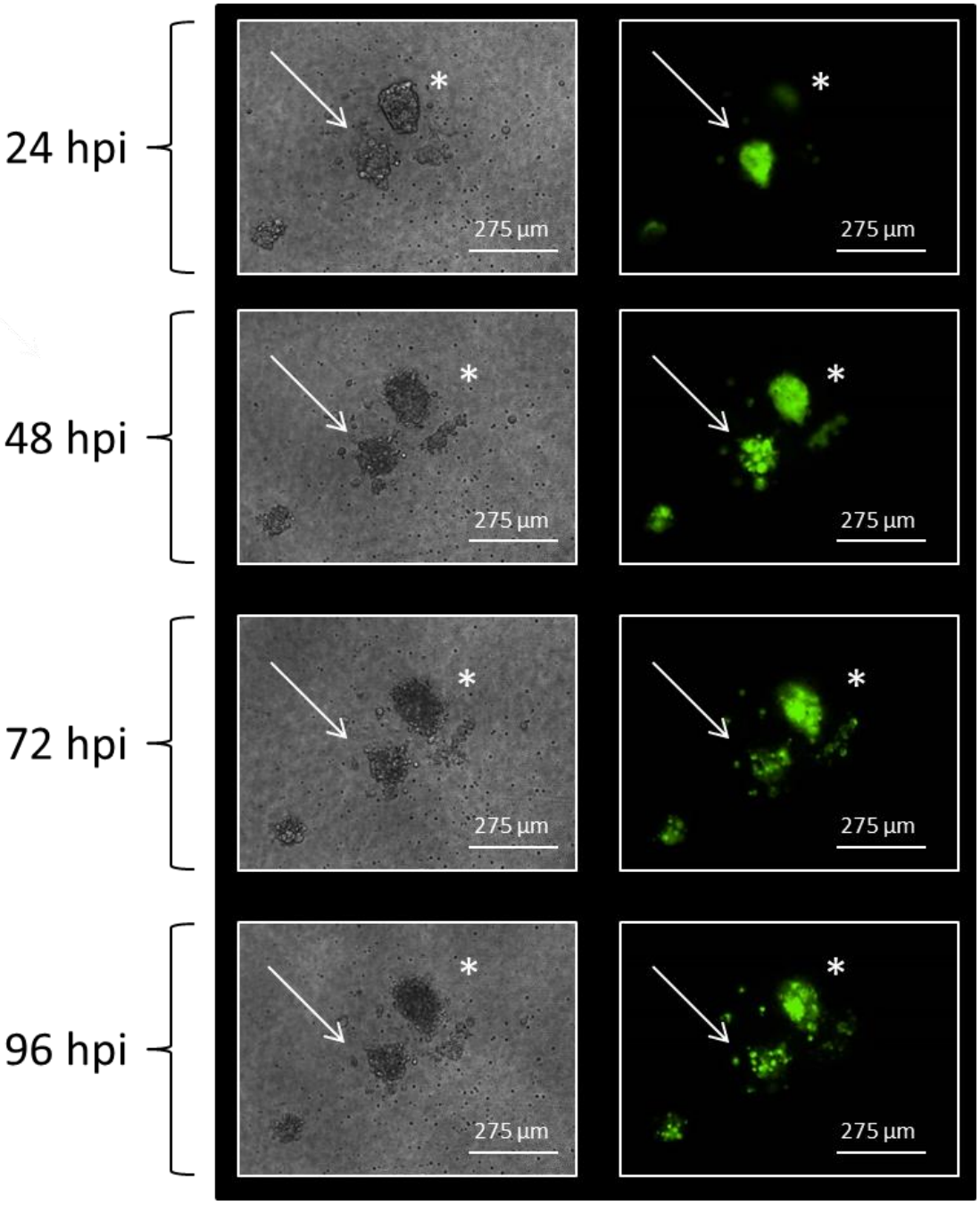

Figure 3-55 Treatment of organoid line C1 with GLV-1h94 MOI 10

The infection of neighbouring organoids can be seen in Figure 3-55. The organoid (marked with an arrow) was fully infected 24 hpi (Figure 3-55). After 72 h there was a reduction of green fluorescence and a fragmentation of the organoid indicating oncolysis caused by the oncolytic virus. The neighbouring organoid (marked with a star) exhibited a weak green fluorescence at 24 hpi and a greater green fluorescence the following 24 h, thereby indicating an

infection from the neighbouring organoid (Figure 3-55). Over the subsequent 48 h the organoid fragmented into several parts accompanied by a reduction of green fluorescence (Figure 3-55).

3.2.3.3 Response of organoid cultures derived from breast cancer cell lines

The effects of a vaccinia virus expressing RFP (GLV-0b347) and a vaccinia virus expressing a suicide gene and GFP (GLV-1h94) were compared in organoid cultures derived from breast cancer cell lines. The breast cancer cell lines T47D, MCF7 and MDA-MB-468 were used for organoid culture setup.

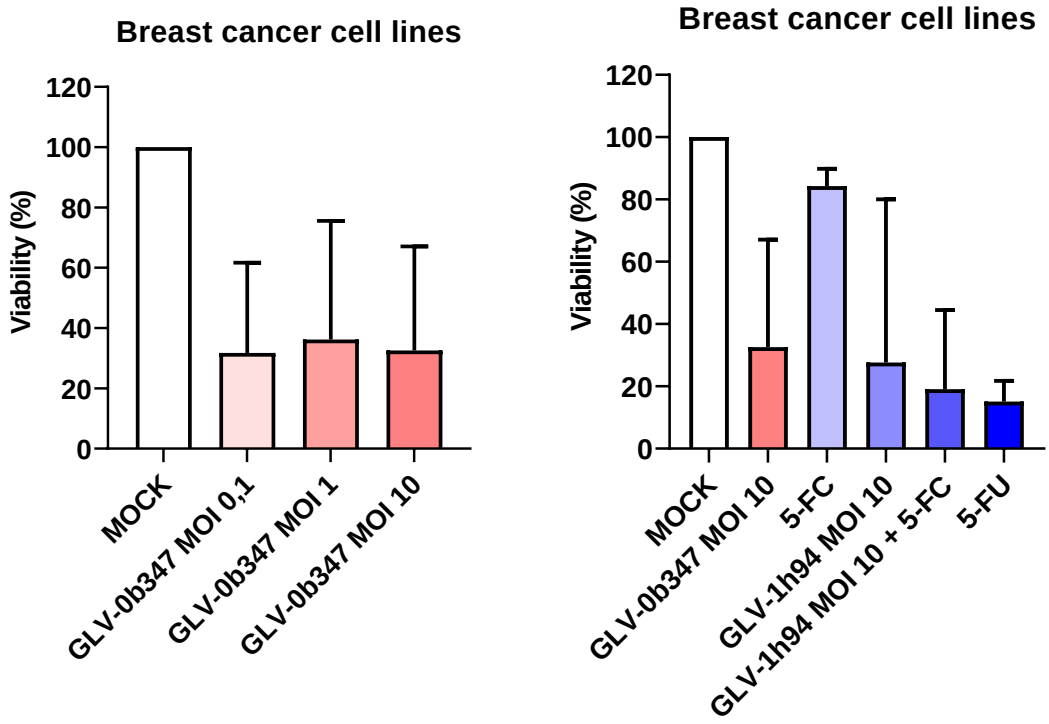

Figure 3-56 The effects of oncolytic vaccinia viruses on organoids derived from breast cancer cell lines (n=3)

There was no difference between the viral titres MOI 0.1, MOI 1 and MOI 10 for GLV 0b347 (Figure 3-56). However, the addition of the oncolytic viruses to the organoid culture resulted in a decrease of viability in compared to the prodrug alone (Figure 3-56). The addition of 5-FC to GLV 1h94 resulted in an additional loss of viability (Figure 3-56). The viability was comparable between the GLV 1h94 with 5-FC and the application of 5-FU alone (Figure 3-56).

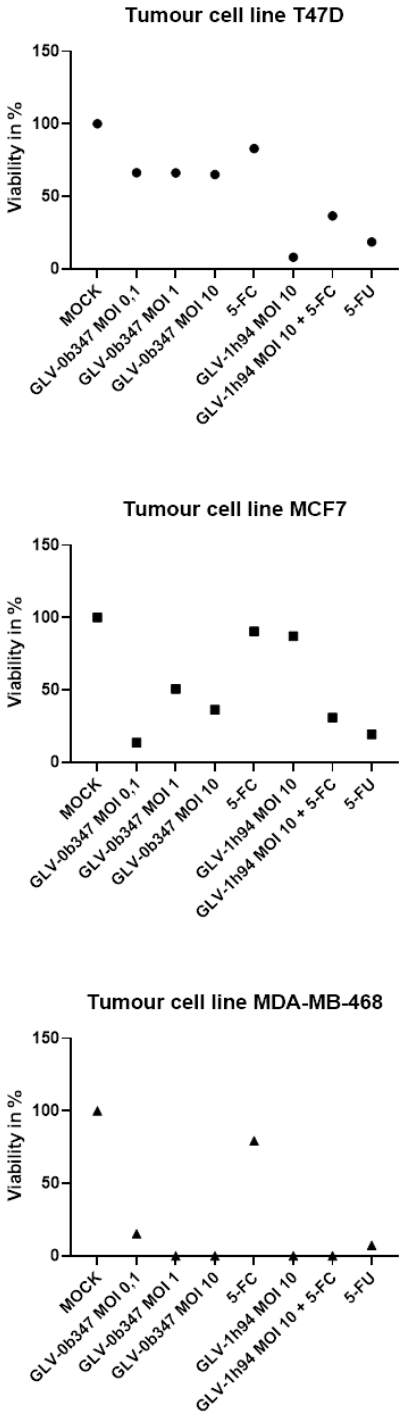

Figure 3-57 The effects of oncolytic vaccinia viruses on organoid lines derived from breast cancer tumour cell lines T47D, MCF7 and MDA-MB-468

Table 18 Viability measurements for T47D, MCF7 and MDA-MB-468 for infection with oncolytic vaccinia viruses

Organoid line	GLV-0b347 MOI 0.1	GLV-0b347 MOI 1	GLV-0b347 MOI 10	5-FC	GLV-1h94 MOI 10	GLV-1h94 MOI 10 + 5-FC	5-FU
T47D	66 %	66 %	65 %	83 %	8%	37 %	19%
MCF 7	14 %	51%	36%	90%	87%	31%	19%
MDA-MB-468	15%	0%	0%	79%	0%	0%	7%

The organoid lines derived from breast cancer cell lines responded differently to the treatment with oncolytic viruses (Figure 3-57). The three organoid lines formed different sizes of organoids (Figure 3-58). The organoid from tumour cell line MCF7 were larger as compared to T47D and MDA-MB-468, whereas organoids derived from MDA-MB-468 were smaller in size (Figure 3-58). The increase of viral concentration resulted in an increase of red fluorescence, an observation that indicates a larger viral spread in GLV 0b347 MOI 10 (Figure 3-58) as seen in the breast cancer and control organoid lines mentioned previously. The increase of viral load did not result in significant lower organoid viability for T47D and MCF 7 (Table 18). However, reduction of organoid viability could be observed for MDA-MB-468 (Table 18).

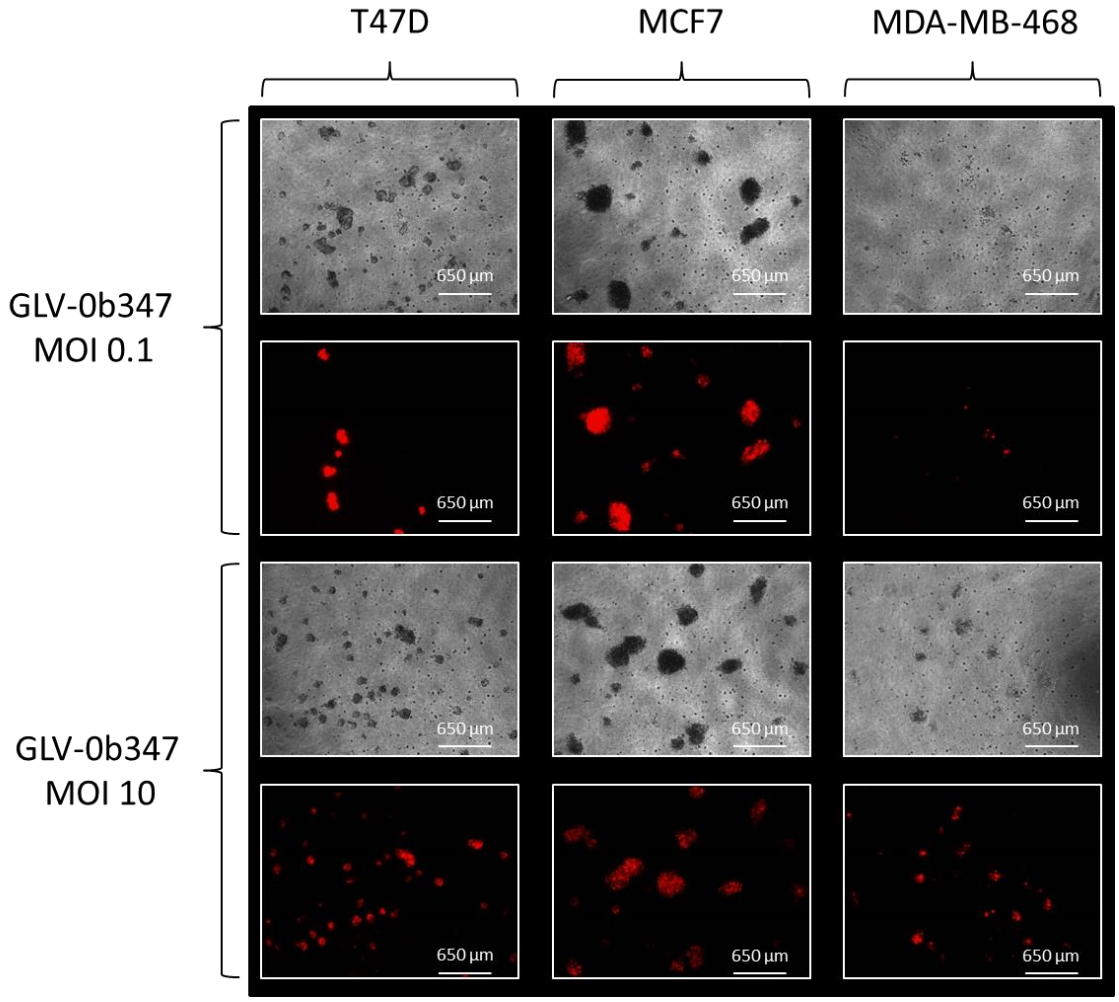

Figure 3-58 Treatment of organoid lines T47D, MCF7 and MDA-MB-468 with GLV-0b347 MOI 0.1 and GLV-0b347 MOI 10 96 hpi

A differential dose response of the tumour cell lines for GLV-1h94 was observed. The viral spread seen by the green fluorescence was comparable to the response of breast cancer and control organoid lines. More green fluorescence can be detected when infecting organoids with GLV-1h94 than infection with GLV-1h94 + 5-FC (Figure 3-59, Figure 3-60, Figure 3-62). The infection of T47D showed a greater reduction in organoid viability for GLV-1h94 (8%) than for GLV-1h94 + 5-FC (36%; Table 18). The infection of MCF7 with GLV-1h94 + 5-FC resulted in a lower organoid viability than the infection GLV-1h94 (Table 18). The infection of MDA-MB-468 with GLV-1h94 and GLV-1h94 + 5-FC resulted in 0% organoid viability as seen by the fully dissolved organoids (Figure 3-62, Table 18). Figure 3-61 shows the full fragmentation of organoids

into single cells. The organoids of tumour cell lines displayed oncolytic activity in the same way as breast cancer and control organoid lines. The organoids fragmented into several parts through oncolysis as seen with breast cancer and control organoid lines (Figure 3-61).

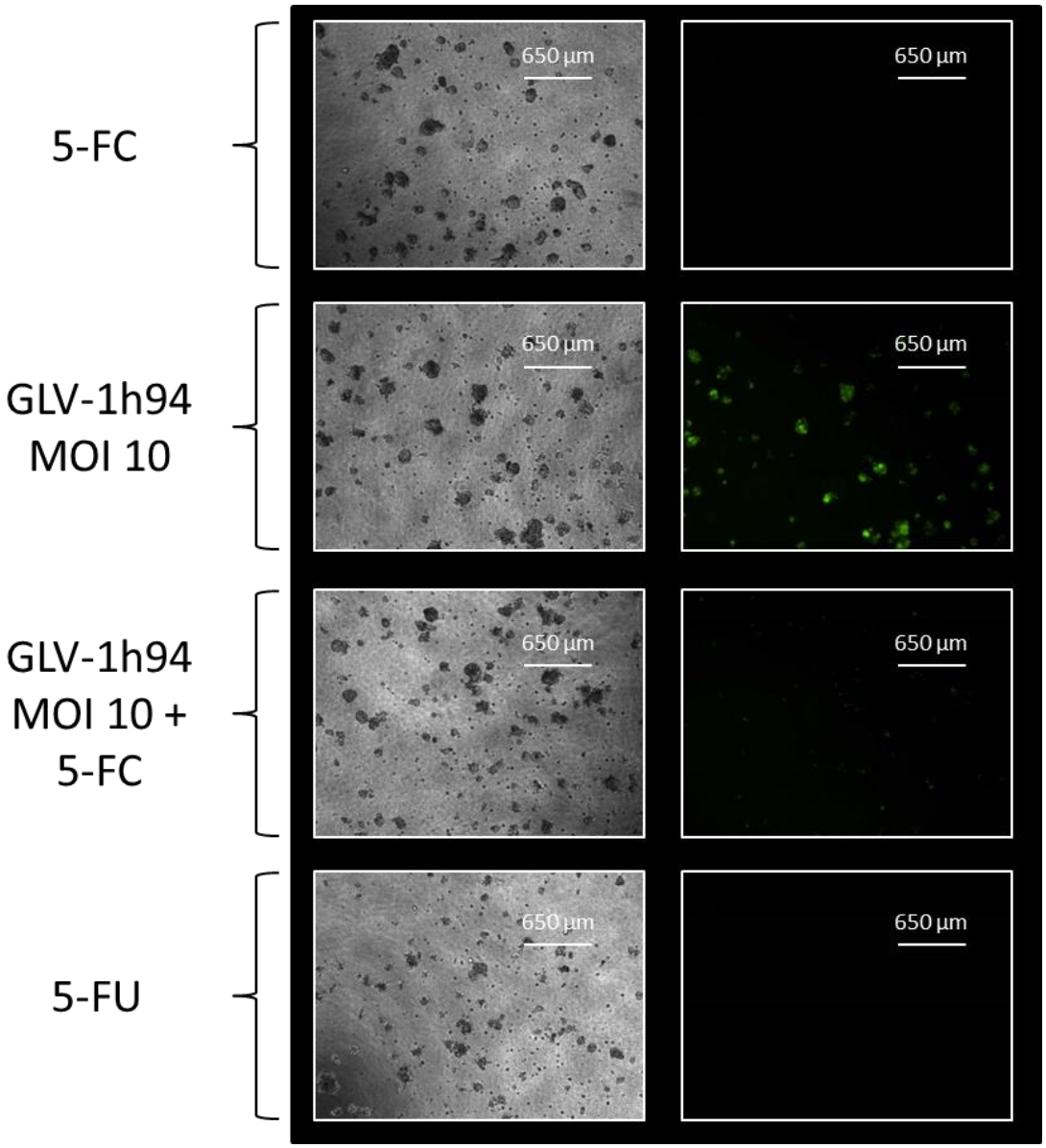

Figure 3-59 Treatment of organoid line T47D with 5-FC, GLV-1h94 MOI 10, GLV-1h94 MOI + 5-FC and 5-FU 96 hpi

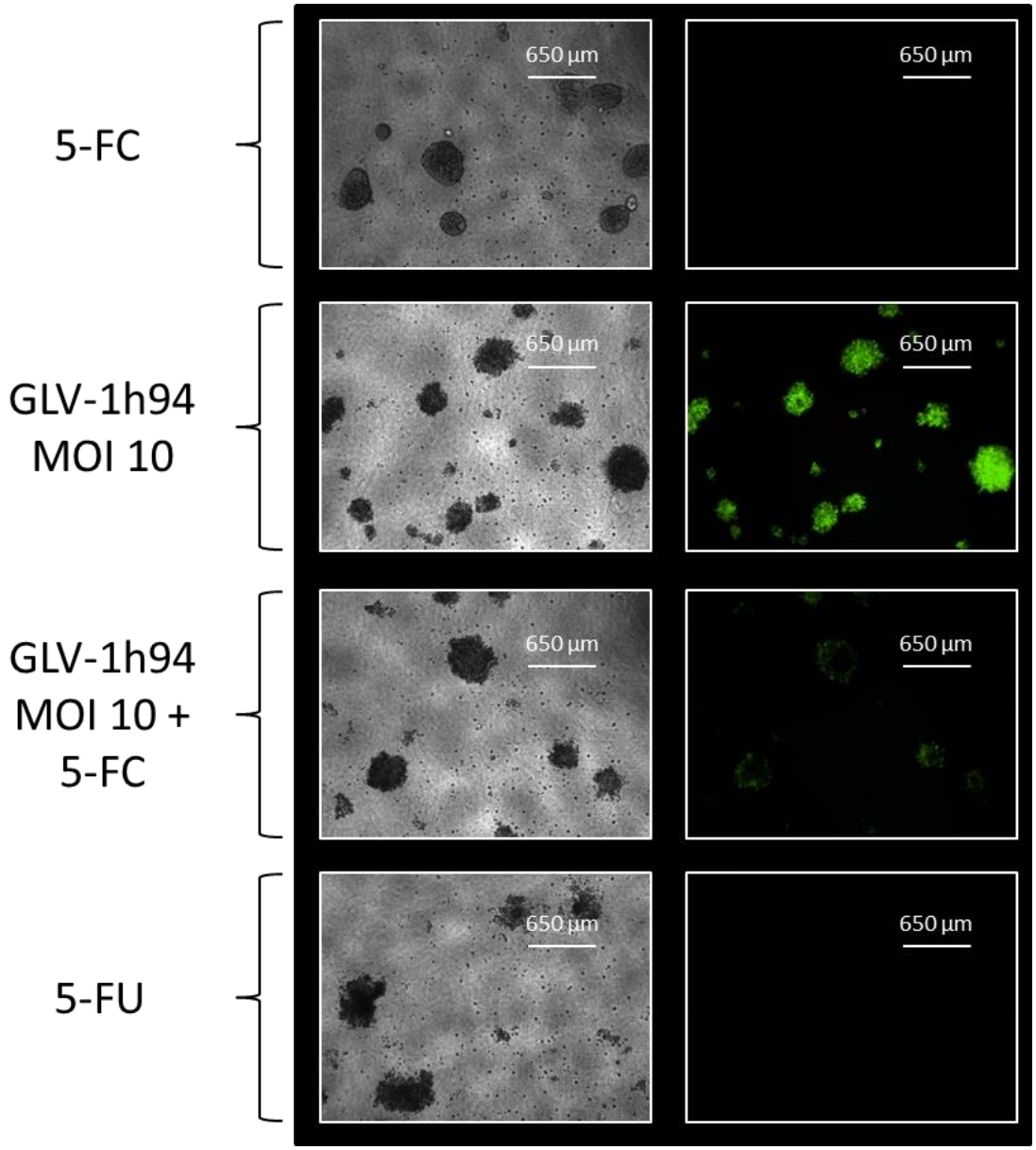

Figure 3-60 Treatment of organoid line MCF7 with 5-FC, GLV-1h94 MOI 10, GLV-1h94 MOI + 5-FC and 5-FU 96 hpi

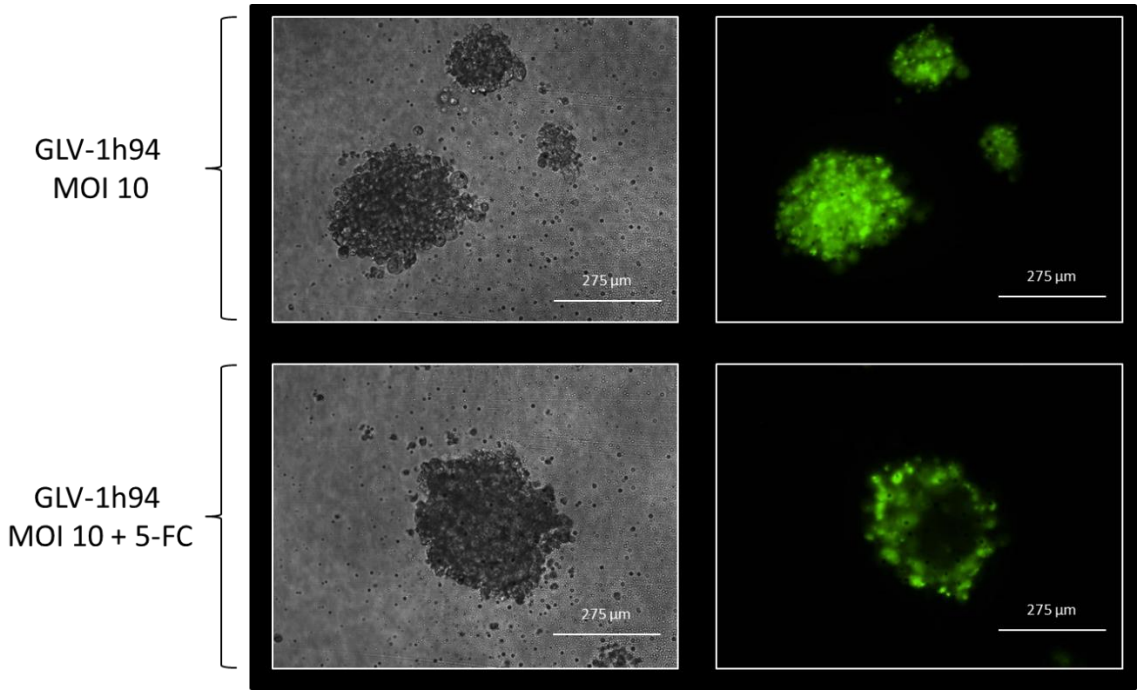

Figure 3-61 Treatment of organoid line MC7 with GLV-1h94 MOI 10 and GLV-1h94 MOI 10 + 5-FC 96 hpi

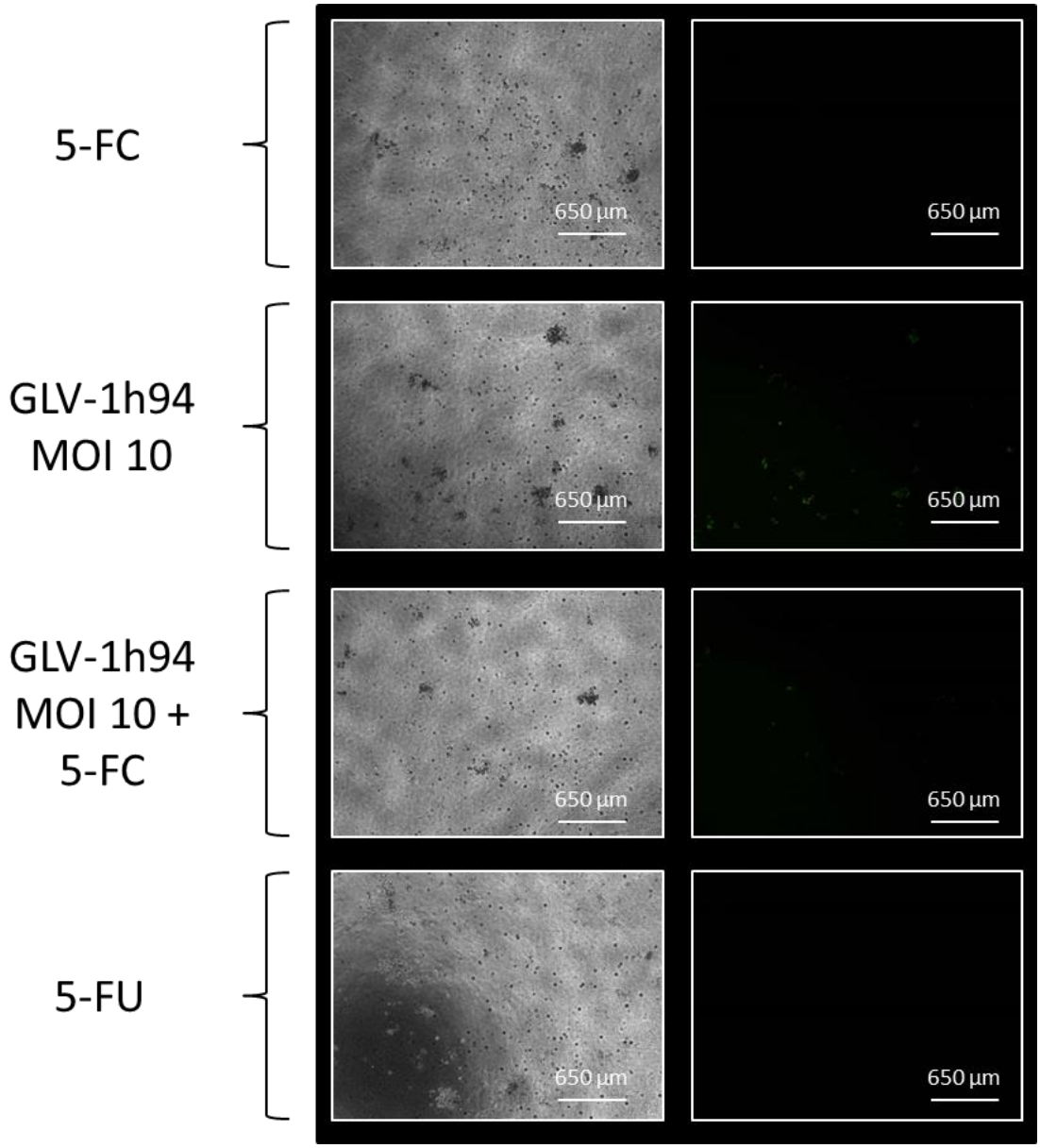

Figure 3-62 Treatment of organoid line MDA-MB-468 with 5-FC, GLV-1h94 MOI 10, GLV-1h94 MOI + 5-FC and 5-FU 96 hpi

4 Discussion

The results of this study show that it was possible to establish organoid cultures from patients with breast cancer and corresponding control tissue. Furthermore, the method allowed the long-term cultivation of such organoids. The findings also showed that it was possible to demonstrate the effects of two different oncolytic viruses, namely measles and vaccinia virus, in the organoid cultures. Indeed, the method was sensitive enough to detect titre-dependent responses and the different effects of oncolytic viruses that had been genetically engineered to express suicide genes provided the appropriate substrate was present in the culture medium. Thus, the model has the potential to determine the most effective and efficient oncolytic virus treatment for breast cancer based on a patient-derived model, thereby allowing improved and personalized treatment of breast cancer in future. There is still an urgent need to develop patient-derived experimental systems such as our organoid model that mimic the response of breast cancer to oncolytic agents in preparation of testing different oncolytic viruses in clinical trials [110].

The treatment options for metastatic breast cancer are limited and currently this stage remains incurable [25]. Therefore, new treatment approaches are needed. New treatment schemes and modalities should emphasize tumour selective treatment and ideally be based on patient specific characteristics of breast cancer. The aim of therapy is to prolong overall survival while at the same time improving or at least stabilizing quality of life.

Oncolytic viruses are emerging as promising agents for the treatment of cancer because they selectively infect and damage cancerous tissues without causing harm to normal tissue [74]. They offer an attractive combination of tumour-specific cell lysis coupled with immune stimulation through release of tumour antigens and/or other signals to overcome immunosuppression in the tumour microenvironment. Oncolytic viruses achieve tumour-specific lysis in three different ways [131]. Firstly, they can enter cells via virus-specific, receptor-mediated mechanisms. Secondly, increased viral replication may be supported by rapid cell division in tumour cells. And thirdly, tumour cells support selective

virus replication because they often demonstrate deficits in antiviral type I IFN signalling [131].

Personalized treatment with oncolytic virotherapy of breast cancer patients relies on the availability of a suitable experimental patient-derived breast cancer model. This will facilitate the transformation of treatment options from bench to bedside. Currently established models for breast cancer research include human tumour cell lines, rodent xenografts, and SCID mice [60, 61, 67]. These models have major disadvantages and may only insufficiently represent the patterns of the original cancer patient tumour tissues [61, 67]. In contrast, a three-dimensional organoid model based on patient-derived tumour samples should be able to recapitulate the structure of the original tumour and capture disease heterogeneity and the characteristics of the patient's individual tumour [60, 71]. Sachs et al. showed the majority of breast cancer organoids matched the original breast cancer characteristics based on typical classifications of breast cancer such as histology [71]. A patient-derived organoid model may therefore allow personalized treatment in the future.

Breast cancer and control organoids were successfully and reproducibly established from tissue samples in this study. Many different tumour samples were used to capture the heterogeneity of breast cancer. The experiments were set out to compare breast cancer organoids and control organoids. When possible, control tissue from breast cancer patients was obtained. As this was not always possible control tissue from patients who did not have breast cancer was obtained to investigate the specificity of the treatment scheme for breast cancer.

Breast cancer and control organoids were cultured individually. The culture medium was the same for both types of organoids. The shape and sizes of organoids varied in both groups. The imaging of the organoids did not allow for a clear differentiation between control and breast cancer organoids. However, the initial growth pattern of the two groups differed. The control organoids initially contained more single cells which then grew into individual organoids. The breast cancer organoids generally contained more cell clusters that grew

into organoids more quickly. This difference in growth pattern indicated a generally higher proliferation rate of tumour cells in comparison to normal cells. After 2-3 passages the single cells grew into organoids in both groups and did not differ in their growth pattern. It was possible to use the organoid model in the longer term (> 10 passages). The utilization of this model for future research should therefore be possible.

The aim of the histological comparison was to compare the expression of ER, PR, Her2 and Ki67 with the original expression rates of the breast cancer tissue sample. The results were available for all breast cancer tissue samples and all breast cancer organoids underwent histological comparison. All organoid cultures (breast cancer and control) were negative for ER, PR and Her2 (view 3.1.3). These findings seemed to contradict the original publications on breast cancer organoids [71]. However, more recently this problem has been found to be the case for organoid cultures derived from breast cancer samples. Goldhammer *et al.* found ER stainings to be unsuccessful in all breast cancer organoid samples used [132]. Sachs *et al.* investigated the ER expression in breast cancer organoids in comparison to breast cancer tissue samples. Not all organoid cultures from ER-positive breast cancer samples yielded ER-positive breast cancer organoids [71]. PR expression rates showed a similar trend, not all PR-positive tumours grew PR-positive organoids [71]. Additionally, breast cancer organoids were classified as ER or PR positive, if more than 1% of the cells in organoids were ER or PR positive. Therefore, organoids with 5% or 100% positive cell were all classified as ER or PR positive organoid lines. The Her2 histological comparison demonstrated similar results [71]. A more recent investigation into the ER expression of breast cancer organoids showed a 10% expression of breast cancer organoids for ER. Low expression rates for PR were detected within breast cancer organoids [133]. Recent research with breast cancer explant cultures grown in three-dimensional matrix scaffolds has shown that ER expression is regulated by matrix stiffness via stress-mediated p38 activation and H3K27me3-dependent epigenetic chromatin remodelling [134]. More research is needed to understand the factors influencing expression

of all the three markers (ER, PR and Her2) in organoid cultures compared to the original breast cancer.

The goal of the study was to determine the effects of oncolytic therapy in organoid cultures derived from breast cancer patients. As no published method for assessing oncolytic virotherapy in an organoid model was available a new protocol needed to be developed. All protocols used in these experiments for oncolytic virotherapy showed a successful oncolytic virotherapy as demonstrated by detection of fluorescence by microscopic imaging and reduction of organoid viability measured with the Cell Titer-Blue Cell Viability Assay. To improve viral spread the time-point of infection was altered in relation to the passaging process to allow infection of organoids in a three-dimensional setup rather than single cells being infected in a three-dimensional setup. This resulted in a more homogenous distribution of the viral infection through the culture setup und enhanced reduction of organoid viability. However, it is important to note that Matrigel can interfere with the Cell Titer-Blue Cell Viability Assay and measurements need to be corrected. Therefore, we set out to test whether single cells contained in the organoid setup interfere with the Cell Titer-Blue Cell Viability Assay. To determine the lowest possible viability, organoids were treated with staurosporine. Staurosporine is a strong inducer of apoptosis and should result in 0% organoid viability [135]. However, this theoretical response was not achieved for all organoid lines as some measurements revealed a viability of up to 20%. Thus the staurosporine vitality measurements were not considered reliable enough to use as a correction factor for the measured organoid viabilities.

Typically, viruses exhibit a specific cellular tropism that determines which tissues and/or hosts are preferentially infected. Oncolytic viruses can be classified into three different groups; (1) oncolytic viruses with natural anti-neoplastic properties, (2) oncolytic viruses designed for tumour-selective replication, and (3) armed oncolytic viruses [115]. Four different oncolytic viruses were tested in the organoid model. Two viruses had a naturally occurring oncolytic activity (MeV-GFP and GLV-0b347) and two viruses had additionally been armed with suicide genes to enhance their naturally occurring

oncolytic activity (MeV-SCD and GLV-1h94). MeV-GFP and GLV-0b347 were genetically modified to express a green fluorescent protein (MeV-GFP) or a red fluorescent protein (GLV-0b347) (Figure 1-2, Figure 1-4).

The insertion of the suicide gene to the measles virus genome allowed evaluation of the additional influence of the suicide gene on organoid viability. The prodrug 5-FC did not significantly reduce organoid viability (Figure 3-22). However, when 5-FC was added to viral infection with MeV-SCD, the oncolytic effects were significantly enhanced and comparable to the cytotoxic effects of the active metabolite 5-FU (Figure 3-22). The trend seen for MeV-SCD could also be seen for GLV-1h94 (Figure 3-39). Numerically, similar results were seen for infection of control organoids. However, most likely due to the small number of control organoid lines, these effects did not reach statistically significance.

GLV-0b347 and GLV-1h94 are both vaccinia viruses, yet include a different genetic backbone. GLV-0b347 includes a *Western Reserve* backbone and GLV-1h94 includes a *Lister* backbone (see 1.5.3). As previous research had demonstrated different distribution rates of the viruses in different types of tissues, vaccinia viruses with different backbones were used for the experiments [127]. However, the reduction in organoid viability between GLV-0b347 MOI 10 and GLV-1h94 MOI 10 was comparable (Figure 3-39), suggesting a similar distribution of different vaccinia viruses in breast cancer tissue.

The spread of oncolytic viruses during the 96 h of infection was not counted as the expression of green and red fluorescent protein and morphological changes were monitored through microscopy. During the time period of 96 h the expression of GFP or RFP increased which can be interpreted as active viral replication in the tumour cells. However, it cannot be excluded that the increase of fluorescence is due to continuous expression of fluorescence from the initial infection. A future modification of this model may be to incorporate other methods to quantify the replication of new oncolytic viruses within the organoids.

The difference in the reduction of organoid viability between breast cancer organoid lines and control organoid lines was small. They responded similarly to the treatment with oncolytic viruses. The spread of oncolytic viruses was comparable over 96 h and visualization of the oncolytic viral infection (expression of fluorescent proteins and morphological changes of the organoids) did not differ. The organoid viability measurements were also similar. Based on the results, a clear distinction between the effects of oncolytic viruses on breast cancer organoid lines and control organoid lines was not possible. This may be because of the lack of immune cells in the organoid model, as oncolytic viruses exert their maximum antitumour effect in the presence of an intact immune system. For example, measles viruses normally induce an IFN-β response which triggers an immune response directed against infected cells [116]. Tumour cells often have mutations in IFN signalling resulting in an enhanced spread of oncolytic viruses throughout the tumour that is facilitated by the subsequent immune response [78]. As breast cancer organoids and control organoids were cultivated in the absence of immune cells the effects of a potential immune response could not be evaluated. Dijkstra *et al.* successfully incorporated peripheral blood monocytes derived from patient blood samples into the corresponding colon and lung cancer organoid setup. The T-cell attack infiltration of the patient's cancer organoids could be measured and showed efficient killing of cancer organoids [136]. The addition of patient-derived peripheral blood monocytes to a breast cancer organoid setup could be a next step to improve the model yet further. This would allow a more accurate representation of the tumour environment and could allow an investigation of the interaction between the immune system and the efficacy of oncolytic viruses.

The incorporation of immune cells into the organoid cultivation would also allow the evaluation of oncolytic viruses that have been engineered to enhance for triggering an immune response against tumour cells specifically. For example, OncoVEX$^{GM\text{-}CSF}$ is a promising oncolytic virus in the category of armed oncolytic viruses. The virus is based on a herpes-simplex virus 1 strand [96]. The virus interferes with the IFN-pathway resulting in enhanced tumour selectivity [135].

An additional genetic modification results in a higher production of class I major histocompatibility complex (MHC) molecules important for triggering an immune response against the host cells [136, 137]. The viral genome has been genetically modified to include a GM-CSF gene [138]. The number of T-cells is reduced by the expression of GM-CSF through an induction of an antigen-specific T-cell response [97]. This virus offers a wide variety of genetic modifications and needs to be compared to other oncolytic viruses in an organoid model. OncoVEX^{GM-CSF} was approved by the United States Food and Drug Administration and the European Medicines Agency to treat advanced melanoma [138].

The protocol could also be used to assess other currently available oncolytic viruses such as OncoVEX^{GM-CSF} and test them on breast cancer organoids to establish a panel most likely to be effective for oncolytic virotherapy of breast cancer. The viruses included in this panel should combine different approaches such as viruses with naturally occurring oncolytic potential, genetically modified virus for tumour selectivity and armed oncolytic viruses for enhanced cell killing or enhanced triggering of an immune response.

In conclusion, this study shows that it was possible to develop a protocol that could be used to assess the effects of different oncolytic viruses on cell viability in established patient-derived organoid cell cultures from breast cancer tissue. The greatest oncolytic effects were observed with oncolytic viruses engineered to express a suicide gene (MeV-SCD; GLV-1h94) in the presence of the prodrug 5-FC. Thus the model provides a promising *in vitro* method for investigating the effects of different oncolytic viruses for treating breast cancer, thereby facilitating the correlation to *in vivo* results. The next step would be to compare and contrast the effects of other oncolytic viruses such as OncoVEX^{GM-CSF} and test them on breast cancer organoids to establish a panel most likely to be effective for oncolytic virotherapy of breast cancer. The viruses included in this panel should combine different approaches such as viruses with naturally occurring oncolytic potential, genetically modified virus for tumour selectivity and armed oncolytic viruses for enhanced cell killing or enhanced triggering of an immune response.

5 Summary

Although several oncolytic viruses have already been tested in early-stage clinical studies of breast cancer, there is still an urgent need to develop patient-derived experimental systems that mimic the response of breast cancer to oncolytic agents in preparation of testing different oncolytic viruses in clinical trials. We addressed this need by developing a protocol to study the effects of oncolytic viruses in stable organoid cell cultures derived from breast cancer tissue and control tissue.

We used an established three-dimensional organoid model derived from tissue of 10 patients with primary breast cancer. Furthermore, we established an organoid model derived from healthy control tissue from 6 patients.

We developed an experimental protocol for infecting organoid cultures with oncolytic viruses and compared the oncolytic effects of a measles vaccine virus (MeV) and a vaccinia virus (GLV) genetically engineered to express either green fluorescent protein (MeV-GFP) and red fluorescent protein (GLV-0b347), respectively, or a suicide gene encoding a fusion of cytosine deaminase with uracil phosphoribosyltransferase (MeV-SCD and GLV-1h94, respectively), thereby enabling enzymatic conversion of the prodrug 5-fluorocytosine (5-FC) into cytotoxic compounds 5-fluorouracil (5-FU) and 5-fluorouridine monophosphate (5-FUMP).

The method demonstrated that all four oncolytic viruses significantly inhibited cell viability in organoid cultures derived from breast cancer tissue. The oncolytic effects of the oncolytic viruses expressing suicide genes (MeV-SCD and GLV-1h94) were further enhanced by virus-triggered conversion of the prodrug 5-FC to toxic 5-FU and toxic 5-FUMP.

The model therefore provides a promising in vitro method to help further testing and engineering of new generations of virotherapeutic vectors for in vivo use.

6 German Summary

Verschiedene onkolytische Viren werden derzeit in frühen klinischen Studien untersucht. Dennoch besteht ein dringender Bedarf zur Etablierung von patientenabgeleiteten Modellen, um das Ansprechen von Mammakarzinomen auf onkolytische Viren vorherzusagen und zukünftige klinische Studien zielgenauer vorbereiten zu können. Um diesen Bedarf zu decken, haben wir ein Protokoll entwickelt, welches die Infektion eines stabilen aus Mammakarzinom- oder Kontrollgewebeproben etablierten Modells mit onkolytischen Viren erlaubt.

Für die Untersuchung wurde ein etabliertes dreidimensionales Organoidmodell verwendet, welches aus Gewebeproben von zehn Patientinnen mit Mammakarzinom stammte. Zusätzlich wurde ein Organoidmodell aus Kontrollgewebeproben etabliert. Wir haben ein experimentelles Protokoll zur Infektion von Organoidkulturen mit onkolytischen Viren entwickelt, um den onkolytischen Effekt von einem Masernvirus (MeV) und Vacciniavirus (GLV) zu untersuchen. Die Viren waren jeweils genetisch verändert zur Expression eines grün fluoreszierenden (MeV-GFP) oder eines rot fluoreszierenden Marker-Proteins (GLV-0b347), oder genetisch verändert zur Expression eines therapeutisch wirksamen Suizidgens, welches für ein Fusionsprotein aus Cytosindeaminase mit Uracil-Phosphoribosyltransferase codiert (MeV-SCD; GLV-1h94). Letzteres ermöglicht hierbei die enzymatische Konversion des Prodrug 5-Fluorocytosin (5-FC) zum zytotoxischen Produkt 5-Fluorouracil und weiter zu 5-Fluorouridinmonophosphat (5-FUMP).

Im Ergebnis gelang die Entwicklung eines Protokolls, mit dem der Effekt zwei verschiedener onkolytischer Virusgruppen in einem von Mammakarzinom- und Kontrollgewebe stammenden Organoidmodell beurteilt werden konnte. Den stärksten onkolytischen Effekt zeigten dabei onkolytische Viren, welche über das eingebrachte Suizidgen (MeV-SCD; GLV-1h94) das Prodrug 5-FC in 5-FU toxifizierten. Auf Basis dieses *in vitro* Modells könnte es möglich werden, künftig für den Patienten individuelle Virotherapeutika bereits vor deren Erstanwendung zu priorisieren.

7 References

1. Siegel, R.L., et al., *Cancer Statistics, 2021.* CA Cancer J Clin, 2021. **71**(1): p. 7-33.
2. Society, A.C., *Cancer Facts & Figures 2019*. 2019, Atlanta: American Cancer Society.
3. Edge, S.B., et al., *AJCC cancer staging manual*. Vol. 7. 2010: Springer New York.
4. Fabbri, A., M.L. Carcangiu, and A. Carbone, *Histological Classification of Breast Cancer*, in *Breast Cancer: Nuclear Medicine in Diagnosis and Therapeutic Options*, E. Bombardieri, L. Gianni, and G. Bonadonna, Editors. 2008, Springer Berlin Heidelberg: Berlin, Heidelberg. p. 3-14.
5. Elston, C.W. and I.O. Ellis, *pathological prognostic factors in breast cancer. I. The value of histological grade in breast cancer: experience from a large study with long-term follow-up.* Histopathology, 1991. **19**(5): p. 403-410.
6. Joe, B.N. *Clinical features, diagnosis, and staging of newly diagnosed breast cancer*. 2020 [cited 2020 29.02]; Available from: https://www.uptodate.com/contents/clinical-features-diagnosis-and-staging-of-newly-diagnosed-breast-cancer?search=classification%20breast%20cancer&source=search_result&selectedTitle=1~150&usage_type=default&display_rank=1#H1583246042.
7. Bleiweiss, I.J. *Pathology of breast cancer*. 2020 [cited 2020 29.02.2020]; Available from: https://www.uptodate.com/contents/pathology-of-breast-cancer?search=breast%20cancer&topicRef=744&source=see_link#H1220079795.
8. Orvieto, E., et al., *Clinicopathologic characteristics of invasive lobular carcinoma of the breast: results of an analysis of 530 cases from a single institution.* Cancer, 2008. **113**(7): p. 1511-1520.
9. Winchester, D.J., et al., *A comparative analysis of lobular and ductal carcinoma of the breast: presentation, treatment, and outcomes.* Journal of the American College of Surgeons, 1998. **186**(4): p. 416-422.
10. Pestalozzi, B.C., et al., *Distinct clinical and prognostic features of infiltrating lobular carcinoma of the breast: combined results of 15 International Breast Cancer Study Group clinical trials.* Journal of clinical oncology : official journal of the American Society of Clinical Oncology, 2008. **26**(18): p. 3006-3014.
11. Li, C.I., R.E. Moe, and J.R. Daling, *Risk of mortality by histologic type of breast cancer among women aged 50 to 79 years.* Archives of internal medicine, 2003. **163**(18): p. 2149-2153.
12. Cristofanilli, M., et al., *Invasive lobular carcinoma classic type: response to primary chemotherapy and survival outcomes.* Journal of clinical oncology : official journal of the American Society of Clinical Oncology, 2005. **23**(1): p. 41-48.
13. Ferlicot, S., et al., *Wide metastatic spreading in infiltrating lobular carcinoma of the breast.* European Journal of Cancer, 2004. **40**(3): p. 336-341.

14. Theodoros Foukakis, M., PhD, Jonas Bergh, MD, PhD, FRCP (London UK). *Prognostic and predictive factors in early, non-metastatic breast cancer*. 2020 [cited 2020 01.03.2020]; Available from: https://www.uptodate.com/contents/prognostic-and-predictive-factors-in-early-non-metastatic-breast-cancer?sectionName=GENOMIC%20PROFILES&search=classification%20breast%20cancer&topicRef=744&anchor=H697669959&source=see_link#H682640025.
15. Harvey, J.M., et al., *Estrogen receptor status by immunohistochemistry is superior to the ligand-binding assay for predicting response to adjuvant endocrine therapy in breast cancer.* Journal of clinical oncology : official journal of the American Society of Clinical Oncology, 1999. **17**(5): p. 1474-1481.
16. Bartlett, J.M.S., et al., *Estrogen receptor and progesterone receptor as predictive biomarkers of response to endocrine therapy: a prospectively powered pathology study in the Tamoxifen and Exemestane Adjuvant Multinational trial.* Journal of clinical oncology : official journal of the American Society of Clinical Oncology, 2011. **29**(12): p. 1531-1538.
17. Colzani, E., et al., *Prognosis of patients with breast cancer: causes of death and effects of time since diagnosis, age, and tumor characteristics.* Journal of clinical oncology : official journal of the American Society of Clinical Oncology, 2011. **29**(30): p. 4014-4021.
18. Purdie, C.A., et al., *Progesterone receptor expression is an independent prognostic variable in early breast cancer: a population-based study.* British Journal of Cancer, 2014. **110**(3): p. 565-572.
19. Loi, S., et al., *Definition of Clinically Distinct Molecular Subtypes in Estrogen Receptor–Positive Breast Carcinomas Through Genomic Grade.* Journal of Clinical Oncology, 2007. **25**(10): p. 1239-1246.
20. Voduc, K.D., et al., *Breast Cancer Subtypes and the Risk of Local and Regional Relapse.* Journal of Clinical Oncology, 2010. **28**(10): p. 1684-1691.
21. Hu, Z., et al., *The molecular portraits of breast tumors are conserved across microarray platforms.* BMC Genomics, 2006. **7**(1): p. 96.
22. Fan, C., et al., *Concordance among Gene-Expression–Based Predictors for Breast Cancer.* New England Journal of Medicine, 2006. **355**(6): p. 560-569.
23. Gonzalez-Angulo, A.M., et al., *Incidence and outcome of BRCA mutations in unselected patients with triple receptor-negative breast cancer.* Clinical cancer research : an official journal of the American Association for Cancer Research, 2011. **17**(5): p. 1082-1089.
24. Livasy, C.A., et al., *Phenotypic evaluation of the basal-like subtype of invasive breast carcinoma.* Modern Pathology, 2006. **19**(2): p. 264-271.
25. Waks, A.G. and E.P. Winer, *Breast Cancer Treatment: A Review.* JAMA, 2019. **321**(3): p. 288-300.
26. (EBCTCG), E.B.C.T.C.G., *Effect of radiotherapy after mastectomy and axillary surgery on 10-year recurrence and 20-year breast cancer mortality: meta-analysis of individual patient data for 8135 women in 22 randomised trials.* The Lancet, 2014. **383**(9935): p. 2127-2135.

27. Moran, M.S., et al., *Society of Surgical Oncology–American Society for Radiation Oncology Consensus Guideline on Margins for Breast-Conserving Surgery With Whole-Breast Irradiation in Stages I and II Invasive Breast Cancer.* Journal of Clinical Oncology, 2014. **32**(14): p. 1507-1515.
28. Park, C.C., et al., *Outcome at 8 Years After Breast-Conserving Surgery and Radiation Therapy for Invasive Breast Cancer: Influence of Margin Status and Systemic Therapy on Local Recurrence.* Journal of Clinical Oncology, 2000. **18**(8): p. 1668-1675.
29. Bodilsen, A., et al., *Importance of margin width in breast-conserving treatment of early breast cancer.* Journal of Surgical Oncology, 2016. **113**(6): p. 609-615.
30. van Maaren, M.C., et al., *10 year survival after breast-conserving surgery plus radiotherapy compared with mastectomy in early breast cancer in the Netherlands: a population-based study.* The Lancet Oncology, 2016. **17**(8): p. 1158-1170.
31. Agarwal, S., et al., *Effect of Breast Conservation Therapy vs Mastectomy on Disease-Specific Survival for Early-Stage Breast Cancer.* JAMA Surgery, 2014. **149**(3): p. 267-274.
32. Hwang, E.S., et al., *Survival after lumpectomy and mastectomy for early stage invasive breast cancer.* Cancer, 2013. **119**(7): p. 1402-1411.
33. Hartmann-Johnsen, O.J., et al., *Survival is Better After Breast Conserving Therapy than Mastectomy for Early Stage Breast Cancer: A Registry-Based Follow-up Study of Norwegian Women Primary Operated Between 1998 and 2008.* Annals of surgical oncology, 2015. **22**(12): p. 3836-3845.
34. Asselain, B., et al., *Long-term outcomes for neoadjuvant versus adjuvant chemotherapy in early breast cancer: meta-analysis of individual patient data from ten randomised trials.* The Lancet Oncology, 2018. **19**(1): p. 27-39.
35. Giuliano, A.E., et al., *Axillary Dissection vs No Axillary Dissection in Women With Invasive Breast Cancer and Sentinel Node Metastasis: A Randomized Clinical Trial.* JAMA, 2011. **305**(6): p. 569-575.
36. Donker, M., et al., *Radiotherapy or surgery of the axilla after a positive sentinel node in breast cancer (EORTC 10981-22023 AMAROS): a randomised, multicentre, open-label, phase 3 non-inferiority trial.* The Lancet. Oncology, 2014. **15**(12): p. 1303-1310.
37. Fisher, B., et al., *Twenty-Year Follow-up of a Randomized Trial Comparing Total Mastectomy, Lumpectomy, and Lumpectomy plus Irradiation for the Treatment of Invasive Breast Cancer.* New England Journal of Medicine, 2002. **347**(16): p. 1233-1241.
38. (EBCTCG), E.B.C.T.C.G., *Effect of radiotherapy after breast-conserving surgery on 10-year recurrence and 15-year breast cancer death: meta-analysis of individual patient data for 10 801 women in 17 randomised trials.* The Lancet, 2011. **378**(9804): p. 1707-1716.
39. (EBCTCG), E.B.C.T.C.G., *Aromatase inhibitors versus tamoxifen in early breast cancer: patient-level meta-analysis of the randomised trials.* The Lancet, 2015. **386**(10001): p. 1341-1352.

40. Pagani, O., et al., *Adjuvant Exemestane with Ovarian Suppression in Premenopausal Breast Cancer.* New England Journal of Medicine, 2014. **371**(2): p. 107-118.
41. Francis, P.A., et al., *Tailoring Adjuvant Endocrine Therapy for Premenopausal Breast Cancer.* New England Journal of Medicine, 2018. **379**(2): p. 122-137.
42. Pan, H., et al., *20-Year Risks of Breast-Cancer Recurrence after Stopping Endocrine Therapy at 5 Years.* New England Journal of Medicine, 2017. **377**(19): p. 1836-1846.
43. Harris, L.N., et al., *Use of Biomarkers to Guide Decisions on Adjuvant Systemic Therapy for Women With Early-Stage Invasive Breast Cancer: American Society of Clinical Oncology Clinical Practice Guideline.* Journal of Clinical Oncology, 2016. **34**(10): p. 1134-1150.
44. Albain, K.S., et al., *Prognostic and predictive value of the 21-gene recurrence score assay in postmenopausal women with node-positive, oestrogen-receptor-positive breast cancer on chemotherapy: a retrospective analysis of a randomised trial.* The Lancet Oncology, 2010. **11**(1): p. 55-65.
45. Duffy, M.J., et al., *Clinical use of biomarkers in breast cancer: Updated guidelines from the European Group on Tumor Markers (EGTM).* European Journal of Cancer, 2017. **75**: p. 284-298.
46. Early Breast Cancer Trialists' Collaborative, G., *Comparisons between different polychemotherapy regimens for early breast cancer: meta-analyses of long-term outcome among 100 000 women in 123 randomised trials.* The Lancet, 2012. **379**(9814): p. 432-444.
47. Arteaga, C.L., et al., *Treatment of HER2-positive breast cancer: current status and future perspectives.* Nature Reviews Clinical Oncology, 2012. **9**(1): p. 16-32.
48. Piccart-Gebhart, M.J., et al., *Trastuzumab after Adjuvant Chemotherapy in HER2-Positive Breast Cancer.* New England Journal of Medicine, 2005. **353**(16): p. 1659-1672.
49. Slamon, D., et al., *Adjuvant trastuzumab in HER2-positive breast cancer.* New England Journal of Medicine, 2011. **365**(14): p. 1273-1283.
50. von Minckwitz, G., et al., *Trastuzumab Emtansine for Residual Invasive HER2-Positive Breast Cancer.* New England Journal of Medicine, 2018. **380**(7): p. 617-628.
51. Pagani, O., et al., *International guidelines for management of metastatic breast cancer: can metastatic breast cancer be cured?* Journal of the National Cancer Institute, 2010. **102**(7): p. 456-463.
52. Stockler, M., et al., *Systematic reviews of chemotherapy and endocrine therapy in metastatic breast cancer.* Cancer Treatment Reviews, 2000. **26**(3): p. 151-168.
53. Geels, P., et al., *Palliative Effect of Chemotherapy: Objective Tumor Response Is Associated With Symptom Improvement in Patients With Metastatic Breast Cancer.* Journal of Clinical Oncology, 2000. **18**(12): p. 2395-2405.
54. Beslija, S., et al., *Third consensus on medical treatment of metastatic breast cancer.* Annals of Oncology, 2009. **20**(11): p. 1771-1785.

55. Cardoso, F., et al., *International Guidelines for Management of Metastatic Breast Cancer: Combination vs Sequential Single-Agent Chemotherapy.* JNCI: Journal of the National Cancer Institute, 2009. **101**(17): p. 1174-1181.
56. Schmid, P., et al., *Atezolizumab and Nab-Paclitaxel in Advanced Triple-Negative Breast Cancer.* New Eng J Med, 2018. **379**(22): p. 2108-2121.
57. Bardia, A., et al., *Efficacy and Safety of Anti-Trop-2 Antibody Drug Conjugate Sacituzumab Govitecan (IMMU-132) in Heavily Pretreated Patients With Metastatic Triple-Negative Breast Cancer.* Journal of Clinical Oncology, 2017. **35**(19): p. 2141-2148.
58. Livraghi, L. and J.E. Garber, *PARP inhibitors in the management of breast cancer: current data and future prospects.* BMC Medicine, 2015. **13**(1): p. 188.
59. Lin, K.Y. and W.L. Kraus, *PARP Inhibitors for Cancer Therapy.* Cell, 2017. **169**(2): p. 183.
60. Drost, J. and H. Clevers, *Organoids in cancer research.* Nature Reviews Cancer, 2018. **18**(7): p. 407-418.
61. Kamb, A., *What's wrong with our cancer models?* Nature Reviews Drug Discovery, 2005. **4**(2): p. 161-165.
62. Liu, X., et al., *ROCK Inhibitor and Feeder Cells Induce the Conditional Reprogramming of Epithelial Cells.* The American Journal of Pathology, 2012. **180**(2): p. 599-607.
63. Ben-David, U., et al., *Patient-derived xenografts undergo mouse-specific tumor evolution.* Nature Genetics, 2017. **49**(11): p. 1567-1575.
64. Byrne, A.T., et al., *Interrogating open issues in cancer precision medicine with patient-derived xenografts.* Nature Reviews Cancer, 2017. **17**(4): p. 254-268.
65. Eirew, P., et al., *Dynamics of genomic clones in breast cancer patient xenografts at single-cell resolution.* Nature, 2015. **518**(7539): p. 422-426.
66. Kresse, S.H., et al., *Preclinical xenograft models of human sarcoma show nonrandom loss of aberrations.* Cancer, 2012. **118**(2): p. 558-570.
67. Bosma, M.J. and A.M. Carroll, *The SCID mouse mutant: definition, characterization, and potential uses.* Annual review of immunology, 1991. **9**(1): p. 323-350.
68. Eiraku, M. and Y. Sasai, *Self-formation of layered neural structures in three-dimensional culture of ES cells.* Current Opinion in Neurobiology, 2012. **22**(5): p. 768-777.
69. Clevers, H., *Modeling Development and Disease with Organoids.* Cell, 2016. **165**(7): p. 1586-1597.
70. Dutta, D., I. Heo, and H. Clevers, *Disease Modeling in Stem Cell-Derived 3D Organoid Systems.* Trends in Molecular Medicine, 2017. **23**(5): p. 393-410.
71. Sachs, N., et al., *A Living Biobank of Breast Cancer Organoids Captures Disease Heterogeneity.* Cell, 2018. **172**(1): p. 373-386.e10.
72. Raimondi, G., et al., *Patient-derived pancreatic tumour organoids identify therapeutic responses to oncolytic adenoviruses.* EBioMedicine, 2020. **56**: p. 102786.

73. Pardoll, D.M., *The blockade of immune checkpoints in cancer immunotherapy.* Nature Reviews Cancer, 2012. **12**: p. 252.
74. Russell, S.J., K.-W. Peng, and J.C. Bell, *Oncolytic virotherapy.* Nature Biotechnology, 2012. **30**: p. 658.
75. Hartkopf, A.D., et al., *Oncolytic virotherapy of breast cancer.* Gynecologic Oncology, 2011. **123**(1): p. 164-171.
76. Binz, E. and U.M. Lauer, *Chemovirotherapy: combining chemotherapeutic treatment with oncolytic virotherapy.* Oncolytic virotherapy, 2015. **4**: p. 39-48.
77. Hartkopf, A.D., et al., *Oncolytic Viruses to Treat Ovarian Cancer Patients - a Review of Results From Clinical Trials.* Geburtshilfe und Frauenheilkunde, 2012. **72**(2): p. 132-136.
78. Kirn, D., R.L. Martuza, and J. Zwiebel, *Replication-selective virotherapy for cancer: Biological principles, risk management and future directions.* Nature Medicine, 2001. **7**(7): p. 781-787.
79. Cutts, F.T. and L.E. Markowitz, *Successes And Failures In Measles Control.* The Journal of Infectious Diseases, 1994. **170**(Supplement_1): p. S32-S41.
80. Anderson, B.D., et al., *High CD46 Receptor Density Determines Preferential Killing of Tumor Cells by Oncolytic Measles Virus.* Cancer Research, 2004. **64**(14): p. 4919.
81. Arakawa, S., et al., *Clinical trial of attenuated vaccinia virus AS strain in the treatment of advanced adenocarcinoma.* Journal of Cancer Research and Clinical Oncology, 1987. **113**(1): p. 95-98.
82. Antonio Chiocca, E., *Oncolytic viruses.* Nature Reviews Cancer, 2002. **2**: p. 938.
83. Martuza, R.L., et al., *Experimental therapy of human glioma by means of a genetically engineered virus mutant.* Science, 1991. **252**(5007): p. 854.
84. Lichty, B.D., et al., *Going viral with cancer immunotherapy.* Nature Reviews Cancer, 2014. **14**: p. 559.
85. Chiocca, E.A. and S.D. Rabkin, *Oncolytic viruses and their application to cancer immunotherapy.* Cancer immunology research, 2014. **2**(4): p. 295-300.
86. Kaufman, H.L., F.J. Kohlhapp, and A. Zloza, *Oncolytic viruses: a new class of immunotherapy drugs.* Nature Reviews Drug Discovery, 2015. **14**: p. 642.
87. McCart, J.A., et al., *Systemic Cancer Therapy with a Tumor-selective Vaccinia Virus Mutant Lacking Thymidine Kinase and Vaccinia Growth Factor Genes.* Cancer Research, 2001. **61**(24): p. 8751.
88. Chalikonda, S., et al., *Oncolytic virotherapy for ovarian carcinomatosis using a replication-selective vaccinia virus armed with a yeast cytosine deaminase gene.* Cancer Gene Therapy, 2008. **15**(2): p. 115-125.
89. Erbs, P., et al., *In Vivo Cancer Gene Therapy by Adenovirus-mediated Transfer of a Bifunctional Yeast Cytosine Deaminase/Uracil Phosphoribosyltransferase Fusion Gene.* Cancer Research, 2000. **60**(14): p. 3813.

90. Dias, J.D., et al., *Targeted Chemotherapy for Head and Neck Cancer with a Chimeric Oncolytic Adenovirus Coding for Bifunctional Suicide Protein FCU1.* Clinical Cancer Research, 2010. **16**(9): p. 2540.
91. Slos, P. and P. Erbs, *Intratumoral delivery of genes: a new weapon against cancer?* 2004, Taylor & Francis.
92. Glazer, R.I. and L.S. Lloyd, *Association of cell lethality with incorporation of 5-fluorouracil and 5-fluorouridine into nuclear RNA in human colon carcinoma cells in culture.* Molecular Pharmacology, 1982. **21**(2): p. 468.
93. Ingraham, H.A., B.Y. Tseng, and M. Goulian, *Nucleotide levels and incorporation of 5-fluorouracil and uracil into DNA of cells treated with 5-fluorodeoxyuridine.* Molecular Pharmacology, 1982. **21**(1): p. 211.
94. Andtbacka, R.H.I., et al., *Talimogene Laherparepvec Improves Durable Response Rate in Patients With Advanced Melanoma.* Journal of Clinical Oncology, 2015. **33**(25): p. 2780-2788.
95. Kaufman, H.L. and S.D. Bines, *OPTIM trial: a Phase III trial of an oncolytic herpes virus encoding GM-CSF for unresectable stage III or IV melanoma.* Future Oncology, 2010. **6**(6): p. 941-949.
96. Hu, J.C.C., et al., *A Phase I Study of OncoVEX GM-CSF, a Second-Generation Oncolytic Herpes Simplex Virus Expressing Granulocyte Macrophage Colony-Stimulating Factor.* Clinical Cancer Research, 2006. **12**(22): p. 6737.
97. Kaufmann, M., et al., *Recommendations from an International Consensus Conference on the Current Status and Future of Neoadjuvant Systemic Therapy in Primary Breast Cancer.* Annals of Surgical Oncology, 2012. **19**(5): p. 1508-1516.
98. Kaufman, H.L., et al., *Local and Distant Immunity Induced by Intralesional Vaccination with an Oncolytic Herpes Virus Encoding GM-CSF in Patients with Stage IIIc and IV Melanoma.* Annals of Surgical Oncology, 2010. **17**(3): p. 718-730.
99. Pesonen, S., et al., *Integrin targeted oncolytic adenoviruses Ad5-D24-RGD and Ad5-RGD-D24-GMCSF for treatment of patients with advanced chemotherapy refractory solid tumors.* International Journal of Cancer, 2012. **130**(8): p. 1937-1947.
100. Yu, Y.A., et al., *Visualization of tumors and metastases in live animals with bacteria and vaccinia virus encoding light-emitting proteins.* Nature Biotechnology, 2004. **22**(3): p. 313-320.
101. Parato, K.A., et al., *The Oncolytic Poxvirus JX-594 Selectively Replicates in and Destroys Cancer Cells Driven by Genetic Pathways Commonly Activated in Cancers.* Molecular Therapy, 2012. **20**(4): p. 749-758.
102. Stojdl, D.F., et al., *VSV strains with defects in their ability to shutdown innate immunity are potent systemic anti-cancer agents.* Cancer Cell, 2003. **4**(4): p. 263-275.
103. Breitbach, C.J., et al., *Intravenous delivery of a multi-mechanistic cancer-targeted oncolytic poxvirus in humans.* Nature, 2011. **477**: p. 99.
104. Liu, T.-C., et al., *The Targeted Oncolytic Poxvirus JX-594 Demonstrates Antitumoral, Antivascular, and Anti-HBV Activities in Patients With Hepatocellular Carcinoma.* Molecular Therapy, 2008. **16**(9): p. 1637-1642.

105. Breitbach, C.J., et al., *Oncolytic Vaccinia Virus Disrupts Tumor-Associated Vasculature in Humans.* Cancer Research, 2013. **73**(4): p. 1265.
106. Breitbach, C.J., et al., *Targeted Inflammation During Oncolytic Virus Therapy Severely Compromises Tumor Blood Flow.* Molecular Therapy, 2007. **15**(9): p. 1686-1693.
107. Breitbach, C.J., et al., *Targeting Tumor Vasculature With an Oncolytic Virus.* Molecular Therapy, 2011. **19**(5): p. 886-894.
108. Fulci, G. and E.A. Chiocca, *Oncolytic viruses for the therapy of brain tumors and other solid malignancies: a review.* Front Biosci, 2003. **8**: p. e346-60.
109. Chiocca, E.A., et al., *A Phase I Open-Label, Dose-Escalation, Multi-Institutional Trial of Injection with an E1B-Attenuated Adenovirus, ONYX-015, into the Peritumoral Region of Recurrent Malignant Gliomas, in the Adjuvant Setting.* Molecular Therapy, 2004. **10**(5): p. 958-966.
110. Carter, M.E., et al., *Clinical Trials of Oncolytic Viruses in Breast Cancer.* Frontiers in Oncology, 2021. **11**(5484).
111. Pol, J., et al., *Trial Watch—Oncolytic viruses and cancer therapy.* OncoImmunology, 2016. **5**(2): p. e1117740.
112. Hartkopf, A.D., et al., *Enhanced killing of ovarian carcinoma using oncolytic measles vaccine virus armed with a yeast cytosine deaminase and uracil phosphoribosyltransferase.* Gynecologic Oncology, 2013. **130**(2): p. 362-368.
113. Udem, S.A. and K.A. Cook, *Isolation and characterization of measles virus intracellular nucleocapsid RNA.* Journal of Virology, 1984. **49**(1): p. 57.
114. Santiago, C., et al., *Distinct kinetics for binding of the CD46 and SLAM receptors to overlapping sites in the measles virus hemagglutinin protein.* Journal of Biological Chemistry, 2002. **277**(35): p. 32294-32301.
115. Hartkopf, A.D., et al., *Oncolytic virotherapy of gynecologic malignancies.* Gynecologic Oncology, 2011. **120**(2): p. 302-310.
116. Krabbe, T. and J. Altomonte, *Fusogenic Viruses in Oncolytic Immunotherapy.* Cancers, 2018. **10**(7).
117. Fishelson, Z., et al., *Obstacles to cancer immunotherapy: expression of membrane complement regulatory proteins (mCRPs) in tumors.* Molecular Immunology, 2003. **40**(2): p. 109-123.
118. Lech, P.J. and S.J. Russell, *Use of attenuated paramyxoviruses for cancer therapy.* Expert Review of Vaccines, 2010. **9**(11): p. 1275-1302.
119. Galanis, E., et al., *Phase I Trial of Intraperitoneal Administration of an Oncolytic Measles Virus Strain Engineered to Express Carcinoembryonic Antigen for Recurrent Ovarian Cancer.* Cancer Research, 2010. **70**(3): p. 875.
120. Tsien, R.Y., *The green fluorescent protein*. 1998, Annual Reviews 4139 El Camino Way, PO Box 10139, Palo Alto, CA 94303-0139, USA.
121. Carter, M.E., et al., *A Three-Dimensional Organoid Model of Primary Breast Cancer to Investigate the Effects of Oncolytic Virotherapy.* Frontiers in Molecular Biosciences, 2022. **9**.

122. Graepler, F., et al., *Bifunctional chimeric SuperCD suicide gene -YCD: YUPRT fusion is highly effective in a rat hepatoma model.* World journal of gastroenterology, 2005. **11**(44): p. 6910-6919.
123. Lampe, J., et al., *An armed oncolytic measles vaccine virus eliminates human hepatoma cells independently of apoptosis.* Gene Therapy, 2013. **20**: p. 1033.
124. Zaoui, K., et al., *Chemovirotherapy for head and neck squamous cell carcinoma with EGFR-targeted and CD/UPRT-armed oncolytic measles virus.* Cancer Gene Therapy, 2012. **19**(3): p. 181-191.
125. Goebel, S.J., et al., *The complete DNA sequence of vaccinia virus.* Virology, 1990. **179**(1): p. 247-266.
126. Zhang, Q., et al., *The highly attenuated oncolytic recombinant vaccinia virus GLV-1h68: comparative genomic features and the contribution of F14.5L inactivation.* Molecular genetics and genomics : MGG, 2009. **282**(4): p. 417-435.
127. Zhang, Q., et al., *Eradication of Solid Human Breast Tumors in Nude Mice with an Intravenously Injected Light-Emitting Oncolytic Vaccinia Virus.* Cancer Research, 2007. **67**(20): p. 10038.
128. Wiedenmann, J., et al., *A far-red fluorescent protein with fast maturation and reduced oligomerization tendency from Entacmaea quadricolor (Anthozoa, Actinaria).* Proceedings of the National Academy of Sciences, 2002. **99**(18): p. 11646.
129. Izmailyan, R. and W. Chang, *Vaccinia Virus WR53.5/F14.5 Protein Is a New Component of Intracellular Mature Virus and Is Important for Calcium-Independent Cell Adhesion and Vaccinia Virus Virulence in Mice.* Journal of Virology, 2008. **82**(20): p. 10079.
130. Raki, M., et al., *Utility of TK/GCV in the context of highly effective oncolysis mediated by a serotype 3 receptor targeted oncolytic adenovirus.* Gene Therapy, 2007. **14**: p. 1380.
131. Lawler, S.E., et al., *Oncolytic viruses in cancer treatment: A review.* JAMA Oncology, 2017. **3**(6): p. 841-849.
132. Goldhammer, N., et al., *Characterization of organoid cultured human breast cancer.* Breast Cancer Research, 2019. **21**(1): p. 141.
133. Rosenbluth, J.M., et al., *Organoid cultures from normal and cancer-prone human breast tissues preserve complex epithelial lineages.* Nature Communications, 2020. **11**(1): p. 1711.
134. Munne, P.M., et al., *Compressive stress-mediated p38 activation required for ERα + phenotype in breast cancer.* Nature Communications, 2021. **12**(1): p. 6967.
135. Bertrand, R., et al., *Induction of a Common Pathway of Apoptosis by Staurosporine.* Experimental Cell Research, 1994. **211**(2): p. 314-321.
136. Dijkstra, K.K., et al., *Generation of Tumor-Reactive T Cells by Co-culture of Peripheral Blood Lymphocytes and Tumor Organoids.* Cell, 2018. **174**(6): p. 1586-1598.e12.

8 Own contribution

Die Arbeit wurde in der Universitätsfrauenklinik Tübingen unter Betreuung von Herrn Prof. Dr. Andreas Hartkopf selbstständig von mir durchgeführt. Die Arbeit mit onkolytischen Viren wurde durch Prof. Dr. Ulrich Lauer mitbetreut.

Die Konzeption der Studie erfolgte durch Prof. Hartkopf, Dr. André Koch und mich in Zusammenarbeit mit Prof. Lauer.

Die Versuche wurden nach Einarbeitung durch Anna Wagner und Dr. Koch von mir eigenständig durchgeführt. Das Anlegen und Kultivieren der Organoid-kulturen von Brustkrebspatienten wurde von mir selbstständig durchgeführt. Mehrere Protokolle zur Infektion der Organoiden mit onkolytischen Viren wurden von mir erprobt und schließlich wurde eine Methode zur weiteren Analytik definiert. Die Quantifizierung der Effekte der onkolytischen Viren auf die Organoidkulturen mittels Cell-Titer Blue Assay wurde von mir selbstständig etabliert und durchgeführt. Die Paraffineinbettung der Organoide erfolgte durch Ingrid Teufel. Die immunhistochemischen Färbungen der Organoidschnitte erfolgten durch das Institut für Pathologie des Universitätsklinikums Tübingen.

Die statistische Auswertung erfolgte eigenständig durch mich.

Ich versichere, das Manuskript komplett selbständig nach Anleitung durch Dr. Koch und Prof. Hartkopf verfasst zu haben und keine weiteren als die von mir angegebenen Quellen verwendet zu haben.

Tübingen, den 16.02.2022

Mary Elisabeth Carter

9 Publications

In Vorbereitung auf meine Doktorarbeit habe ich eine Literaturrecherche zu den aktuellen publizierten klinischen Studien mit onkolytischen Viren bei Mammakarzinom durchgeführt. Aus diesen Daten ist ein Review entstanden mit meiner Erstautorenschaft unter der Betreuung durch Dr. Koch, Prof. Lauer und Prof. Hartkopf. Dieses Review wurde am 23.12.2021 in *Frontiers in Oncology* unter dem Titel „Clinical Trials of Oncolytic Viruses in Breast Cancer" publiziert [110].

Während der Verfassung meiner Doktorarbeit habe ich einen Teil meiner Daten als Manuskript bei *Frontiers in Molecular Biosciences* im *Research Topic Oncolytic Virotherapy* zur Publikation eingereicht. Die hierfür verwendeten Daten wurden durch mich erhoben, ausgewertet und von mir als erstes Manuskript verfasst. Hierbei wurde ich u.a. durch Prof. Hartkopf, Dr. Berchtold, Prof. Lauer und Dr. Koch betreut, die das Konzept des Projektes mitentwickelt haben und an der Ausarbeitung der finalen Version des Manuskriptes beteiligt waren. Das Manuskript wurde am 11.02.2022 bei *Frontiers in Molecular Biosciences* im *Research Topic Oncolytic Virotherapy* unter dem Titel „A three-dimensional Organoid Model of Primary Breast Cancer to Investigate the Effects of Oncolytic Virotherapy" mit meiner Erstautorenschaft publiziert [121].

10 Acknowledgement

An dieser Stelle bedanke ich mich bei all denjenigen, die mir eine Anfertigung dieser Doktorarbeit ermöglicht haben.

Mein Dank geht vor allem den folgenden Personen, ohne deren Unterstützung diese Doktorarbeit nicht zustande gekommen wäre:

Mein Dank gilt zunächst meinem Doktorvater, Herrn Prof. Dr. Andreas Hartkopf, für die hervorragende wissenschaftliche Betreuung der Arbeit und die stetige Unterstützung. Sowohl der konstruktive als auch der fachliche Austausch waren stets eine besondere Bereicherung und eine große Hilfe für mich.

Mein Dank gilt zudem Herrn Prof. Dr. Ulrich Lauer für die Mitbetreuung des Projektes und der Arbeit sowie die fachliche und persönliche Unterstützung. Den regen Austausch, die Unterstützung bei den Publikationen und die professionelle Unterstützung schätze ich sehr.

Ebenfalls gilt mein Dank Herrn Dr. André Koch und seiner Arbeitsgruppe für die wissenschaftliche Zusammenarbeit im Rahmen des Projektes. Die Zeit war von sehr interessanten und anregenden fachlichen Gesprächen geprägt und von gegenseitiger Unterstützung.

Ebenfalls gilt mein Dank Frau Dr. Susanne Berchtold und der Arbeitsgruppe von Prof. Dr. Lauer für die wissenschaftliche Zusammenarbeit und Kooperation im Rahmen dieses Projektes. Die Zusammenarbeit war durch regen Ideenaustausch und eine angenehme Atmosphäre geprägt.

Bei meiner Familie und Martin Pietzsch möchte ich mich ganz herzlich für die geduldige, aufmerksame und hilfreiche Unterstützung während des Projektes, dem Verfassen meiner Arbeit und meines gesamten Studiums danken.

Außerdem gilt mein Dank dem IZKF Promotionskolleg der Medizinischen Fakultät Tübingen für die ideelle und finanzielle Förderung meines Projektes.